6-12-2018

Process intervention for water recovery in food manufacture

Christian Michael Wisniewski
Rowan University

PROCESS INTERVENTION FOR WATER RECOVERY IN FOOD MANUFACTURE

by

Christian M. Wisniewski

A Thesis

Submitted to the
Department of Chemical Engineering
College of Engineering
In partial fulfillment of the requirement
For the degree of
Master of Science in Chemical Engineering
at
Rowan University
May 24, 2018

Thesis Chairs: C. Stewart Slater, Ph.D.
Mariano J. Savelski, Ph.D.

Acknowledgments

I would like to thank my advisors Dr. C. Stewart Slater and Dr. Mariano J. Savelski for the opportunity to work on this project and their guidance throughout the project. I acknowledge the Rowan Engineering Clinic students: Sabrina Abrenica, Richard Bartell, John Borovilas, Don Dunner, Luke Howard, Glen Kartalis, Brandon Lawrence, Drew Skiba, Paul Tozzi, and Andrew Warne for their help during the 2016-17 and 2017-18 academic years. I also appreciate the assistance of Nestlé-USA and Jim Barden, Fredéric Bodo, Erica Grun, John Morton (former Rowan student), and Eugene Williford. Finally, I acknowledge the support of the U.S. Environmental Protection Agency through the Pollution Prevention grant program (NP96271316-1).

Abstract

Christian M. Wisniewski
PROCESS INTERVENTION FOR WATER RECOVERY IN FOOD MANUFACTURE
2017-2018
C. Stewart Slater, Ph.D.; Mariano J. Savelski, Ph.D.
Master of Science in Chemical Engineering

A case study has been conducted for the recovery of water from complex wastewater at a soluble coffee manufacturing factory. The study has evaluated separation methods for process intervention based on environmental and economic assessments. Water recovery was identified in two possible wastewater streams at the factory: the overall plant effluent and an intermediate stream before it enters on-site pre-treatment. A novel vibratory field membrane separation was tested at the laboratory scale using real factory wastewater and scaled-up using appropriate design protocols. Recovery of water from the intermediate stream proved the most effective, both environmentally and economically. The full-scale vibratory membrane process recovers 100,000 gallons of water per day that meets specifications for the factory cooling tower. The proposed design reduced the daily well water with draw by 21% and the amount of wastewater discharged from the factory by 28.5%. Annual operating costs were reduced by 22.5% and total life cycle emissions were reduced by 27.8%. These reductions are mainly the result of the reduced volume of wastewater discharged from the factory and the reduced energy requirement of the on-site pre-treatment processes. The vibratory membrane process for water recovery presents favorable economics, even after capital costs are considered. The net present value after 10 years is $485,300, while the payback time is under three years.

Table of Contents

Table of Contents (Continued)

Table of Contents (Continued)

List of Figures

List of Tables

Chapter 1

Introduction

This project focuses on the implementation of process intensification (water and waste reduction) techniques to improve the efficiency of food manufacturing facilities. The broad goals of pollution prevention are achieved by reduction in the generation of greenhouse gas (GHG) emissions, reduction in the use of water, associated reduction in energy utilization, and potential reduction in hazardous waste materials. This is specifically accomplished by working with Nestlé USA, the world's largest food company, at their Freehold, New Jersey manufacturing plant.

Based on background research and discussions with food industry representatives, challenges of this sector have been identified to be related to inefficiencies in water utilization. This project evaluates and proposes to improve food processing platforms through process intensification techniques. The term, process intensification, is a broad term, which is used to describe approaches to reduce water use and waste generation. The primary focus of this activity is related to water conservation by proposing a fully-integrated food manufacturing platform, using the Nestlé production facility in Freehold, NJ as the case study. The Freehold, NJ plant produces Nescafé Clasico®, Nescafé Clasico Decaf®, Nescafé Taster's Choice®, Nescafé Taster's Choice Decaf®, and Nescafé Taster's Choice Gourmet® freeze-dried and spray-dried instant (i.e. soluble) coffee products. Current food manufacturing operations, as described in the following section, have inefficiencies in their water and energy use, which leads to GHG emissions and associated environmental impacts.

Through this case study, an evaluation of methods to optimize Nestlé's processes has been conducted. The process intensification approach will also have a potential impact on other Nestlé facilities, and that of other food manufacturers.

Chapter 2

Background

Water Use in the Food and Beverage Industry

The food and beverage industry contributes to a high amount of global water and energy use. High water demands show a requirement for an investigation towards optimization for recovery and recycle of it. A recent study has estimated that the demand for agricultural production will increase 70% by 2050, because of rising global populations [1]. It should be noted that freshwater water around the world is mostly used for irrigation purposes. According to the AQUASTAT database provided by the Food and Agriculture Organization of the United Nations, agriculture is responsible for the consumption of 69% of all freshwater that is currently withdrawn in the world, as shown in Figure 1 [2].

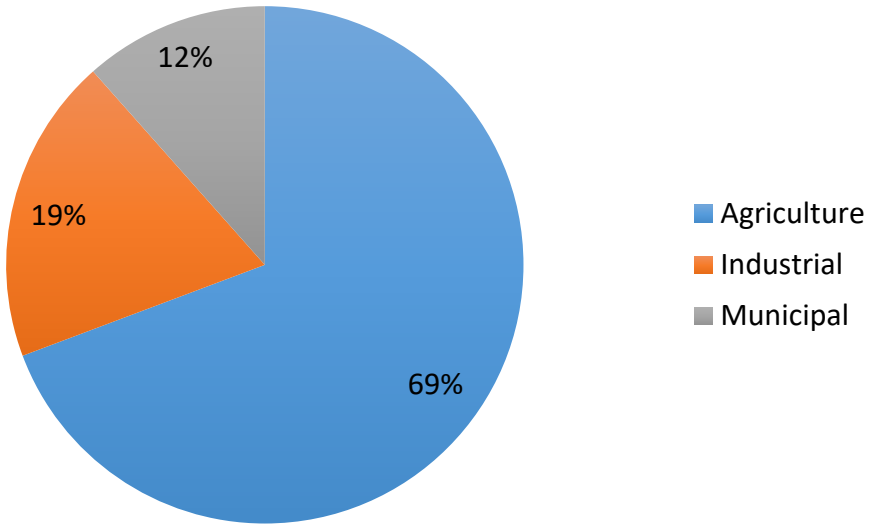

Figure 1. Worldwide freshwater withdrawal by sector [2]

Water use by sector in North America is not dominated by agricultural use, but rather industrial use, as shown in Figure 2. Freshwater use in industrial applications is at 47% of the total water use while agriculture usage is at 40%. In the United States, water use is even more shifted to industrial purposes at about 51% of the total freshwater withdrawn and about 36% is used for agriculture [2].

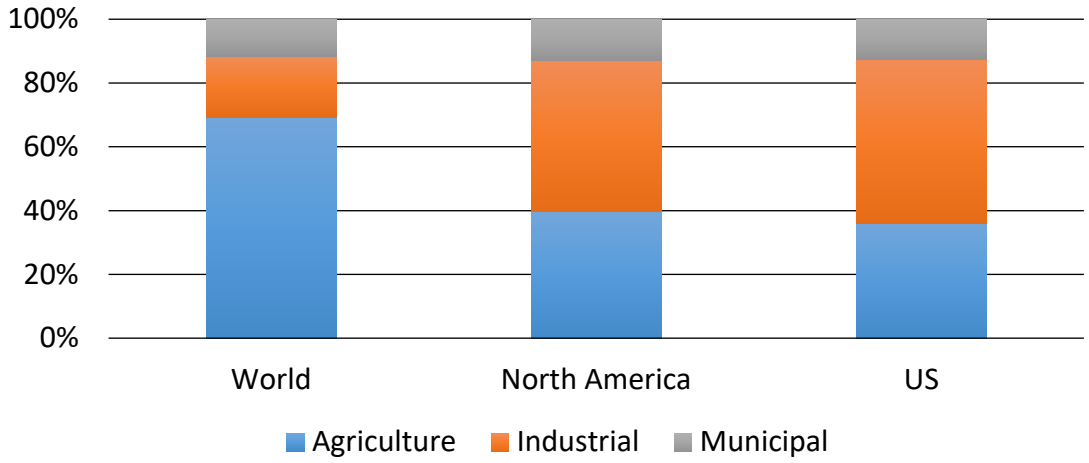

Figure 2. Comparison of freshwater withdrawal worldwide, North America, and the United States [2]

Food production and processing accounts for 5% of commercially-used water consumption in the United States [3]. Water can be used as a food product ingredient and/or for various aspects of food processing/manufacturing operations. Water is also used for various process and cleaning steps, including heating, pasteurizing, chilling, blanching, chilling, cooling, steam production, washing, rinsing, sanitizing, disinfecting, and others [4], [5]. Water can also be used to transport raw materials in food manufacture [6]. Since water can be used in a multitude of ways, the food manufacturing

industry has a high water utilization per finished product. Some cases show ratios upwards of 1,000 times the mass of the finished product, even for those cases where water is not an ingredient in the finished product [5], [7], [8], [9]. Figure 3 shows a comparison of the water consumption associated with the production of various food products.

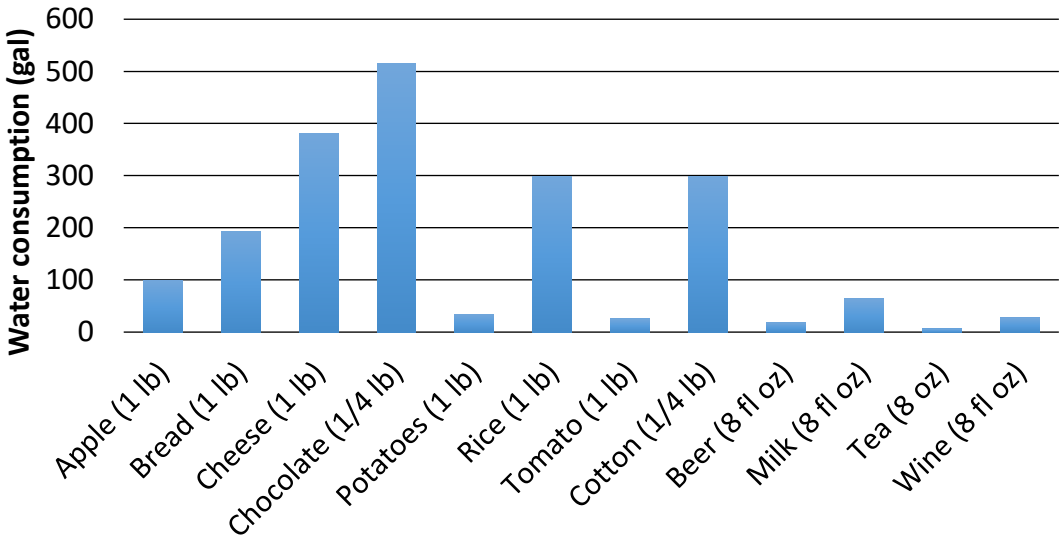

Figure 3. Comparison of the water consumption for various food/beverage products [9]

A major concern with water use in food manufacture is that most water used in processing does not end up in the final product, but rather as waste [7]. One approach to evaluate the total water use over the life cycle of the production of a food product is a water footprint analysis. The "water footprint" concept is defined as "an indicator of freshwater use that looks not only at direct water use of a consumer or producer, but also at the indirect water use [10]." A water footprint assessment aims to complete three main tasks. The first is to quantify the water footprint of a process, product, producer, or

consumer or to quantify the water footprint of a specified region. The second is to assess the sustainability of the water footprint from an environmental, social, and economic standpoint. The third is to formulate a strategy to respond to the water footprint [10]. An important concept in the water footprint assessment is the differentiation between sources of freshwater. Water sourced from the surface or ground is referred to as blue water. Water from precipitation that has not run off to surface sources, but is stored in the soil, is referred to as green water. The final type of water considered is grey water. Grey water is the freshwater needed to assimilate waste and is quantified as the amount of freshwater needed to dilute pollutants to conform to water quality standards [10].

The production of crops and their derived products presents a case of high water consumption from a water footprint assessment. The water footprint of crop production can be calculated by determining the evapotranspiration and yield associated with a crop [11]. Evapotranspiration is the process by which water enters the atmosphere from the land by evaporation from soil and other areas and transpiration from plants [12]. The evapotranspiration of a crop is affected by climate characteristics, crop characteristics, and the availability of soil water. Allen et al. have provided methods for evaluating the evapotranspiration for crops [11], [13]. The yield of a crop is affected by a water stress factor, the evapotranspiration of a crop, and the total water requirement of a crop [14]. The global averages of the water footprint breakdown of various crop products can be seen in Figure 4.

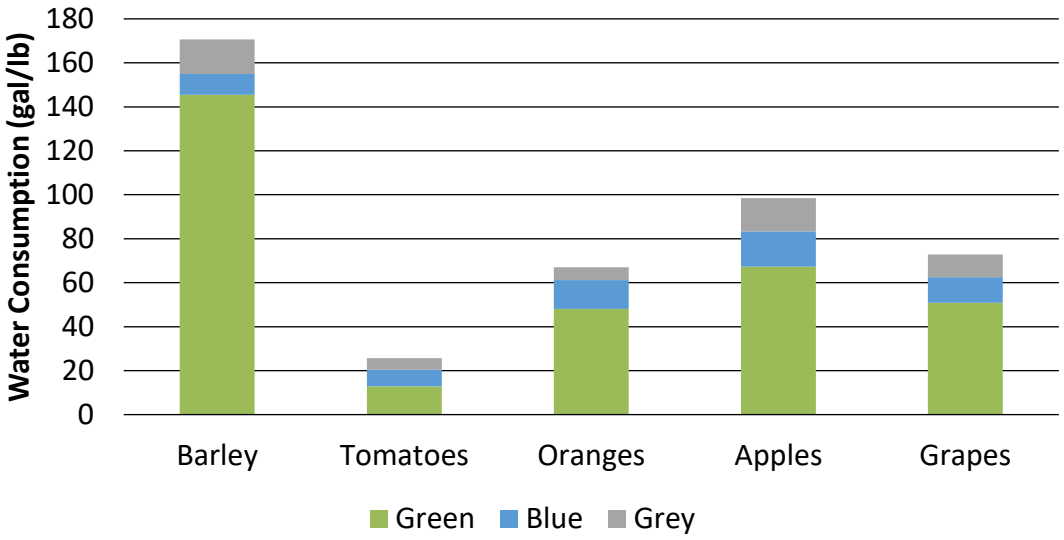

Figure 4. Global water footprint of different crops

To determine the water footprint of products derived from crops (e.g. juices), a product fraction and a value fraction are incorporated [11]. The product fraction is the amount of product that is generated per the amount of input of crop. The value fraction of a product is the ratio of the market value of the product to the combined market value of all products derived from the input crop [11]. The global averages of various products that are derived from crops are shown in Figure 5. This figure also reveals that the production of various juices from the original crops requires more water by a factor of 1.3 for grape juice, up to a factor of 5 for concentrated tomato juice. It is important to note the large water consumption for chocolate and coffee manufacturing. Figure 5 shows the water consumption of these products in gal/ (1/2-lb finished goods). A discussion of water use in coffee is provided in a later section of this project. Chocolate and coffee beans cultivation and processing are responsible for the high water footprint.

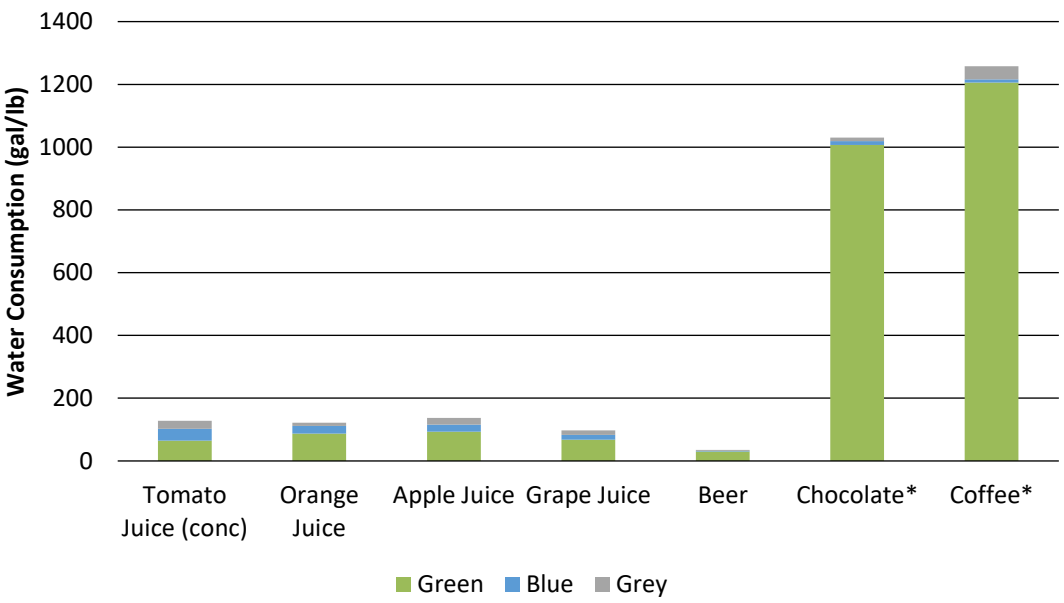

Figure 5. Global water footprint of various products derived from crops (*chocolate and coffee are in gal/(1/2-lb finished goods) to better display data) [11]

Water Use Issue Examples in Crop-derived Products

As an example on how this analysis is used, sample products derived from crops will be discussed. Among products shown in Figure 5, beer has the smallest water footprint; however, with a global average of nearly 300 gallons of water used per gallon of beer, water consumption per product is significant [11]. In the production of beer, water use can be assigned to four categories: crop cultivation, crop processing, brewing and bottling, and waste disposal [15]. Crop cultivation is the most water intensive step and consists direct water for crops, irrigation systems, and water used for farm machinery and transport. Crop processing involves direct water use for cleaning and other processes and water related to energy use in processing steps. Brewing and bottling consists of direct water use for brewing and cleaning, waste generation, and water used for

manufacture of other raw materials. Waste disposal involves any water requirement used for recycling of cans, bottle, and kegs [15].

Case studies provided by SABMiller plc (acquired by AB InBev in October 2016 [16]) offer insight to the water footprint of beer production at two production regions, in South Africa and in the Czech Republic. Annual production of beer among seven breweries in South Africa was 687 million gallons in 2007. Water availability in South Africa has been a pressing issue, with many regions of the country in danger of extremely scarce levels by 2025 [15]. The annual water footprint for beer production was 137 billion gallons, or about 199 gallons of water per gallon of beer. About 98.3% of the water footprint among breweries in South Africa was attributed to crop growth, both from local cultivation and import of crops [15]. The remainder is dominantly brewing and bottling at 1.4% and crop processing and waste disposal totaling the balance. The water footprint among the Czech Republic includes three breweries, two malting plants, and thirteen distribution centers [15]. Annual beer production in the Czech Republic in 2008 totaled 223 million gallons. The annual water consumption for beer production was 10.3 billion gallons, or 46 gallons of water per gallon of beer. Again, the water footprint is predominantly made up from crop cultivation, at about 95% of the total water footprint. About 4.4% of the water footprint is accounted for by brewing and bottling, with the balance as crop processing and waste disposal [15]. A comparison between the studies shows that location is an important factor for the water footprint of a product. Overall, it can be concluded between the two cases that total water consumption of beer production is significantly influenced by crop production, and only a small percentage is used during manufacturing operations. While this percentage is small, the actual volume of water

used during such operations remains high. Water use during brewing and bottling totaled nearly 9 billion gallons per year between the two cases [15].

Soft drinks, specifically, sugar-containing carbonated beverages, are another crop-derived beverage product with a significant water use per product. The amount of water required to produce this product varies on the source and type of sugar crop used for the final product [17]. The final water footprint, however, shows the same trend that the majority of water use occurs in the crop production stages of the product. In a recent study, the water footprint of sugar-containing carbonated beverages was assessed [17]. The water footprint of the product with sugar derived from sugar cane, sugar beet, or high fructose corn syrup from different countries was evaluated. It was found that the water consumption varies between 150 to 300 liters of water per 0.5 liter product, including water requirements for packaging materials and water and energy used during operation [17]. The common theme among all assessments is that at least 99.7% of all water consumed is used in the supply chain and the remainder as water as the raw ingredient. Of the supply chain water, 94.5 – 97% of the water is consumed for products derived from crops: sugar, caffeine, and vanilla extract. Caffeine was assumed to be sourced from coffee beans and vanilla extract from vanilla beans [17].

Issues Associated with High Water Use

High water footprints are stereotypical of the food and beverage industry. This presents a significant cause for concern as the demand for food production rises, and freshwater is not a limitless resource. Water demand is also influenced by a rising global population, urbanization, energy, and trade [18]. Water use in energy production is affected by many sectors, including agriculture and manufacturing. Urbanization causes

high, localized withdrawal of freshwater. Unstainable growth in each of these factors contribute to the unstable demand for water. A response to this growth in the form of sustainable development and optimization is required in order to achieve water security for future generations.

Water availability and use faces a variety of challenges by region. Currently, water availability in developing nations remains scarce, resulting in over 660 million people in these regions without safe drinking water [19]. In developed regions of the world, such as North America and Europe, water-related challenges concern development and implementation of new technologies to use and reuse water more efficiently [18]. Within the Pacific region and Asia, sanitation and access to safe water by mending pollution issues are main concerns. In Latin America, establishment of the right to clean water and sanitation is a priority. Challenges pertaining to water in Africa include achieving sustainable participation in global trade and developing better access to natural water resources [18].

Specifically, in New Jersey, stress on freshwater supply and use is elevated by the state's high and growing population density [20]. In 2010, estimated freshwater use in New Jersey totaled over 1.9 billion gallons among all sectors [21]. Figure 6 shows water use by sector in 2010. It can be observed that over half of freshwater use was for public supply, followed by thermo-electric power generation at 27%. Based solely on public water supply, it can be estimated that water use per person was about 123 gallons per day. Industrial freshwater draw only contributes to 4% of the total. The "other" category consists of water used for irrigation, livestock, domestic supply, and mining. In addition to on-site wells, Nestlé-Freehold draws water from the borough of Freehold in

Monmouth County. Upon further investigation, this county accounts for 2% of industrial freshwater use in New Jersey in 2010 [21]. It is expected that a portion of this is caused by instant coffee processing.

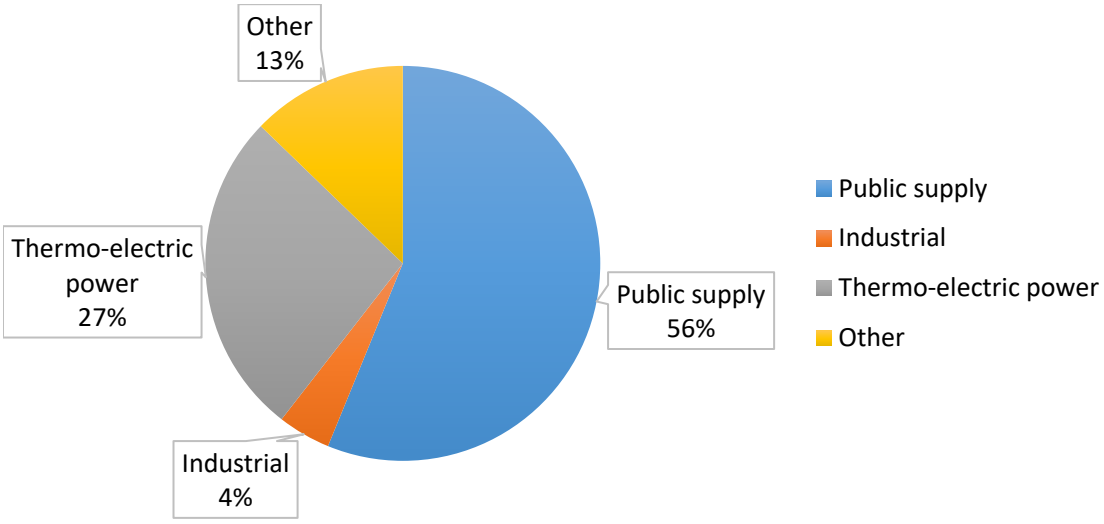

Figure 6. Freshwater use by sector in New Jersey in 2010 [21]

Chapter 3

Water Use in Coffee Manufacture

Green Coffee Processing

Water is used extensively throughout the entire coffee manufacturing process. A significant portion of water used to make coffee and coffee products is consumed before coffee beans even reach a processing plant. As is the case with worldwide freshwater use, most water needed for coffee production is consumed for the agriculture of the coffee plant. The virtual water content of coffee beans at different stages of processing, by country, was investigated in a recent study, both by wet processing and dry processing [22]. The virtual water content is defined as the overall amount of water required to produce the product. Both types of processing begin with harvesting the fresh "cherry" from the coffee plant. The wet processing method begins with a more in-depth cherry selection process in which cherries reside in a flotation tank [23]. Therefore, wet processing is generally considered to produce a higher quality coffee product. The stages included in wet processing include pulped cherry, wet parchment coffee, dry parchment coffee, hulled beans, green coffee, and roasted coffee. The stages included in dry processing include the dried cherry, hulled beans, green coffee, and roasted coffee [22]. The stages for both processing methods are shown in Figure 7.

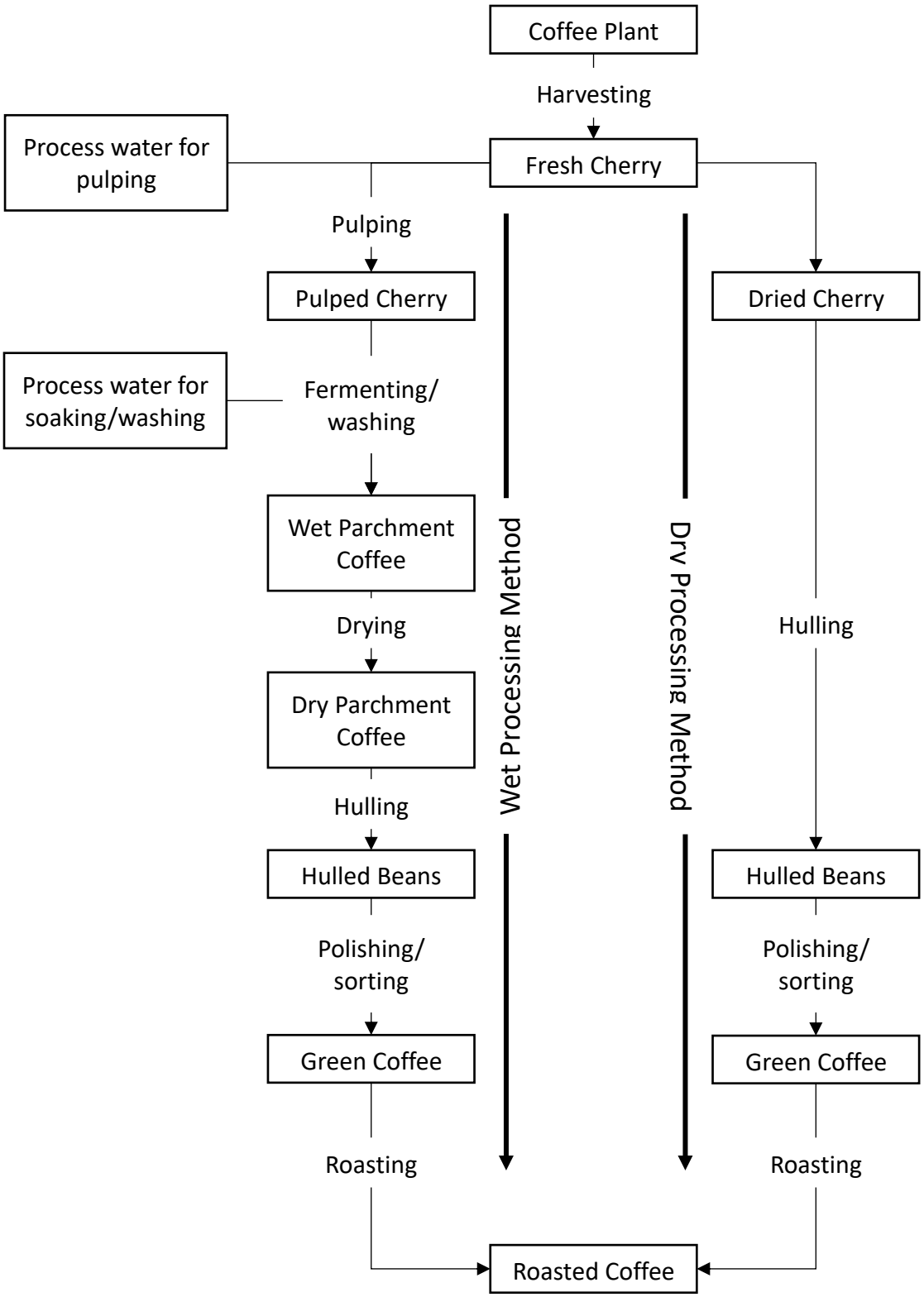

Figure 7. Flow chart of stages in both wet and dry processing methods for roasted coffee from the coffee plant; adapted from Chapagain and Hoekstra [22]

The water requirement associated with the fresh cherry is determined by the water requirement of the coffee plant and the amount of fresh cherries yielded. After the amount of water required for the fresh cherry is determined, the additional steps are calculated considering two factors. The first factor is whether the step requires additional processing water. This factor only needs to be considered for two steps in the wet processing method, shown in Figure 7. Water is needed to pulp the fresh cherry and to soak and wash the pulped cherry for fermentation to wet parchment coffee [22]. The second factor is a product fraction introduced in between in each step; it can be considered as the ratio of the amount of the resulting product to the original product [22]. For example, between the green coffee and roasted coffee stage, a 16% weight reduction of the green coffee is observed because of losses in moisture content [24]. Therefore, the product fraction between the green coffee and roasted coffee steps is 84%, or 0.84. The virtual water content of the original product is divided by the product fraction to determine the virtual water content of the resulting product [22]. Thus, each resulting product will have a higher virtual water content than the original product before it.

There are no current studies relating the water footprint of green coffee processing to consumption rates in the United States. The top countries that exported unroasted (green) coffee, by trade value in USD, in 2016 can be seen in Figure 8 [25]. The dominant region of coffee exports to the United States are from South America. These countries are shared to similar degrees for coffee imported by the Netherlands.

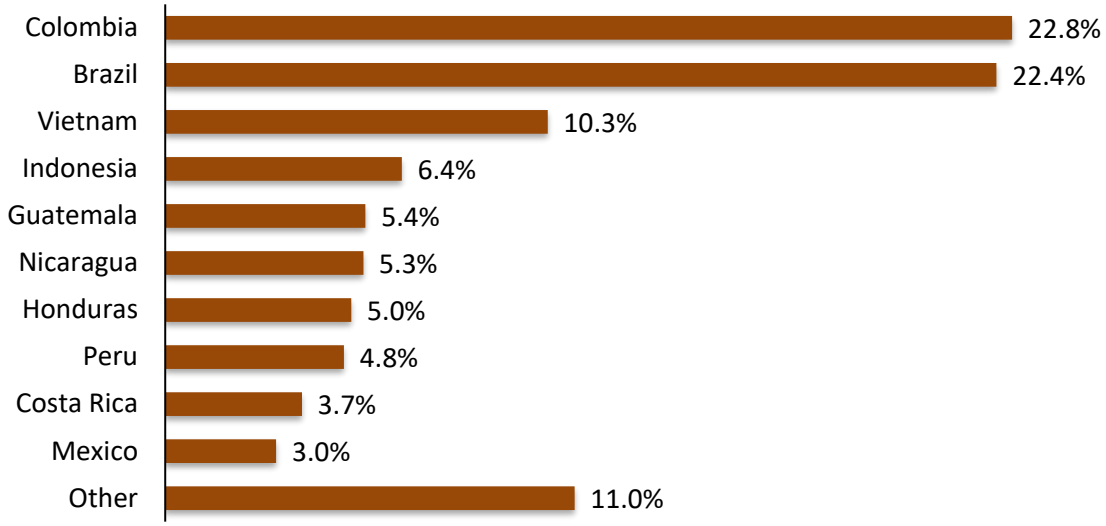

Figure 8. Top countries that exported unroasted (green) coffee to the United States in 2016 by trade value in USD [25]

The virtual water content of coffee in the United States can be estimated, assuming water use for transportation is consistent with that reported for the water footprint of coffee imports to the Netherlands [22]. Table 1 shows the breakdown of the virtual water content of green coffee in the United States.

Table 1

Virtual water content of green coffee from top countries that export to the United States

Country	Virtual Water Content (gal/ton) – Wet Processing [26]	Virtual Water Content (gal/ton) – Dry Processing [26]	Percent of Total Import
Colombia	2,909,000	2,895,000	22.8%
Brazil	4,535,000	4,521,000	22.4%
Vietnam	1,219,000	1,204,000	10.3%
Indonesia	6,387,000	6,372,000	6.4%
Guatemala	3,580,000	3,566,000	5.4%
Nicaragua	5,463,000	5,449,000	5.3%
Honduras	4,560,000	4,546,000	5.0%
Peru	3,915,000	3,900,000	4.8%
Costa Rica	2,019,000	2,004,000	3.7%
Mexico	5,835,000	5,820,000	3.0%
Other	4,225,000	4,210,000	11.0%
Weighted Average	3,823,000	3,808,000	

In order to determine the virtual water content of instant coffee powder, a scaling factor is applied to account for further product manufacturing processes. It was found that for every 1 lb of instant coffee powder produced, 2.3 lbs of green coffee are required [22]. Table 2 shows the virtual water content of the final, roasted coffee bean product by different preparations of one 4 fl oz cup of coffee. It can be seen that a standard cup of coffee requires 39 gallons water to make. The virtual water content of instant coffee powder per pound is much higher than that of typically brewed, ground coffee; however, less powdered coffee solids are required to make a cup of instant coffee than the amount of roasted, ground coffee needed to make a typically brewed cup. Therefore, the virtual water content per cup of instant coffee is less than that of a standard, strong, or weak cup of filter-coffee. The virtual water content is nearly identical between wet and dry processing methods. In dry processing, more weight is removed between production

steps than in wet processing, thus more water is needed to generate the same quantity of product.

Table 2

The virtual water content of one cup of coffee by different preparations [22]

Wet Processing			
	Virtual water content (gal/lb)	Amount of coffee product per cup (oz/cup)	Virtual water content per cup (gal/cup)
Standard cup*	1,911	0.247	29
Strong cup*	1,911	0.353	42
Weak cup*	1,911	0.176	21
Instant coffee	4,396	0.071	19
Dry Processing			
	Virtual water content (gal/lb)	Amount of coffee product per cup (oz/cup)	Virtual water content per cup (gal/cup)
Standard cup*	1,904	0.247	29
Strong cup*	1,904	0.353	42
Weak cup*	1,904	0.176	21
Instant coffee	4,380	0.071	19
* Brewed from roasted, ground coffee			

Water Use in Soluble Coffee Manufacture

The extensive water use in the manufacture of instant coffee is especially interesting because instant coffee powder finished products contain no water at all. Water consumption in instant coffee manufacture includes applications such as cooling, steam production, equipment operations, intermediate production steps, and cleaning and sterilization [27]. A general schematic of the production of instant coffee can be seen in Figure 9. Instant coffee powder production begins with green beans, as with all coffee products. The green beans are roasted and ground at the manufacturing plant. Roasting the beans develops flavor and aroma of the coffee product; grinding the roasted beans is

required so that soluble solids and volatile substances can be extracted during brewing to produce the extract that once dried, becomes instant coffee [27]. Water used in the extraction is heated to high temperature, around 175 °C, under pressure, to maintain the liquid phase [28]. The extraction process removes soluble and volatile flavor and aroma compounds from the ground, roasted beans. The most common type of equipment used in instant coffee manufacturing for extraction on an industrial scale is the percolation battery [27]. The percolation battery consists of a series of columns used to extract the soluble compounds from the coffee grounds continuously. Once a column is exhausted, it is isolated from the battery and the spent grounds are discharged. The column is then refilled with fresh coffee and replaced in the battery as a "fresh column" once the next column becomes exhausted [27]. An efficient extraction process yields a soluble-solids concentration of around 15 – 25 weight% [27].

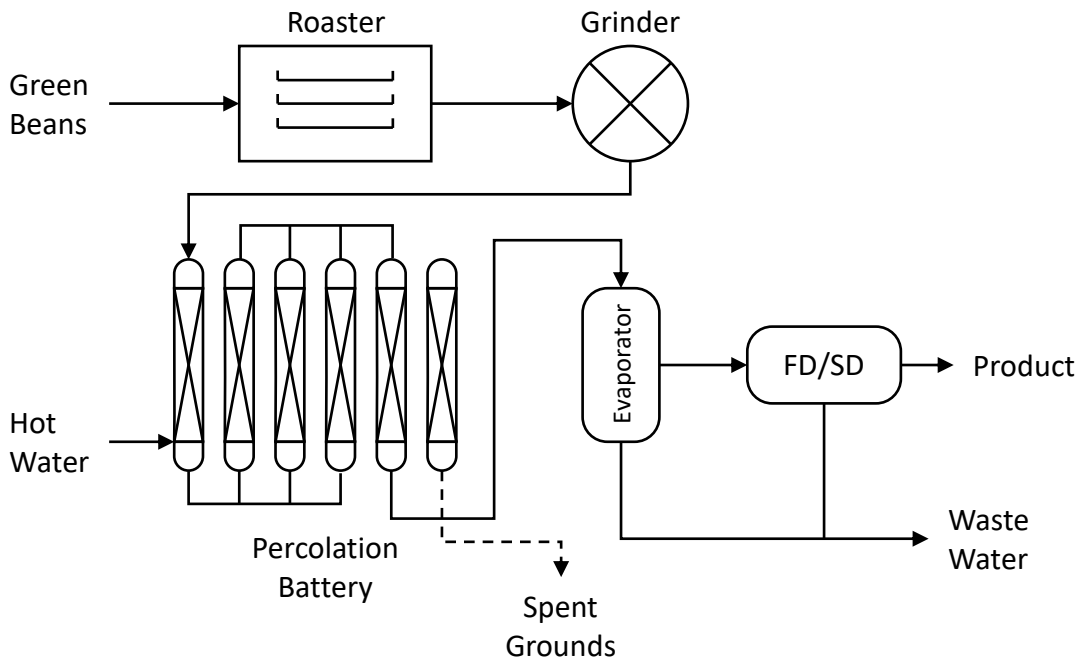

Figure 9. General schematic of the soluble coffee manufacture process; FD/SD: free-dry/spray-dry

Efficiency of percolation battery cycles is determined by two important factors: the cycle time and the weight of extract drawn off per cycle [27]. The cycle time is assessed by the difference in time between placing a fresh column on stream and the conclusion of drawing off extract from that column. Cycle time is crucial because it also determines other time dependent factors, including productivity. The amount of drawn extract and its soluble solids concentration determines the yield of the process [27]. The amount of water required for coffee extraction can vary depending on different factors, including, the original moisture content of the fresh grounds, the volume of the extraction vessel, and the flowrate and temperature the of water through the percolation battery [27]. A typical water to coffee ratio is 3:1 for such extraction processes [27]. Thus, the

extraction of soluble solids in 1,000 lbs of coffee, by percolation battery, requires 3,000 lbs of water.

The drained extract must then be dried to remove water from the product. Prior to drying, the coffee extract is typically concentrated by vacuum evaporation to around 40 – 60% solids by weight to reduce drying time and energy [29], [30]. Through pre-concentration, a fraction of volatile compounds is lost and must be reintroduced to produce the desirable flavor profiles of the product [27]. In order to remove nearly all water from the extract, which is required for the finished instant coffee product, one of two methods of drying must be used. The first is spray-drying, in which water is evaporated by a stream of hot dry air. The other method is freeze-drying, in which the extract is frozen and placed under very low pressure. A small amount of heat is gradually added to remove water in the frozen extract by sublimation [27]. Freeze-drying low temperatures help reduce deterioration of flavor/aroma and microbiological activity. It is widely considered that instant coffee products dried by this method are of higher quality [30]. Instant coffee product quality is determined by flavor/aroma and solubility. Given the extreme processing conditions, however, freeze-drying is the most expensive drying technique in dehydrated food and beverage product manufacture.

A mass balance around the starting point of the extraction process determines the total amount of water required for the manufacture of 1 lb of instant coffee powder, starting with roasted and ground beans. Figure 10 shows the flows described in the mass balance.

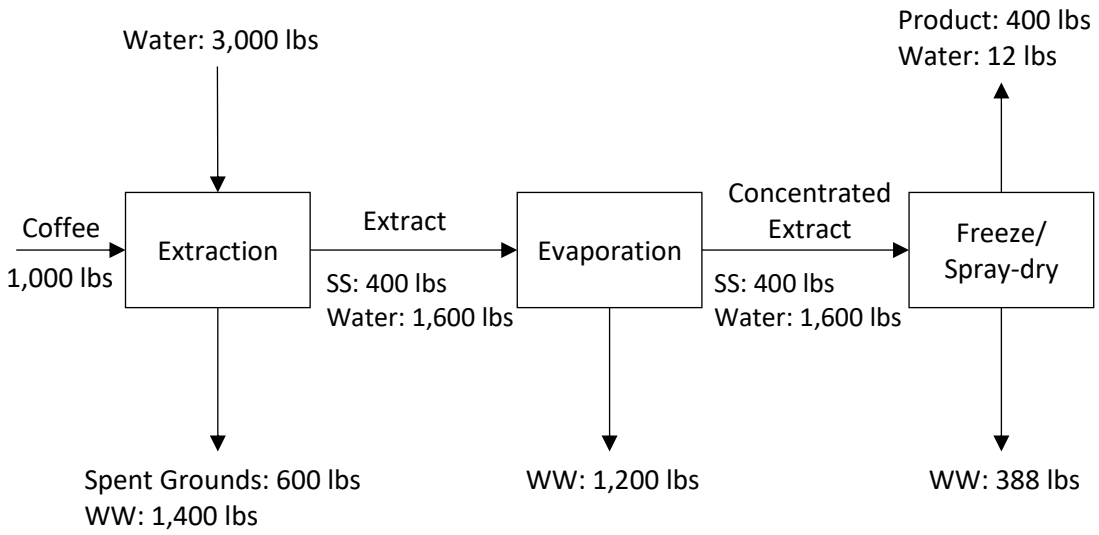

Figure 10. Flow diagram accompanying mass balances for instant coffee powder manufacturing starting from the extraction; SS: soluble solids, WW: wastewater

An example process for using 1,000 lbs of roasted and ground coffee is described. For efficient extraction, a water to coffee ratio of 3:1 is used (Equation 1).

$$3\frac{lb\ Water}{lb\ Coffee} \times 1{,}000\ lbs\ Coffee = 3{,}000\ lbs\ Water \quad (1)$$

In practice, a factor known as the draw-off factor is used as the ratio of the amount of extract drawn to the amount of roasted coffee in the percolation battery. A factor of 2 is suggested for use in mass balance calculations by Clarke and Macrae [27]. Therefore, 2,000 lbs of extract will be drawn from this process, while a total of 2,000 lbs of water and spent grounds are removed as waste. The coffee extract stream is typically between 15 – 25% soluble solids [27]. It will be assumed that the extract stream is 20% soluble solids. Thus, 400 lbs of soluble solids are estimated using Equation 2.

$$Soluble\ solids = 0.20 \times 2000lbs = 400\ lbs\ Soluble\ solids \quad (2)$$

The extract is then concentrated through evaporation to 40 – 60 % soluble solids by weight [29], [30]. It will be assumed that the extract is concentrated to 50% soluble solids, and any loss of soluble solids caused by evaporation is negligible (Equation 3).

$$Concentrated\ extract = \frac{400\ lbs\ Soluble\ solids}{0.50} = 800lbs\ total \quad (3)$$

The amount of water that is removed, or wastewater generated, in the evaporation process can be calculated in Equation 4.

$$WW_{evap} = 0.80\ (2000\ lbs) - 0.50\ (800\ lbs) = 1200\ lbs \quad (4)$$

Within the drying process, the coffee extract is dried to moisture contents between 2 – 5%, by weight [27]. It will be assumed that the moisture content of the final product is 3% by weight. It will also be assumed that the loss of soluble solids during drying is negligible. The total amount of instant coffee product (including final moisture content) can be calculated in Equation 5.

$$Product = 400\ lbs\ Soluble\ solids + 0.03\ (400\ lbs) Water = 412\ lbs \quad (5)$$

The amount of water removed, or wastewater generated, during drying can also be calculated, as in Equation 6.

$$WW_{dry} = 0.97(400lbs) = 388\ lbs \quad (6)$$

The total amount of water per instant coffee product is calculated in Equation 7.

$$\frac{Water}{Product} = \frac{3000\ lbs\ Water}{412\ lbs\ Product} = 7.3\frac{lbs\ Water}{lb\ Product} = 0.87\frac{gal\ Water}{lb\ Product} \quad (7)$$

In conclusion, the instant coffee manufacturing process is very water intensive, requiring about 7.3 lbs of water, or 0.87 gal of water, per pound of product. This number could even be larger when considering other processes at the plant, including, green bean cleaning, roasting, aroma recovery, packaging, and utilities. One study has shown that almost 4 gal of water per pound of product may be required when considering these processes [31]. Thus, a large amount of wastewater is generated throughout the process. Specifically, wastewater generation can be observed in three different stages of production. The first of which is during the extraction process. The amount of wastewater generated can be calculated in Equation 8.

$$WW_{extraction} = Water_{in} - Water_{extract} = 3000\ lbs - 0.80\ (2000\ lbs) = 1400\ lbs \quad (8)$$

Nearly half of the input water becomes wastewater during the extraction process. The extraction wastewater has a significant suspended solids concentration because of spent grounds in it. Wastewater pre-treatment is required for this stream before it can be discharged. This wastewater can also be characterized by high concentrations of chemical and biochemical oxygen demands, a dark brown color and mild acidity. Therefore, a significant amount of energy will be required to treat this wastewater, especially if production volumes are high.

Wastewater is then generated during evaporation and drying. Purification of this stream may be less energy intensive since there are no spent grounds, and thus a low solids loading. Recovery and reuse of the wastewater for utilities generation is a relatively simple consideration. Typical contaminants within this wastewater water are volatile flavor and aroma compounds from the coffee extract. Color will also be affected by these contaminants. While this wastewater may not be as difficult to treat as the extraction wastewater, there is still a significant volume of wastewater produced. The amount of wastewater produced is calculated in Equation 9.

$$WW_{evap+dry} = WW_{evap} + WW_{dry} = 1200\ lbs + 388\ lbs = 1588\ lbs \quad (9)$$

Therefore, the total amount of wastewater generated in instant coffee manufacturing is calculated in Equation 10.

$$WW_{total} = WW_{extraction} + WW_{eavp+dry} = 1400\ lbs + 1588\ lbs = 2988\ lbs \quad (10)$$

It can be seen that 99.6% of the water that enters the production process becomes wastewater. Therefore, 7.25 lbs of wastewater are generated for every pound of product.

The highly water intensive process presents problems as water is not a limitless resource and the demand for water use continues to rise [18]. Initial discussions with Nestlé have revealed that the design of their existing production facilities (which dates back to the 1940s [32]) did not include any techniques for water reuse, material recovery, or efficient energy management. At that time, and for many years after the original plant commissioning, water supply from the municipality and wastewater discharge were never

issues from a cost or environmental standpoint. This being a standard practice of food manufacturers at the time. Wastewater treatment costs have since risen and reflect a more water and environmentally conscious standpoint. Specifically, bulk wastewater discharge fees for the Nestlé Freehold plant have increased by nearly 6% over the last 10 years from a rate of $3,732/MMgal to $3,960/MMgal [33]. This project focuses on improving the operation through recommending retrofits for the existing plant. A thoroughly integrated plant operation plan that can minimize water use and provide the most energy efficient techniques for water recovery will be developed. As an integral part of the project, process intensification (water and waste reduction) methods/ approaches that can guide engineers in developing new facilities or renovating existing ones. The following sections explain various methods for the recovery of process wastewaters in the food industry and how they can be applied to wastewaters generated by the instant coffee industry.

Chapter 4

Methods to Recover and Reuse Water from Waste

The degree of treatment for any type of wastewater depends on its end use, whether it be for water recovery, for reuse, or simply for discharge [34]. For the case of water recovery, or reclaimed water, more advanced techniques for treatment are required if the water is to be used for human consumption products. If the reclaimed water is only to be used for processes where potential for human contact is not an issue, such as utilities generation, a wide range of conventional, secondary treatment methods is available [34]. Secondary treatment methods are defined as "any process designed to degrade the biological content of wastewater," whereas, advanced treatment methods are defined as "treatment processes designed to remove pollutants that are not adequately removed by conventional secondary treatment processes [35]." Figure 11 shows general schematic of a process implementing both secondary and advanced purification methods for the use of reclaimed water.

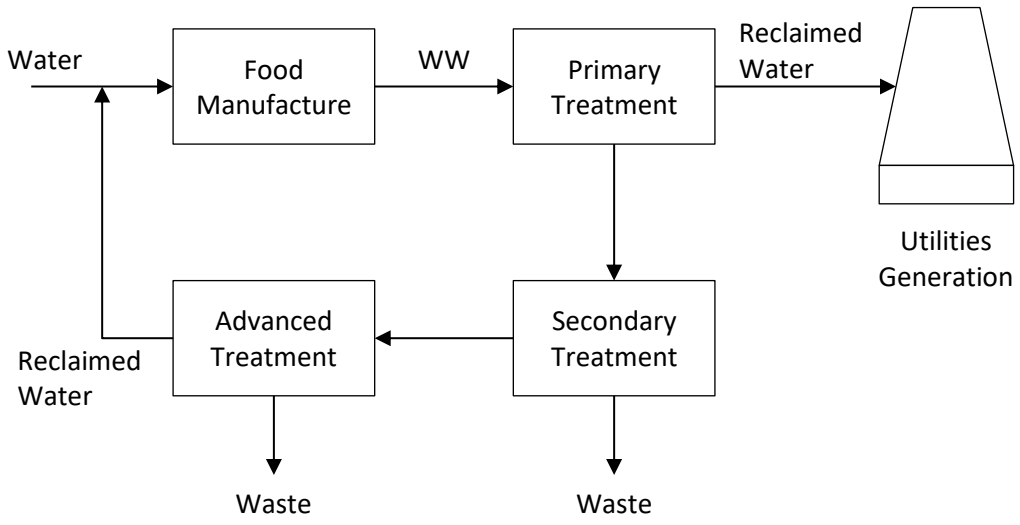

Figure 11. General schematic showing the processes needed to implement reclaimed water in different aspects of a food manufacturing operation; WW: wastewater

Instant coffee wastewater is mildly acidic and is characterized by high values of common wastewater contaminants, such as chemical oxygen demand (COD), biological oxygen demand (BOD), total suspended solids (TSS), and conductivity. Typical values of pH and each of these contaminants can be found in Table 3. In addition, typical values of pH and these contaminant concentrations for process wastewater samples obtained from Nestlé are given in Table 3. While the waste is not considered toxic, the contaminant levels are too high to be discharged to the environment and wastewater treatment is required.

Table 3

Typical ranges of values of coffee wastewater contaminants

Contaminant	Range	Current Data*
pH	4.5 – 5.9 [36], [37]	3.86 – 8.38
COD (ppm)	5,000 – 22,000 [36], [37]	1,000 – 3,000
BOD (ppm)	2,000 – 12,000 [36], [37]	<300
TSS (ppm)	1,400 – 2,000 [36]	30 – 300
Conductivity (µS/cm)	310 – 3,900 [37], [38]	900 – 6,500
* Values are lower than typical ranges since current wastewater samples obtained have undergone pretreatment processes		

As stated, many different techniques or separations have been applied to wastewater streams for treatment for various reuse applications. Some common and novel techniques have been applied to treat the high COD, BOD, and suspended solids level in coffee wastewater. Table 4 provides a summary of the various separation processes that have been considered and explored, comparing advantages and disadvantages.

Table 4

Summary table of potential processes for the purification of coffee wastewater

Separation Method	Advantages	Disadvantages
Adsorption	• Simple, well understood • Continuous operation • Published study w/ coffee wastewater	• Adsorbent regeneration can be costly/water intensive
Slow Sand Biofiltration	• Highly cost-effective • Simple design, low maintenance • Continuous operation	• Requires large footprint for high throughput systems • Biological layer can be disrupted with sudden changes in waste
Electrochemical Oxidation	• Can be cost-effective • Good removal of contaminants	• Batch operation • Difficult scale-up
Ozonation	• Simple lab-scale set-up • Good removal of organics	• Batch operation • Difficult scale-up
Membranes (General)	• Low-energy operation • Continuous operation	• Performance degradation due to fouling
Microfiltration	• Low operating pressures • Removes most suspended solids/particulates	• Does not remove small contaminants
Ultrafiltration	• Moderate operating pressure • Removes most solids and some smaller colloids	• Does not remove ions (conductivity) • Susceptible to fouling
Nanofiltration	• Removes smaller molecules • Can remove some ions	• Requires high pressure • Susceptible to fouling
Reverse Osmosis	• Removes contaminants down to the ionic level	• Requires high pressure • Highly susceptible to fouling

Adsorption

Adsorption is a well understood process used to separate contaminants from a stream by adherence to a material, known as an adsorbent [39]. Adsorbents are

characterized by the amount of surface area they provide, their material of manufacture, selectivity to specific solutes, their ability to be regenerated, and cost [40]. The selection of a proper adsorbent for a process will determine how effective the adsorption is. Commercial adsorption processes are typically carried out in a continuous column operation in which the adsorbent particles form a packed bed [39]. Adsorption is achieved when contaminant solute molecules or ions penetrate the pores of the adsorbent and adhere to the surface. Adsorption is a conventionally method used for the purification of industrial wastewater streams [34].

In a study by Devi et al., batch adsorption had been applied to a coffee processing wastewater stream to reduce organic pollutants [37]. Specifically, the goal was to reduce the amount of COD and BOD in the wastewater prior to discharge for irrigation and other horticultural uses. The batch adsorption process uses activated carbon generated from avocado peels, and the results are compared to a process that uses commercially available granular activated carbon, sourced from coal [37].

The raw coffee wastewater presented high COD and BOD concentrations of 22,000 mg/L and 12,000 mg/L respectively. The study monitored the effect of adsorption time and adsorbent dose in wastewater samples [37]. It was found that avocado peel activated carbon was able to perform similarly to the commercially available activated carbon. At the optimal conditions, samples treated with avocado peel activated carbon showed a reduction in COD concentration of 98.20% and BOD of 99.18%. The samples treated with commercially available activated carbon showed a reduction in COD concentration of 99.02% and BOD by 99.35% [37]. Thus, according to this one study,

adsorption appears to be effective for treating a coffee wastewater effluent with a high range of organic loading.

Coffee processing wastewater, whether in crop processing or instant coffee processing, is commonly characterized by a dark brown color given by tannins, melanoidins, and other organics [36], [41], [42]. Adsorption is known to effectively remove color in wastewater streams, especially the removal of color from textile industry wastewater [43], [44], [45]. Furthermore, one such study has shown the capability of adsorption to lower COD and BOD concentration in textile wastewater, as well [45]. Thus, a parallel can be drawn between color removal in coffee wastewater and textile wastewater. Among such studies, both batch adsorption and continuous adsorption in a fluidized bed were evaluated (results shown in Table 5) [44], [45].

Table 5

Adsorption results in textile wastewater treatment for a batch and continuous study [44], [45]

Batch Study [45]			
	Initial concentration	Final concentration	Percent removal
COD	1625.8 ppm	0 ppm	100%
BOD	1002.4 ppm	11.2 ppm	99%
Color	350.2 Hazen	0 Hazen	100%
Continuous Fluidized Bed Study [44]			
	Initial concentration	Final concentration	Percent removal
COD	525.32 ppm	125.77 ppm*	76%
BOD	210.6 ppm	18.67 ppm*	91%
Color	520 Hazen	385.67 Hazen*	26%
* Average among three different adsorbent sizes analyzed			

In batch studies, COD, BOD, and color removal were maximized at nearly 100%, 99%, and 100%, respectively [45]. In the continuous fluidized bed configuration, COD, BOD, and color removal were achieved at 76%, 91%, and 26%, respectively [45]. While color removal was noticeably lower in the continuous method, it was recommended that a higher load of activated carbon be used to increase the surface area available for mass transfer within the fluidized bed.

Preliminary research has been conducted for the use of nanoparticle adsorption to purify the coffee wastewater. Nanoparticles, specifically nanoadsorbents, offer a key advantage over bulk adsorbents, such as activated carbon. They are able to be chemically synthesized with additional functional groups to improve their affinity for specific contaminants in wastewaters [46]. Nanoadsorbents have been used for water purification in various industrial wastewaters, such as those of the food and textiles [47], [48], [49].

In conclusion, it appears that adsorption has potential in instant coffee wastewater purification for reuse in various applications.

Slow Sand Biofiltration

Another traditional and widely used wastewater treatment technique that has been considered for water recovery from coffee wastewater is slow sand biofiltration [50]. This technology was chosen for review because of its simplicity, scalability, and applicability in industrial wastewater treatment. Slow sand biofiltration has been employed for many years and is capable of removing organic and inorganic particulates and microbial contaminants from wastewater streams [50]. In a slow sand biofiltration unit, water flows through a bed of sand particles. Over time, a biologically active layer is generated at the top of the sand bed called the schmutzdecke [51]. A variety of different

microorganisms can be present in the schmutzdecke, including, algae, plankton, diatoms, protozoa, rotifers, and bacteria [52]. Dissolved oxygen in the influent wastewater stream is crucial for growth and maintaining the schmutzdecke. The purity of reclaimed water from a slow sand biofiltration unit will not be high until the schmutzdecke layer is completely formed [51]. Within the schmutzdecke, organic materials are broken down and a majority of suspended solids in the influent wastewater stream are removed. Any remaining solids are removed while the wastewater stream passes through the rest of the sand bed [52]. To enhance the performance of a slow sand biofiltration bed for industrial wastewater streams with a high organic load, granular activated carbon can be added to the sand to remove organic compounds by adsorption [51].

Slow sand biofiltration systems can be categorized by the driving force pushing water through the bed. The two categories are pressure filters and gravity filters [52]. Pressure filters are typically better suited for industrial applications and consist of a closed vessel. The influent is pushed through from the top of the bed by a pump. Gravity filters are more commonly used for purification of drinking water in developing countries. They have an open top and are commonly constructed as concrete boxes. The influent is fed at the top of the system and moves through the sand bed by gravity [52]. Both types of filters consist of the same components in the sand bed, shown in Figure 12. Above the schmutzdecke is a supernatant layer of water that is held to a specified height. Below the sand bed is a layer of gravel to support the weight of the sand bed. Over time, debris is captured in the sand bed, causing clogging and an increased pressure drop. Backwashing the system is necessary to remove the debris and return to normal

operation; however, this disrupts the schmutzdecke and it will need sufficient time to be regenerated.

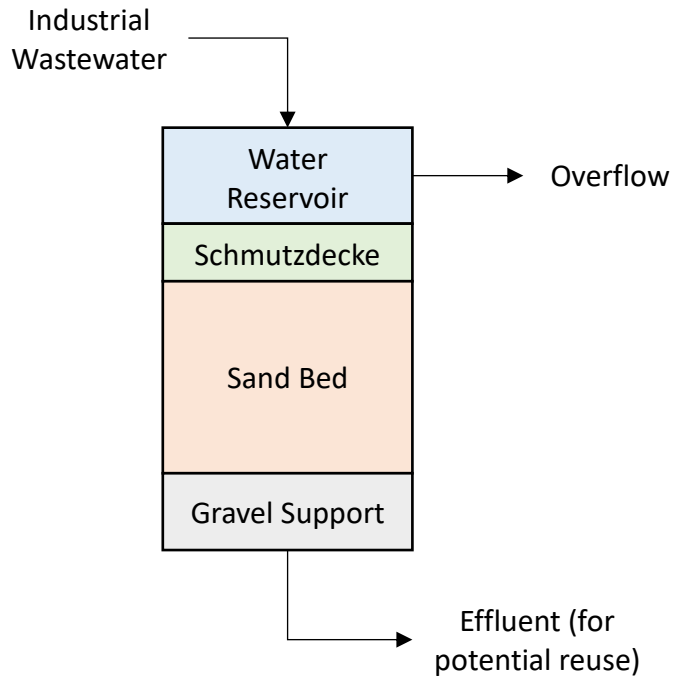

Figure 12. Simplified diagram depicting the layers of a slow sand biofiltration system

Slow sand biofiltration has been applied for water recovery from different food manufacturing wastewaters characterized by high COD, BOD, and TSS concentrations among various studies [53], [54], [55], [56]. These studies can be applied to draw parallels to coffee wastewater, since there is a lack of current studies of slow sand biofiltration implemented for such wastewater. Table 6 summarizes the results of the various food manufacturing wastewater streams. It can be seen that slow sand biofiltration systems are effective in reclaiming water with reduced organic loads in food manufacturing wastewater streams. The studies show a wide range of contaminant

concentrations of COD, BOD, and TSS in the wastewater stream. In each study, slow sand biofiltration provided acceptable or even excellent removal of such contaminants in effluents to be implemented as reclaimed water. The application to various ranges of contaminants can be applied to recovery of water from food wastewater and, more specifically, coffee processing wastewater since it shares this characteristic.

Table 6

Summary table of results of slow sand biofiltration applied to various food manufacturing waste and wastewaters

Potato Farm Wastewater [53]		
	Initial Concentration (mg/L)	Percent Reduction in Final Concentration
COD	-	-
BOD	360	93%
TSS	260	85%
Turkey Processing Wastewater [54]		
COD	-	-
BOD	530	>99%
TSS	-	-
Swine Manure [55]		
COD	1,000 – 16,600	84% *
BOD	400 – 8,600	87% *
TSS	1,000 – 17,500	98% *
Olive Oil Extraction Wastewater [56]		
COD	148,000	65%
BOD	-	-
TSS	-	-
* Average percent reduction among samples		

Slow sand biofiltration has distinct benefits and drawbacks as a water recovery process. The following are listed benefits for this process [52]:

1. The simple design and construction results in a low cost and construction time and ease of operation.

2. Essentially the only maintenance of the system is cleaning the filter bed.
3. Regular flushing for removal of wash water is not required.

The drawbacks of this process are listed, as well [52]:

1. A large amount of area is required for high throughput systems. For example, a plant that processes 50 million m^3 of water annually requires 20,000 m^2 just for the slow sand biofiltration. This does not include any potential pretreatment processes.
2. Precautions for freezing may be required in colder climates (e.g. winter months).
3. The biological layer can be disrupted in systems where the influent wastewater is susceptible to sudden changes in composition.

Electrochemical Oxidation

A more novel technique that has been studied for water recovery in food and coffee applications has also been considered. Electrochemical oxidation is considered an advanced oxidation process which can offer high contaminant removal in industrial wastewaters [57]. The process is achieved by the reactions between electrical energy and chemical change to remove impurities from a liquid product. An amount of wastewater is added to a reactor and electrical energy is added by a pair of electrodes, an anode and cathode, or a set of electrode pairs. The efficacy of electrochemical oxidation can be determined on the basis of a variety of conditions. One such important factor is the selection of material for the electrodes. The efficiency of a process and the final concentration of the treated wastewater are highly dependent on the characteristics of the anode material [57].

The length of time for electrolysis is a key factor for contaminant removal. Longer times result in better removal of contaminants. High conductivities of the wastewater to be treated are required for efficient processing. Typically, wastewater effluents do not possess an adequate conductivity to be effective. To overcome this, electrolyte solutions must be added to such wastewaters. Thus, the amount, type, and concentration of electrolyte solution are an important factor in electrochemical oxidation [57]. The type of electrolyte solution added to a wastewater effluent will result in a change of pH in the treated wastewater. Varying the applied voltage shows a directly proportional effect on the removal efficiency of various contaminants [57]. This is expected as an increase in electrical energy will produce a higher rate of oxidation in the reactor.

Electrochemical oxidation has been applied in various food processing wastewaters for water reuse, including instant coffee [38], [57], [58]. A study by Cárdenas, et al. on the treatment of instant coffee wastewater by electrochemical oxidation evaluated efficacy based on COD and color removal. The wastewater was pretreated by coagulation-flocculation processes to remove suspended solids. Results of the study can be seen in Table 7. Percent removals are expressed after 120 minutes of electrolysis.

Table 7

Results of purifying instant coffee wastewater by electrochemical oxidation [38]

		Percent removal by electrolyte addition	
	Initial conditions *	0.1 M NaCl	0.01 M HCl
COD (mg/L)	2,600	86%	35%
Color (m^{-1})	39.1	99%	99%
* Initial conditions for electrochemical oxidation are the conditions after coagulation-flocculation processes			

Electrochemical oxidation of the instant coffee wastewater shows a significant reduction in color at a removal of 99% for each electrolyte addition. There is a noticeable difference in performance of COD removal depending on the electrolyte addition. COD removal was 51% higher when 0.1 M NaCl was used as the electrolyte. It was expected that this difference was based on the concentration of the electrolyte addition and the active chlorine ion it provides [38].

Electrochemical oxidation has also been evaluated for water reclamation from sugar beet wastewater. This wastewater has similar characteristics to that of coffee wastewater such as high BOD (4,000 – 7,000 mg/L) and COD (10,000 mg/L). Güven et al. have provided a study for lowering the COD (initial concentration: 6,300 mg/L) from simulated beet sugar wastewater [57]. Tests were conducted for 8 hr of electrolysis. The highest reported COD reduction was 86.4%. This result was achieved after 4 hr of run time at the full wastewater concentration and with the highest tested electrolyte concentration (50 g/L NaCl) and highest applied voltage (12 V).

Based on the existing published results, electrochemical oxidation shows potential for the recovery of water in the instant coffee industry. As a water recovery process, it is non-specific and could be applied to a variety of wastewaters [57]. It should be noted

that suspended solids have not been discussed and pretreatment measures may be required. Electrochemical oxidation may present an economical alternative to other wastewater treatment processes, as high temperatures are not required.

Ozonation

Ozonation is a chemical process capable of purifying industrial wastewater with the goal of water recovery and reuse. This recovery process is able to remove both organic and inorganic compounds from wastewater via oxidation by ozone (O_3) [59]. The weakest bond in the ozone molecule will readily break in a solution (e.g. wastewater) to stabilize itself. In the presence of impurities, the third oxygen atom will bond to such compounds, causing the impurities to change structure and become inactive or fall apart and become destroyed. The chemical structure of the compound being oxidized will determine the by-products of the reaction. Often, the by-products are biodegradable, making ozonation an appealing and green wastewater purification process [60].

Ozonation studies and experimentation require an understanding of the principles by which the process operates. Ozone is highly corrosive; therefore, the experimental system must be constructed of corrosions resistant materials (stainless steel, glass, etc.) [59]. More cost-effective materials such as PVC may be used, however, they may need replacement more frequently. Ozone must be generated per experiment or purification process since the molecule is so unstable. There are two methods for practical generation of ozone in bench and full-scale applications: electrical discharge and electrolysis [59]. Electrical discharge units are most commonly found for lab-scale experiments, and the studies that have been reviewed for this project have uses this method. Electrical discharge uses air or pure oxygen as the source for ozone production. Ozone is generated

from the energy from electrons in an electric field between electrodes [59]. The oxygen in air or the pure oxygen is ionized, generating ions and radicals.

The efficacy of an ozonation experiment or process is dependent on a variety of factors. The first of which is the type and flowrate of feed gas; or, the source for ozone production. Ozone can be produced from pure oxygen or air. Higher feed gas flowrates generate more ozone; however, the concentration of ozone will not increase linearly since there will be more oxygen or air present. As expected, systems that use pure oxygen can generate higher concentrations of ozone than those using air for the same feed gas flowrate. Pure oxygen is more common in industrial applications [59]. Air provides less oxygen for ozone generation; however, it can be cost-effective and viable in systems that do not require high amounts of ozone. The amount of ozone that is produced is also dependent on amount of applied voltage to the feed gas, such that, higher amounts of power result in greater production [59].

There are no current studies for the use of ozonation in coffee wastewater purification; however, current studies have used ozonation for the purification of other industrial wastewaters with similar characteristics. Such industries include food [61], [62], textiles [63], and dyes [64]. Each of these wastewaters can be characterized with moderate to high concentrations of contaminants, namely, COD and color. Studies conducted for these wastewaters analyzed the efficacy of removal of COD and color by ozonation. Among these studies, ozonation was used both independently as a purification method and/or was sequenced with additional processes. For the purposes of this discussion, results pertaining to contaminant removal via ozonation solely will be considered. A summary table of contaminant removal can be seen in Table 8.

Table 8

COD and color removal achieved by ozonation (note experimental conditions were different for each study)

Industrial Wastewater Source	Initial COD (mg/L)	Max COD Removal	Max Color Removal
Food (olive mill) [61]	3,000	93%	-
Food (molasses) [62]	885	45%	87%
Textiles* [63]	464 / 1,154	96% / 88%	99% / 99%
Dye (actual waste) [64]	5,000	30%	43%
* A low and a high concentration wastewater sample were studied (low/high)			

As can be seen, ozonation applications to industrial wastewater effluents can provide moderate to excellent COD and color removal. COD removal varies significantly among wastewater types. Upon further investigation, it can be observed that the pH values of the streams are different. The wastewaters with higher removals (olive oil mill and textiles) had pH values that were more basic (12 and 9.5, respectively) [61], [63]. Those with lower COD removal (molasses and dye) had lower pH values (7.9 and 8.6, respectively) [62], [64]. The ozonation study on dye wastewater was conducted on three different COD concentrations and multiple pH values ranging from 3 – 11. The results presented in Table 8 reflect the highest concentration tested. At a COD concentration 2,000 mg/L COD removal increased to about 75% [64]. When studying the effect of pH, COD removal was at its greatest at 11 (~80%) and its lowest at 3 (~28%). Thus, it can be expected that better removal of COD will be observed with higher pH values. Since coffee wastewater is mildly acidic, one approach would be to investigate efficiency at various pH values by adding buffers.

Membrane Separations

Membrane separations have a significant role in food and beverage industry in the pretreatment of water to be used at the plant and for treatment of generated wastewater for recovery of water [65]. Membrane separation processes can be applied to treat food and beverage wastewater streams through removal of dissolved species according to molecular size to recover water for reuse. Membranes provide an attractive separation process because the low operating costs and energy requirements, the high product quality and yields, and the minimal amounts of chemical additives [66]. In addition, membrane systems do not require high temperatures for operation, allowing temperature sensitive materials to be processed with this type of separation. The membrane is a semi-permeable material that acts as a barrier to allow substances of specific size to permeate it. Substances that are unable to permeate the membrane remain in a concentrated retentate stream. A simple schematic of a membrane separation process is shown in Figure 13.

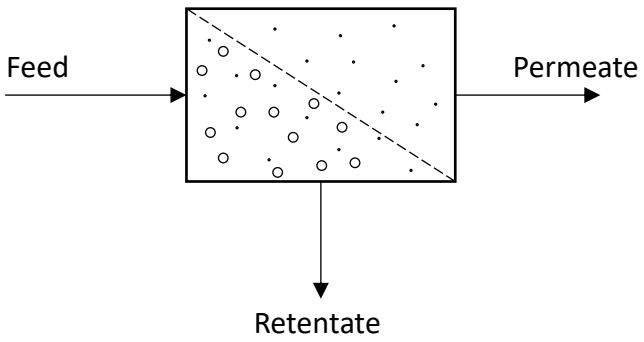

Figure 13. Simplified membrane schematic illustrating the location of specified streams

The most common types of membrane separation process applied in the food and beverage industry are pressure-driven. Pressure is applied on the feed side of the membrane and a pressure drop is observed across the membrane, known as the transmembrane pressure [67]. The transmembrane pressure is determined using Equation 11.

$$TMP = \Delta P = \frac{P_F + P_R}{2} - P_P \quad (11)$$

The transmembrane pressure is a function of the pressure of the feed, P_F, retentate, P_R, and permeate, P_P. It is the average pressure between the feed and the retentate minus the pressure of the permeate.

Transmembrane pressure varies by the type of membrane separation that is being implemented [67]. There are four main types of pressure-driven membrane systems: microfiltration, ultrafiltration, nanofiltration, and reverse osmosis. Table 9 shows different types of membrane systems and their respective range of pore sizes and operating transmembrane pressures [67], [68]. Transmembrane pressures and pore sizes are typically within these ranges. The specific ranges of transmembrane pressure are also dependent on the properties of the materials of which a membrane is manufactured. Pressure-driven membrane systems are useful for treating high-strength food and beverage wastewaters or for secondary and advanced treatment of conventionally treated industrial wastewater for reuse or recovery of valuable compounds [6].

Table 9

Typical pore size and transmembrane pressure for each type of membrane system

Membrane System	Pore Size (µm) [68]	Molecular Weight Cut-off [69]	Transmembrane Pressure (psi) [67]
Microfiltration	> 0.1	> 100	< 44
Ultrafiltration	0.003 – 0.1	20 – 150	44 – 103
Nanofiltration	0.001 – 0.005 [70]	2 – 20	147 – 441
Reverse Osmosis	< 0.001	< 2	147 – 1,100

The amount of throughput per membrane area, or flux, is an important factor for consideration when implementing a membrane system. The flux through a membrane is a function of operating transmembrane pressure, ΔP, the thickness of the membrane, L_m, and the permeability, $\mathcal{P}_m$, of a solvent through a membrane. Flux can be calculated according to Equation 12.

$$J_w = \frac{\mathcal{P}_m}{L_m}\Delta P = A_w \Delta P \tag{12}$$

The permeability of a solvent through the membrane is a lumped parameter of the product of the solubility and diffusivity of a solvent. The permeability of a solvent divided by the thickness of the membrane is often combined to one term, A_w, known as the solvent permeability constant. The solvent permeability constant is expressed as the mass of solvent over the quantity of time, area, and pressure (e.g. [kg solvent/(s·m^2·atm)]). Typically, flux increases as pore size increases. Flux can be greatly affected by pore size of a membrane as smaller pore sizes reduce the amount of substances that can permeate a membrane. Therefore, different membrane systems are

application dependent based on the contaminant to be removed; this is consistent in the food and beverage manufacturing industry.

Microfiltration is a membrane system used to separate particulates from a liquid stream [71]. Microfiltration is often used a first step in membrane separation processes to reduce the volume through steps that may require higher operating pressure or are more energy intensive. This type of membrane system has been used extensively in the food and beverage industry. One common application is the use of microfiltration in food wastewater treatment to reduce contaminant loads before further purification methods are applied or to recover valuable substances [66]. Among common food applications, microfiltration is used in the pretreatment of margarine manufacturing wastewater. The effluent from margarine production can cause problems in further treatment such as high costs for sludge disposal, coating in treatment plants, and saponification of fats in equalization tanks [66]. Thus, applying microfiltration before treatment can reduce the chemical oxygen of margarine wastewater from between 5,000 – 10,000 mg/L to under 250 mg/L. Microfiltration can also be used in processing steps for specific products. For instance, microfiltration is commonplace in the dairy industry for bacteria removal, fat removal from whey, and enrichment of milk for cheese manufacturing [72].

Ultrafiltration is similar to microfiltration that is used to concentrate particulates in process streams, however, such systems are characterized by a smaller typical pore size. Pore sizes in ultrafiltration membranes are orders of magnitude smaller than those of microfiltration membranes [71]. The separation achieved in ultrafiltration can be done based on the pore size of the membrane or through interactions between the membrane and molecules in the system. For instance, the separation can occur caused by charges on

molecules or their affinity for the membrane material [67]. Ultrafiltration is commonly found in processing steps in the dairy industry for the concentration of whey proteins and manufacture of some cheeses [72]. Ultrafiltration can also be used for the recovery of lactose and whey proteins in dairy wastewater effluents [73]. Recovery of lactose in the permeate can be achieved up to 100% while the concentrate is rich in protein at up to 95% [73]. The remaining water from these processes can then be further treated for possible reuse applications.

Nanofiltration systems are characterized by an even smaller pore size than ultrafiltration systems. Nanofiltration is typically used to remove substances in the molecular size range, including, sugars, pesticides and herbicides, dye, and aqueous salts, to an extent [68]. Separations achieved by nanofiltration can be affected by the charge and the size of the particle [70]. Particles can be separated based on charge because the fixed charge on nanofiltration membranes generated by the dissociation of membrane surface groups [70]. Nanofiltration membrane systems can be applied in a variety of ways within the food industry. Such applications include the beverage, dairy, and sugar industries [74]. Within the beverage industry, a simulated nanofiltration process design was studied as a replacement for traditional evaporation for the production of a juice concentrate [75]. It was found that the membrane process reduced production costs by over 40%, indicating the potential not only for cost reduction, but possible reduction of energy and recovery of water [75]. Nanofiltration membranes have also been applied to treatment of returned process water in the sugar industry. A recent study has investigated the effects of various operating parameters on a nanofiltration process for sugar beet press water [76]. Treating the press water before it is returned to the diffuser improves

efficiency because of the decreased final purification of impurities reintroduced by the press water. High rejection of sucrose (>95%), sodium (>73%), and potassium (>65%) was reported in each trial, indicating less removal of impurities required in purification steps [76].

Reverse osmosis membranes require the highest operating transmembrane pressure among all types of pressure driven membranes. In addition, reverse osmosis membranes have the smallest nominal pore size, and are essentially non-porous [70]. Reverse osmosis systems allow liquid (solvent) to pass and retain most solutes, including ions [70]. High pressures are required in these systems to overcome the osmotic pressure of a solution. The osmotic pressure of a solution is the threshold pressure which must be overcome for reverse osmosis to occur [39]. The higher the concentration of ion producing solute (salts) in the solution, the greater the osmotic pressure will be. The osmotic pressure, π, can be calculated as in Equation 13; where n is the amount of solute, V_m is the volume of pure water associated with n solute, R is the gas constant, and T is the temperature. The amount of solute per volume pure water can be expressed as the concentration, c_i.

$$\pi = \frac{n}{V_m} RT = c_i RT \tag{13}$$

In microfiltration, ultrafiltration, and most nanofiltration systems, ions freely pass through the membrane and osmotic pressure can be considered negligible. Therefore, to calculate the flux in a reverse osmosis system, the osmotic pressure term must be considered; the equation for flux becomes Equation 14.

$$J_w = \frac{\mathcal{P}_m}{L_m}(\Delta P - \Delta\pi) = A_w(\Delta P - \Delta\pi) \quad (14)$$

The change in osmotic pressure reflects the difference in solute concentration between the feed and permeate. It is often calculated using a concentration gradient across the membrane as in Equation 15; where c_F is the concentration of solute in the feed and c_P is the concentration of solute in the permeate.

$$\Delta\pi = RT(c_F - c_P) \quad (15)$$

The most popular application of reverse osmosis membranes is desalination of seawater and brackish water for potable water use [77]. The osmotic pressure required to overcome in the desalination of seawater is about 370 psi [39]. In wastewater treatment, reverse osmosis is typically implemented as a final processing step for water for reuse and recovery of valuable substances in a wastewater stream [77].

Reverse osmosis systems are used for water reuse from wastewater in various food industry applications. As with other membrane systems, reverse osmosis membranes are commonly found in the dairy industry, specifically within wastewater treatment for water recovery. One study has shown the efficacy of reverse osmosis for the purification of wastewater for reusable water in the dairy industry [78]. Recovery of potable water from the wastewater was achieved between 90 – 95% for reuse [78]. Reverse osmosis has also been studied for the treatment of wastewaters from olive mills. Olive mill wastewater is characterized with substantial concentrations of COD (~40 g/L) and high conductivity (~5.3 mS/cm) [79]. Samples were pretreated with centrifugation and ultrafiltration. After pretreatment, COD concentration was around 17.7 g/L and

conductivity was unaffected at around 5.2 mS/cm. When processed with reverse osmosis at 25 bar, COD concentration was reduced by 96% and conductivity was reduced by over 93% for both reverse osmosis membranes tested [79].

It can be seen that larger pore size membranes (microfiltration and ultrafiltration) typically are used as pretreatment processes for water recovery. In addition, they are often used directly in process steps. In order to recover potable water for reuse smaller pore size membranes (nanofiltration and reverse osmosis) are needed. An efficient process for water recovery by membrane systems could incorporate smaller pore size membranes for pretreatment and recovery of valuable substances before the wastewater is further purified by smaller pore size membranes. Thus, waste and wastewater generation can be minimized, and more water can be recovered for reuse in both utilities generation and process steps. While literature on membrane processes used in coffee manufacturing is limited, this technology has been proposed for an alternative to evaporation in soluble coffee manufacture [80]. Membrane process may not be typically found in coffee manufacturing or wastewater purification because of potential foulants in the processing streams.

Dynamic Vibratory Membrane Filtration

Membrane performance is faced with a common issue among all types of membrane systems. Fouling in membrane systems can be caused by different types of contaminants that affect how much a system can process by reducing the effective permeability of a membrane. Some main types of contaminants include particulates, organics, and dissolved salts [81]. Minimization of surface fouling can be achieved by increasing the shear rate at the membrane surface. In cross-flow filtration systems, high

shear conditions are generated at the interface between the liquid and membrane surface by a high liquid velocity [82]. Contaminants causing fouling can also be removed from the membrane surface by cleaning. Reversible fouling is often caused by suspended solids in a process stream. The second type of fouling is irreversible fouling, which occurs within the pores of a membrane [81]. The fouling cannot be relieved by physical cleaning. Chemical cleaning methods are required to restore a membrane to its original permeability if it is irreversibly fouled. As mentioned prior, dissolved organic material can adsorb to the inside of the pores of a membrane, causing it to plug and be irreversibly fouled. Both types of fouling can be observed in Figure 14. As can be seen, the largest particles can group together and cause surface fouling (reversible), forming a layer over pores. This blocks the smallest particles to be able to leave in the permeate stream. Some particles enter the pores and adhere to the walls, causing irreversible fouling.

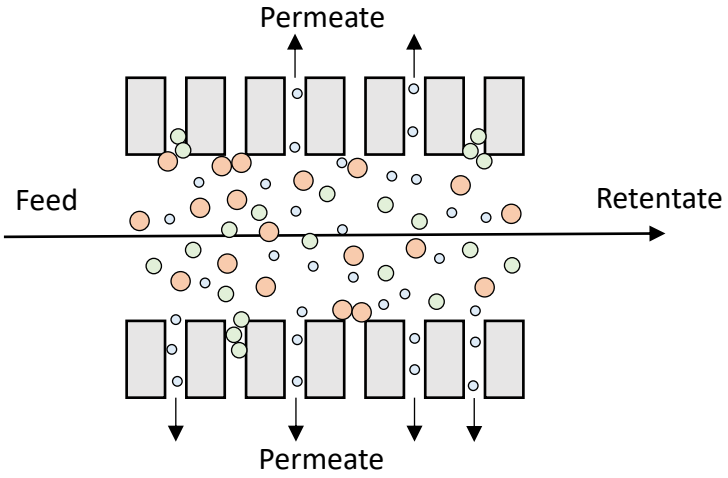

Figure 14. Diagram of cross-flow filtration membrane system showing both reversible and irreversible fouling

Efforts have been made to reduce the amount of fouling in membrane systems. As mentioned, surface fouling is reversible and can even be managed while operating by generating high shear regions at the membrane surface. Not all surface fouling, however, can be completely eliminated by such means due to limitations in the amount of shear that can typically be produced by cross-flow alone. In addition, in order to generate high shear regions by high velocities, a higher amount of energy is required. Alternative methods have been investigated to incorporate higher shear at the liquid-membrane interface without requiring a substantial amount of energy. Vibratory membranes have been studied in a variety of applications for high shear enhanced membrane separations. Vibration at the membrane wall generates high shear regions without the requirement of high liquid velocities in the system.

One such vibratory system has been developed by New Logic Research, Inc., called "Vibratory Shear Enhanced Processing," or V-SEP. Figure 15 displays a comparison between the surface phenomena in a conventional cross-flow membrane system and that achieved by a vibrating membrane system [83]. As can be seen, high shear generated by vibrating the membrane surface reduces almost all surface fouling in the membrane system. In conventional cross-flow systems, the highest velocities are towards the center of flow in low viscosity fluids. High shear rates are therefore found near the center and drop near the wall. Thus, it is not economical to attempt to generate high shear rates simply by high fluid velocity. Vibration allows for an economical method to generate high shear rates at the membrane surface that can be an order of magnitude higher than can be achieved by high fluid velocities [83].

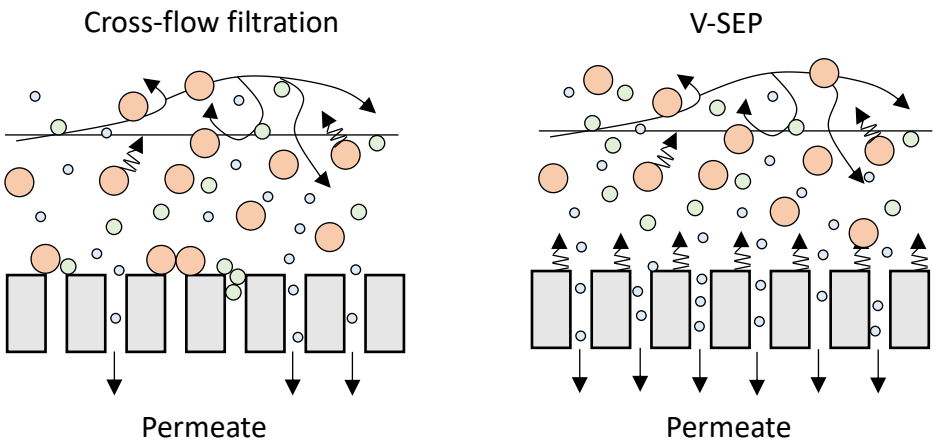

Figure 15. Comparison between cross-flow filtration and vibratory membrane separation systems; adapted from New Logic Research, Inc. [83]

Shear rate at the membrane surface for a V-SEP system can be calculated according to the operating parameters of the system, as shown by Akoum, et al [84]. The maximum shear rate was derived using SI units which are shown for each term throughout the derivation when appropriate. Flow induced by torsional oscillations of two parallel disks was first described by Rosenblat [85] for Newtonian fluids in the geometry given in Figure 16. The transverse velocity, V [m/s], is determined as in Equation 16.

$$V = r\Omega e^{2\pi iFt} \tag{16}$$

It can be seen that the transverse velocity is a function of the radius, r [m], frequency, F [Hz], and the amplitude of angular velocity, Ω [rad/s] at the boundary conditions $z = 0, h$. Where h [m] is the vertical distance about the axis of symmetry between the two disks.

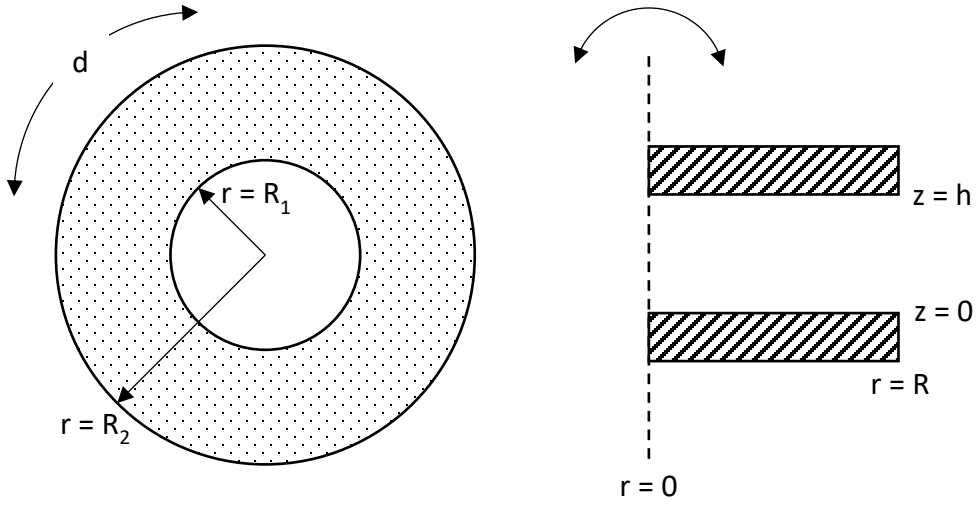

Figure 16. Geometry of parallel plates oscillating torsionally at displacement, *d*, with an incompressible fluid between

Vibrational settings on the V-SEP system are commonly expressed as the azimuthal displacement, *d* [m], caused by the oscillations. This displacement can be expressed as function of the radius, amplitude of angular velocity, and frequency (Equation 17). The greatest such displacement can be observed at the outermost radius, R_2.

$$d = \frac{R_2 \Omega}{\pi F} \tag{17}$$

Flow regime of the fluid between the oscillating plates can be described by it Reynolds number, *Re*. In this case, the Reynolds number is calculated in Equation 18 and is a function of the vibrational frequency and the kinematic viscosity of the fluid, *v* [m^2/s].

$$Re = \frac{2\pi F h^2}{\nu} \tag{18}$$

The shear rate, γ [s^{-1}], is equal at the surface of each plate. It changes with respect to both time, *t*, and radial position, *r* and is calculated in Equation 19.

$$\gamma\,(r,t) = \left.\frac{\partial V}{\partial z}\right|_{z=0} = \left.\frac{\partial V}{\partial z}\right|_{z=h} = \frac{r\Omega}{h}\sqrt{\frac{Re}{2}}G(t) \tag{19}$$

Where *G(t)* is a periodic function of time which represents oscillations. Akoum et al. report that the maximum value of *G(t)* is $2^{1/2}$ and the time average of its absolute value is $2/\pi$ [84]. Therefore, the function for the maximum shear rate achieved at the outer radius of the membrane can be expressed in Equation 20.

$$\gamma_{max} = \frac{R_2\Omega\sqrt{Re}}{h} = \frac{R_2}{h}\left(\frac{d\pi F}{R_2}\right)\sqrt{\frac{2\pi F h^2}{\nu}} = 2^{1/2}d(\pi F)^{3/2}\nu^{-1/2} \tag{20}$$

Therefore, it can be seen that maximum shear rate is a function of the azimuthal displacement, vibrational frequency, and kinematic viscosity of the fluid. The kinematic viscosity of the retentate is assumed to be the most representative of the fluid that the membrane surface contacts. Assuming water as the fluid, cross flow systems are limited in their capability of generating shear rates higher than 1.0 – 1.5 x 10^4 inverse seconds [83]. Vibration enhances the maximum shear rate up to 1.01 x 10^5 inverse seconds.

The integration of vibration to generate high shear regions has been investigated in various applications. Vibratory membrane separation systems have been studied in the

food and beverage industry [86], [87], [88], water and wastewater purification [89], [90], [91], [92], [93], and bioprocessing [84], [94]. Within the food and beverage industry, vibrating membrane modules have been applied primarily in the dairy industry for the concentration of proteins from milk. Vibrating membranes have also been applied in different industries for water and wastewater purification and water recovery. Notably, V-SEP technology has been used for water purification achieve zero-liquid discharge operation at a Nestlé Waters bottled water plant in Thailand [89]. Other applications include desalination and purification of effluents from the dairy and textile industries. Bioprocessing applications of vibrating membrane systems include dewatering microalgae for biofuels and filtration of fermentation broths for both yeast and bovine serum albumin removal. There is a lack of current studies on the application of vibrating membrane systems in instant coffee wastewater purification for water reuse, however, effective parallels can be drawn with similar types of industrial wastewaters.

As mentioned prior, instant coffee wastewater is characterized by a mild acidity, dark brown color, and appreciable levels or contaminants, including COD, BOD, TSS, and conductivity. Typical values can be seen in Table 3. Many food industry wastewater effluents share similar attributes. One such industry is the dairy industry. Typical values of dairy wastewater contaminants can be found in Table 10. Shete and Shinkar have shown that contaminant values can differ greatly among the various production processes and quantity of production within the dairy industry [95]. As can be seen by comparing Table 3 and Table 10, the ranges of contaminant concentrations in the dairy wastewater effluents are very similar to those of the coffee wastewater effluents. Therefore, it can be

expected that vibratory membrane studies conducted for treating dairy wastewater can be reasonably applied to instant coffee wastewater.

Table 10

Typical ranges of concentrations of dairy wastewater contaminants

Contaminant	Range
pH	4.6 – 8.3 [90], [91], [95]
COD (ppm)	2,100 – 36,000 [90], [91], [95]
BOD (ppm)	1,040 – 4,800 [95]
TSS (ppm)	1,200 – 5,800 [95]
Conductivity (µS/cm)	1,580 – 2,700 [90], [91]

Vibratory shear enhanced membrane systems used for dairy wastewater treatment have the primary goal of purifying wastewater to potable water for reuse. One study has compared the performance of ultrafiltration, nanofiltration, and reverse osmosis membranes in a vibratory shear enhanced system in the treatment of dairy wastewater [90]. Performance of shear enhanced membrane systems can be evaluated by various metrics. The first of which is the reduction of surface fouling and improvement of steady state permeate flux. In order to determine the reduction of flux degradation, experiments were conducted until steady state flux was observed (typically at least two hours). Steady state flux increase was observed in all cases. In the ultrafiltration and reverse osmosis systems, steady state flux increased by a factor of two when vibration was applied. In the nanofiltration system, steady state flux increased by nearly three times [90]. The total resistance from fouling was decreased in each case as well, mainly due to the decrease in polarization on the membrane surface [90].

Performance of the vibratory system can also be evaluated in terms of efficiency for the removal of contaminants. In this study, the removal of COD was compared between the case with and without vibration for shear enhancement. An observable increase in COD rejection was only found in the ultrafiltration case. COD rejection increased from 28% to 40%. The nanofiltration and reverse osmosis membranes were already effective for COD rejection without vibration since these membranes have lower molecular weight cut-offs [90].

Vibratory membrane systems are especially advantageous due to generating high shear while reducing the total energy requirement of a membrane system. In the dairy wastewater study, the energy requirement per volume of permeate produced while operating with and without vibration was studied with varying operating transmembrane pressures. At low operating pressures, runs conducted without vibration were less energy intensive for each type of membrane; however, steady state flux achieved without vibration is lower. In the ultrafiltration and nanofiltration systems, a threshold is achieved as operating pressure increases in the system. At this threshold, the energy required to run the system with vibration becomes lower than running the system without vibration. This is important as higher transmembrane pressure is required to generate higher flux, and thus, more wastewater can be processed for a lower amount of energy. This was not the case for the reverse osmosis system, however. The energy requirement for experiments done with vibration were higher than those without vibration as transmembrane pressure was increased [90]. Reverse osmosis membranes are designed to withstand higher pressures. It is possible that the operating pressure threshold was not achieved due to the fact the pressures tested were not high enough to obtain it.

Chapter 5

Environmental and Economic Assessment Methods

The food manufacturing industry is diverse, yet similar inefficiencies are prevalent. The main issues in food manufacturing are related to water and energy use. The relationship between these components has recently been described by the water-energy-food nexus concept [96]. This concept "…describes the complex and inter-related nature of our global resources systems [96]." Understanding this relationship is vital for the efficient use of the limited resources available and reduction of waste generation. Many processes in food product manufacturing are highly water and energy intensive. As previously stated, water plays a major role in food manufacturing. Associated energy consumption for these processes can reach high amounts. In the United States, the food and beverage industry accounted for 6.6% of total energy use of all manufacturing industries [97]. Thermal energy is used for processes such as cooking and drying while electrical energy is used for pumping, cooling, milling, and other processes [98]. High energy use in the food industry presents environmental concerns because energy is generated from non-renewable resources, such as oil, gas, and coal. The methodology of the life cycle assessment and economic analysis have been performed according to established methods in past work by Pastore 2016 [99].

Life Cycle Assessment

The environmental assessment for the current processes and the proposed recovery processes has been conducted through a life cycle assessment (LCA). An LCA is a cradle to grave analysis of the environmental impact associated with all stages of a product's life. This can include raw material extraction and product manufacturing, use,

and disposal; depending on how the boundaries and selected. The overall goal of the LCA conducted is to identify the reduced environmental impact associated with water reuse in manufacturing processes at the Nestlé plant.

The boundaries of the LCA, shown in Figure 17, include the inlet to the factory processes and the outlet of the cooling towers and on-site wastewater pretreatment process. Defining the specific boundaries for the LCA is necessary to determine the impacts from the plant processes and streams that will be included. The LCA boundaries are provided as two cases. In Base Case 1, the factory drying processes, cooling towers, and wastewater pretreatment process are within the LCA boundaries. The energy requirements for these processes are currently unknown; however, these emissions will not change as no process modifications will be implemented. Therefore, the only change in the LCA will be the amount of water used, wastewater discharged, and energy requirements associated with any recovery processes. The amount of energy required for pumping from on-site wells and processes in the on-site pretreatment process will be also reduced as a result of water reuse. Therefore, the LCA of these process steps will be quantified to determine the reduced environmental impact. This will include the cradle to grave analysis including the production of process water, treatment of wastewater, primarily nonhazardous, and electricity or steam needed for recovery processes. Base Case 2 provides similar LCA boundaries as Base Case 1, however, utilities and emissions associated with the wastewater pretreatment processes will be included. Water will be recovered prior to the pretreatment processes, thus, the energy required for such processes will be reduced.

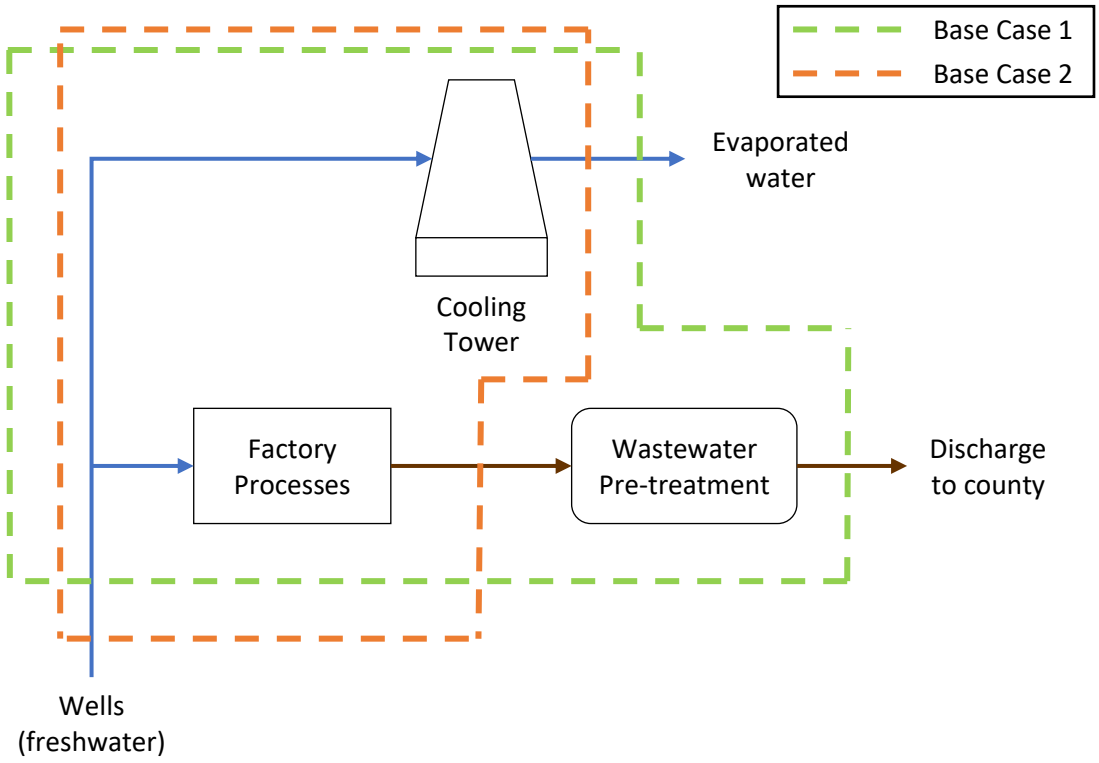

Figure 17. Current Nestlé process with LCA boundaries

The impacts associated with the water entering the factory processes and the water leaving production either as treated wastewater or evaporated water from the cooling towers are included in the selected LCA boundaries. The impact associated with these process streams includes the emissions and resources used for their manufacture and disposal. The water use and waste generated for the base case (current Nestlé process) is being determined for this case study. The process requires 172 MMgal (million gallons) of water annually. Of this, about 4% is used for mechanical pump seals and is recycled as feed to the cooling tower systems. The remainder is wastewater from the extraction process, containing the spent grounds. The factory wastewater is pretreated before being it is discharged to the county municipal wastewater treatment plant. Based on organic material and solids loadings, it can be estimated that the

wastewater discharged is 0.01% hazardous, and the remainder nonhazardous [100]. The LCA from the base case will be compared to that of the proposed case where water recovery techniques are implemented.

The boundaries of the LCA pertain to processing methods that occur at the plant. Thus, the water requirements associated with agriculture and transportation of the green coffee beans will not be included. Since no process modifications will be done for roasting and grinding the beans, it will be considered there is no change associated with the water requirements of these processes. The current overall manufacturing processes at the Nestlé Freehold, NJ plant draws approximately 470,000 GPD of water. Of this, 120,000 GPD are used for utilities generation in the cooling tower and pump seal water. The remainder of the water is used in processing. As explained in the Water Use in Soluble Coffee Manufacture section, nearly all processing water becomes wastewater. Thus 350,000 GPD of wastewater are generated at the plant.

The current Nestlé process will be broken into two base case scenarios. Base Case 1 will evaluate recovery of water from the overall plant effluent. Base Case 2 will evaluate water recovery from wastewater before it is pretreated in the on-site processes. Thus, a difference in environmental impacts and operating costs will be shown and described in the following sections.

Life Cycle Inventories

The first step in this study will be an analysis of the life cycle inventory of each input and output. A life cycle inventory (LCI) is a summary of all the emissions associated with a given process. In this case, the LCI for the manufacture or disposal of a chemical or utility was determined on a certain basis, such as 1 lb or 1 MJ. This summary

consists of all emissions released to soil, water, and air; from the manufacture or disposal process. In addition to emission data, the LCI contains data on water and energy use. The cumulative energy demand (CED) is used to express energy use of the process. The CED is the overall energy required for the defined manufacture or disposal process [101].

LCIs of the manufacture of water and disposal of wastewater for the Nestlé process were generated. This includes the freshwater used for processing and disposal of nonhazardous wastewater. Utilities associated with processing and potential recovery processes are also included. The LCI of a recovery process can be evaluated based on its required energy, whether it be electricity or steam. The emissions associated with producing that amount of energy will be analyzed and added to the overall LCA of the process.

All LCIs were found using SimaPro® Version 8. SimaPro® is an LCA software tool, which contains inventory databases. This software quantifies emissions associated with raw material use, energy use, for processes in its databases. These processes include the manufacture of certain chemicals and utilities, and the disposal of some materials [102]. The Life Cycle Inventories generated in SimaPro® were exported to Microsoft® Excel, where a developed template is to organize the data. The template was used to calculate the total emissions and the emissions to air, water, and soil for the process. In addition, the emissions of common pollutants were calculated. These pollutants include CO_2, CO, CH_4, NO_X, non-methane volatile organic compounds (NMVOC), particulates, and SO_2 emissions released into the air, and VOC emissions released into the water. The water use and Cumulative Energy Demand were also calculated using the template. The

following subsections detail the LCIs associated with the raw materials, processes, and utilities of the Nestlé process.

Freshwater. Water withdrawn for the instant coffee manufacturing process at the Nestlé plant is sourced from on-site wells and the municipal water supply. Based on information by Nestlé staff, water purity required for the manufacturing process must meet public drinking water standards. The SimaPro® database contains an LCI for drinking water treated from groundwater and surface water. Since the freshwater is withdrawn mainly from on-site wells, the inventory for drinking water sourced from groundwater is used. Groundwater pretreatment processes were modeled in SimaPro® as aeration, filtration, softening, and disinfection [103].

The LCI for the production of 1 lb of drinking water sourced from groundwater obtained using SimaPro® is shown in Table 11. The total emissions are low; however, air emissions make up about 98% of the total emissions. Of the air emissions, CO_2 emissions make up 99% for the production drinking water from groundwater. The amount of energy needed to produce 1 lb of drinking water from groundwater is 0.00218 MJ. In the Nestlé process, a significant amount of water is currently used; therefore, the total life cycle emissions and energy demand of the process are significantly high.

Table 11

LCI for the production of 1 lb of drinking water from groundwater

Total Air Emissions (lb)	5.60E-04
CO_2 (lb)	5.55E-04
CO (lb)	9.12E-08
CH_4 (lb)	6.09E-07
NO_X (lb)	-
NMVOC (lb)	1.90E-08
Particulate (lb)	1.72E-06
SO_2 (lb)	6.05E-07
Total Water Emissions (lb)	1.23E-05
VOCs (lb)	2.08E-12
Total Soil Emissions (lb)	6.87E-09
Total Emissions (lb)	**5.72E-04**
CED (MJ)	2.18E-03

Nonhazardous wastewater disposal. Wastewater that is generated at the Nestlé plant is pretreated to specified concentration levels for COD, BOD, and suspended solids. The wastewater is then discharged to the public utilities authority for further treatment. Thus, the wastewater undergoes typical, nonhazardous wastewater treatment processes. The LCI for the treatment of 1 lb of wastewater was found using SimaPro ®. Included in the SimaPro® modeled treatment processes are mechanical, biological, and chemical treatment processes [104].

The LCI data for the treatment of 1 lb of nonhazardous wastewater are shown in Table 12. This table shows that 0.0280 lb of total emissions are generated from the treatment of 1 lb of nonhazardous wastewater. These emissions consist mostly of emissions to air, which total 0.0277 lb or 99% of the total emissions. CO_2 contributes to 99% of the air emissions. The remaining 1% of air emissions is mainly CH_4, NO_X, and SO_2. Emissions to water contribute to 1% of the total emissions, while emissions to soil

are negligible. The amount of energy needed for the treatment of 1 lb of nonhazardous wastewater is 0.0780 MJ.

Table 12

LCI for the treatment of 1 lb of nonhazardous wastewater

Total Air Emissions (lb)	2.77E-02
CO_2 (lb)	2.75E-02
CO (lb)	2.27E-06
CH_4 (lb)	2.43E-05
NO_X (lb)	5.74E-05
NMVOC (lb)	7.64E-07
Particulate (lb)	7.55E-07
SO_2 (lb)	2.76E-05
Total Water Emissions (lb)	3.59E-04
VOCs (lb)	8.88E-11
Total Soil Emissions (lb)	3.04E-07
Total Emissions (lb)	**2.80E-02**
CED (MJ)	7.80E-02

Hazardous wastewater disposal. Nearly all wastewater that is discharged to county wastewater treatment plant is considered nonhazardous. BOD and TSS are considered as "hazardous" waste under the Clean Water Act [100]. Wastewater polluted with BOD and TSS does not require incineration for treatment but does require additional treatment processes. The model of the LCI used for wastewater containing BOD and TSS was found using SimaPro ®. The LCI entry is described as wastewater, organic contaminated [105]. This model accounts for mechanical, biological, and chemical treatment steps and also includes processes for sludge treatment associated with higher concentrations of BOD and TSS [105].

The LCI data for the treatment of 1 lb of hazardous wastewater are shown in Table 13. This table shows that 0.0829 lb of total emissions are generated from the treatment of 1 lb of hazardous wastewater. These emissions consist mostly of emissions to air, which total 0.0810 lb or 99% of the total emissions. CO_2 contributes to 99% of the air emissions. The remaining 1% of air emissions is mainly CH_4 and SO_2. Emissions to water contribute to 1% of the total emissions, while emissions to soil are negligible. The amount of energy needed for the treatment of 1 lb of hazardous wastewater is 0.223 MJ.

Table 13

LCI for the treatment of 1 lb of hazardous wastewater

Total Air Emissions (lb)	8.10E-02
CO_2 (lb)	8.05E-02
CO (lb)	6.55E-06
CH_4 (lb)	7.05E-05
NO_X (lb)	-
NMVOC (lb)	2.22E-06
Particulate (lb)	2.15E-06
SO_2 (lb)	7.93E-05
Total Water Emissions (lb)	1.98E-03
VOCs (lb)	2.58E-10
Total Soil Emissions (lb)	8.84E-07
Total Emissions (lb)	**8.29E-02**
CED (MJ)	2.23E-01

Electricity. The electricity at the Nestlé Freehold plant comes from the local electrical grid. However, SimaPro® does not have a process to model electricity generation in central New Jersey. The processes in SimaPro® for electricity generation may not be accurate for New Jersey because these processes may not use the fuels typically used in New Jersey. In order to accurately model electricity generation in New

Jersey, a custom model was created in SimaPro®. The custom model uses data from the U.S. Energy Administration. In New Jersey, electricity is generated from coal, natural gas, nuclear power, and renewable resources. The quantity of electricity generated by each energy source in 2015 is shown in Table 14 [106]. Table 14 shows that the most common fuels used to produce electricity in New Jersey are natural gas and nuclear power, accounting for 95.5% of electricity generation. The remaining 4.5% of electricity is generated from coal and renewable resources.

Table 14

Net electricity generation by source in New Jersey for 2015 [106]

	Coal	**Natural Gas**	**Nuclear**	**Other Renewables**	**Total**
Electricity by Source (GWh)	1,759	36,974	33,262	1,574	73,569
Percentage of Total Electricity (%)	2.4	50.3	45.2	2.1	

The model created in SimaPro® consisted of a combination of all resources used to generated electricity in New Jersey. The percentages associated with each fuel type are shown in Table 14. In SimaPro®, the inputs used to create 1 MJ of electricity in New Jersey were 0.024 MJ of electricity from coal, 0.503 MJ of electricity from natural gas, 0.452 MJ of electricity from nuclear power, and 0.021 MJ of electricity from biomass. The LCI data for each source of electricity was based off of averaged data from power plants in the United States, which produce electricity from the specified resource. Biomass was chosen to represent renewable resources because the renewable resources used in New Jersey to generate electricity consisted mostly of biomass [106].

The LCI data for the production of 1 MJ of electricity in New Jersey is provided in Table 15. The total emissions released to the environment for the production of 1 MJ of electricity are 0.261 lb. These emissions consist mostly of emissions to air, which total 0.229 lb or 87.4% of the total emissions. CO_2 contributes to 98% of the air emissions released from electricity generation. The remaining 2% of air emissions is mainly CH_4 and SO_2. Emissions to water contribute to 12.5% of the total emissions, while emissions to soil are trace. The CED to produce 1 MJ of electricity is 3.95 MJ.

Table 15

LCI for the manufacture of 1 MJ of electricity in New Jersey

Total Air Emissions (lb)	2.29E-01
CO_2 (lb)	2.25E-01
CO (lb)	1.57E-04
CH_4 (lb)	1.13E-03
NO_X (lb)	1.80E-04
NMVOC (lb)	7.13E-05
Particulate (lb)	5.95E-05
SO_2 (lb)	1.97E-03
Total Water Emissions (lb)	3.28E-02
VOCs (lb)	1.00E-07
Total Soil Emissions (lb)	1.43E-06
Total Emissions (lb)	**2.61E-01**
CED (MJ)	3.95E+00

Steam. The Nestlé Freehold, NJ plant produces steam using natural gas. In this process, natural gas is combusted to provide heat energy to boil water, thus generating steam. In SimaPro®, the LCI data for process steam generated from natural gas were used to model the steam generation process at the Nestlé Freehold Plant. The LCI for the generation of process was calculated on a 1 MJ basis, using SimaPro®. In Table 16, it is

shown that 0.148 lb of total emissions is generated from the manufacture of 1 MJ of process steam. These emissions consist mostly of emissions to air, which total 0.147 lb or about 99.5% of the total emissions. CO_2 contributes to 99.7% of the air emissions released from electricity generation. The remaining 0.3% of air emissions is mainly CH_4, CO, and SO_2. Emissions to water and soil are trace. The amount of energy needed to manufacture 1 MJ of process steam is 1.19 MJ.

Table 16

LCI of the manufacture of 1 MJ of steam produced by natural gas

Total Air Emissions (lb)	1.47E-01
CO_2 (lb)	1.47E-01
CO (lb)	5.27E-05
CH_4 (lb)	2.34E-04
NO_X (lb)	0.00E+00
NMVOC (lb)	1.25E-06
Particulate (lb)	1.77E-06
SO_2 (lb)	5.09E-05
Total Water Emissions (lb)	7.12E-04
VOCs (lb)	7.99E-09
Total Soil Emissions (lb)	2.78E-06
Total Emissions (lb)	**1.48E-01**
CED (MJ)	1.19E+00

Life Cycle Emissions of the Nestlé Process

The LCIs for each component of the Nestlé process will be used to perform an LCA. Equation 21 is used to calculate the life cycle emissions of Base Case 1 of the Nestlé process. The total life cycle emissions and life cycle CO_2 emissions for each component of the process will be determined based on the annual use of water and generation of waste. The only impact of utility use included in the LCA of Base Case 1

of the coffee product manufacture will that of the electricity requirement by the well pumps. No other utilities will be included in this LCA because these impacts will not change with the addition of the proposed purification processes.

$$LCE_{Nestlé,BC1} = m_{water}LCI_{water} + m_{HW}LCI_{HW} + m_{NHW}LCI_{NHW} + E_{pump}LCI_E \quad (21)$$

In the above equation, m_{water} is the amount of water that is withdrawn for manufacturing and utilities, in lb/yr. m_{HW} and m_{NHW} are the amounts of hazardous and nonhazardous waste generated by the current operation at the Nestlé plant, in lb/yr. LCI_{water} is the life cycle inventory for the production of process water on a 1 lb basis. It should be noted that hazardous waste is the BOD and TSS discharged as discussed in the earlier section describing the mass flows. LCI_{HW} and LCI_{NHW} are the life cycle inventories for the disposal of hazardous and nonhazardous waste on a 1 lb basis. E_{pump} is the electricity required by the well pumps to pump freshwater to the factory processes and cooling tower. LCI_E is the life cycle inventory of electricity on a 1 MJ basis.

An alternative base case for the current process will also be considered, in which the operating energy associated with the on-site wastewater pretreatment is included. This will be Base Case 2. This is necessary to calculate since there will be a reduction in the volume of wastewater that is pretreated on-site, thus the operating energy of such processes is reduced. The majority of energy associated with the on-site pretreatment processes is that of the energy required to operate the blower pumps in the aeration lagoon. Equation 22 shows a similar equation as Equation 21; however, it includes the electricity required for the blowers of the aeration lagoon.

$$LCE_{Nestlé,BC2} = m_{water}LCI_{water} + m_{HW}LCI_{HW} + m_{NHW}LCI_{NHW} + (E_{pump} + E_{Blowers})LCI_E \quad (22)$$

Table 17 presents the mass and energy flows for both base cases used in this study. Material flows (water and wastewaters) are the same for each base case. The difference in the bases cases are in the total electricity requirements. It can be seen that the blowers require a considerable amount of electricity. Thus, reducing the volume of wastewater that will be pretreated will have a beneficial effect on the environmental assessment process.

Table 17

Mass and energy flows of each base case of the current processes at the Nestlé plant

Flows	**Base Case 1**		**Base Case 2**	
Freshwater	$1.72x10^8$	gal/yr	$1.72x10^8$	gal/yr
	$1.43x10^9$	lb/yr	$1.43x10^9$	lb/yr
Nonhazardous wastewater	$1.28x10^8$	gal/yr	$1.28x10^8$	gal/yr
	$1.06x10^9$	lb/yr	$1.06x10^9$	lb/yr
Hazardous wastewater	$1.14x10^5$	lb/yr	$1.14x10^5$	lb/yr
Electricity (pumps)	$1.30x10^6$	MJ/yr	$1.30x10^6$	MJ/yr
Electricity (blowers)	N/A		$8.00x10^6$	MJ/yr

In Table 17, the mass flowrate of hazardous wastewater in the process is the sum of the masses of BOD and TSS that are in the plant effluent. Nestlé is under contract with the Ocean County Utilities Authority such that only and the excess of a concentration of BOD or TSS of 300 mg/L each is considered hazardous wastewater. Based on wastewater discharge data, the average concentrations of BOD and TSS in the effluent have been estimated to be 352 and 355 mg/L, respectively. Thus, the total mass

flowrate of hazardous wastewater can be calculated as the product of the concentrations of each BOD and TSS and the volumetric flowrate of the wastewater effluent. This calculation is shown in Equation 23.

$$HW = (BOD + TSS) \times NHW_{volumetric} \tag{23}$$

$$HW = \left[\left(352\frac{mg}{L} - 300\frac{mg}{L}\right) + \left(355\frac{mg}{L} - 300\frac{mg}{L}\right)\right] \times 1.28 \times 10^6 \frac{gal}{yr} \times \frac{3.785\ L}{gal} \times \frac{2.2046\ lb}{10^6\ mg} = \mathbf{1.14 \times 10^5 \frac{lb}{yr}}$$

The life cycle emissions associated with the Base Case 1 of the Nestlé process are shown in Table 18. The total life cycle emissions are the sum of the emissions associated with water use, nonhazardous and hazardous wastewater disposal, and electricity required for the pump. A considerable portion of the total life cycle emissions are to the air at 98.8%. Furthermore, CO_2 emissions contribute 99.3% of the total air emissions. Nonhazardous wastewater disposal attributes to 96% of the total emissions. This is based on the high volume of wastewater that is generated and must be treated. Therefore, a reduction in the amount of wastewater that is discharged has the potential for a strong decrease in the total life cycle emissions of the current Nestlé process.

Table 18

Life cycle emissions associated with the Base Case 1 current Nestlé process

	Freshwater	NHW	HW	Electricity	Total
Total Air Emissions (lb/yr)	8.01E+05	2.95E+07	9.24E+03	2.97E+05	**3.06E+07**
CO_2 (lb/yr)	7.93E+05	2.93E+07	9.18E+03	2.92E+05	**3.04E+07**
CO (lb/yr)	1.30E+02	2.42E+03	7.47E-01	2.04E+02	**2.75E+03**
CH_4 (lb/yr)	8.71E+02	2.59E+04	8.04E+00	1.47E+03	**2.82E+04**
NO_X (lb/yr)	0.00E+00	6.11E+04	0.00E+00	2.34E+02	**6.13E+04**
NMVOC (lb/yr)	2.72E+01	8.13E+02	2.53E-01	9.26E+01	**9.33E+02**
Particulate (lb/yr)	2.46E+03	8.04E+02	2.45E-01	7.73E+01	**3.34E+03**
SO_2 (lb/yr)	8.65E+02	2.94E+04	9.05E+00	2.56E+03	**3.28E+04**
Total Water Emissions (lb/yr)	1.76E+04	3.82E+05	2.26E+02	4.26E+04	**4.43E+05**
VOCs (lb/yr)	2.97E-03	9.45E-02	2.94E-05	1.30E-01	**2.27E-01**
Total Soil Emissions (lb/yr)	9.82E+00	3.24E+02	1.01E-01	1.86E+00	**3.35E+02**
Total Emissions (lb/yr)	**8.18E+05**	**2.98E+07**	**9.46E+03**	**3.39E+05**	**3.10E+07**
CED (MJ/yr)	3.12E+06	8.30E+07	2.54E+04	5.13E+06	**9.13E+07**

The life cycle emissions associated with the Base Case 2 of the Nestlé process are shown in Table 19. The total life cycle emissions are the sum of the emissions associated with water use, nonhazardous and hazardous wastewater disposal, and electricity required for the pump. Similar to Base Case 1, a considerable portion of the total life cycle emissions are to the air at 98.1%. Furthermore, CO_2 emissions contribute 99.2% of the total air emissions. Nonhazardous wastewater disposal still accounts for a majority of the total emissions, even when including the electricity required for the blowers. When compared to Base Case 1, the total emissions associated with electricity increase by a factor of approximately 7. This is a considerable increase; however, the life cycle emissions associated with electricity are only 7% of the total emissions of Base Case 2. Nonhazardous wastewater disposal accounts for 90% of the total emissions while the

remaining 3% is caused by freshwater procurement and hazardous wastewater disposal. Therefore, a reduction in the amount of wastewater that is sent to pretreatment will show favorable decreases in the emissions associated with nonhazardous wastewater disposal and electricity.

Table 19

Life cycle emissions associated with the Base Case 2 current Nestlé process

	Freshwater	**NHW**	**HW**	**Electricity**	**Total**
Total Air Emissions (lb/yr)	8.01E+05	2.95E+07	9.24E+03	2.13E+06	**3.24E+07**
CO_2 (lb/yr)	7.93E+05	2.93E+07	9.18E+03	2.09E+06	**3.22E+07**
CO (lb/yr)	1.30E+02	2.42E+03	7.47E-01	1.46E+03	**4.01E+03**
CH_4 (lb/yr)	8.71E+02	2.59E+04	8.04E+00	1.05E+04	**3.73E+04**
NO_X (lb/yr)	0.00E+00	6.11E+04	0.00E+00	1.67E+03	**6.28E+04**
NMVOC (lb/yr)	2.72E+01	8.13E+02	2.53E-01	6.63E+02	**1.50E+03**
Particulate (lb/yr)	2.46E+03	8.04E+02	2.45E-01	5.53E+02	**3.82E+03**
SO_2 (lb/yr)	8.65E+02	2.94E+04	9.05E+00	1.83E+04	**4.86E+04**
Total Water Emissions (lb/yr)	1.76E+04	3.82E+05	2.26E+02	3.05E+05	**7.05E+05**
VOCs (lb/yr)	2.97E-03	9.45E-02	2.94E-05	9.29E-01	**1.03E+00**
Total Soil Emissions (lb/yr)	9.82E+00	3.24E+02	1.01E-01	1.33E+01	**3.47E+02**
Total Emissions (lb/yr)	**8.18E+05**	**2.98E+07**	**9.46E+03**	**2.43E+06**	**3.31E+07**
CED (MJ/yr)	3.12E+06	8.30E+07	2.54E+04	3.67E+07	**1.23E+08**

Alternative processes, which include purification/recovery methods, proposed to the current Nestlé process have been designed to reduce environmental impact through water recovery and waste minimization. Figure 18 shows the two alternative processes considered as they relate to each of the base case scenarios. Case 1 relates to Base Case 1. Utilities of the on-site wastewater pretreatment process are not included since the overall effluent is the target stream for recovery. Thus, there is no reduction associated

with the utilities of the pretreatment processes. Case 2 targets a lower strength wastewater stream from the steam injectors in the factory processes. Recovering water from this stream will reduce the volume of water treated in the pretreatment processes; thus, the energy required will be decreased.

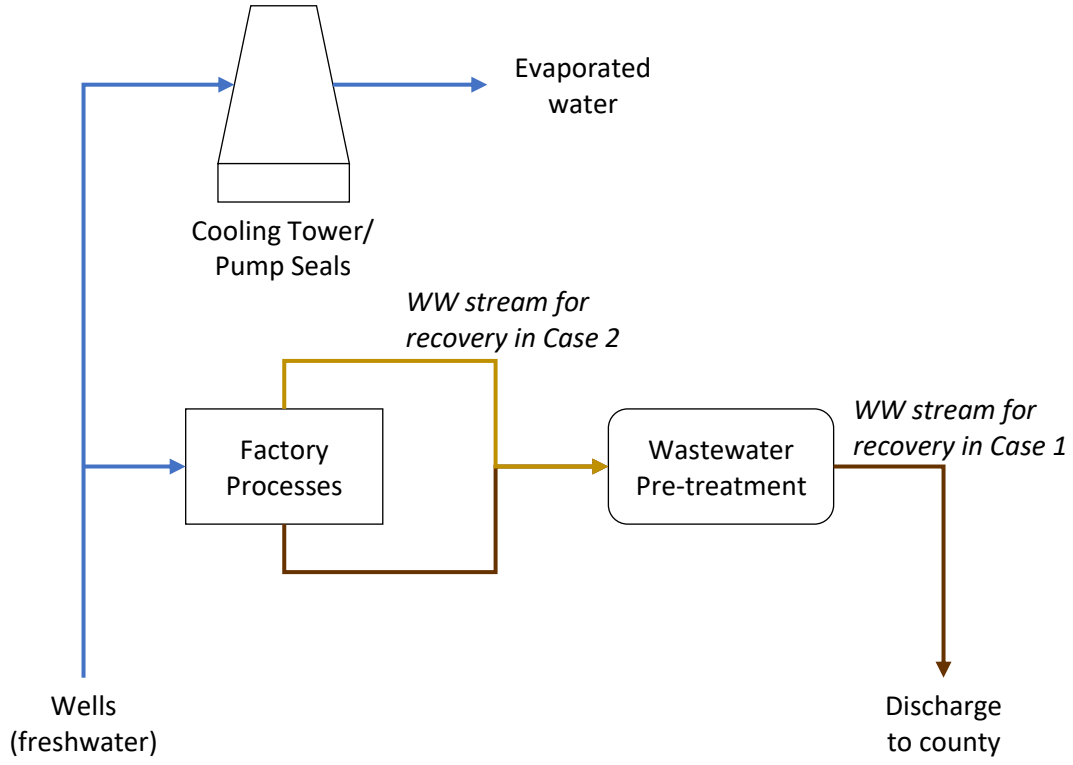

Figure 18. Simplified process flow diagram depicting wastewater streams for recovery in each case

The life cycle emissions of recovery processes will be calculated using Equation 24.

$$LCE_{AP} = (m_{water} - r_{water}) \cdot LCI_{water} + m_{HW,\ AP} \cdot LCI_{HW} + m_{NHW,\ AP} \cdot LCI_{NHW} + S \cdot LCI_S + E \cdot LCI_E \quad (24)$$

The life cycle emissions generated with the alternative process can be estimated using a similar equation to that of the current process, except that the emissions associated with recovered water and the amount of waste reduced are not included. The recovered water is given as r_{water} in lb/yr. The reduced amounts of wastewater are given as $m_{HW,\ AP}$ and $m_{NHW,\ AP}$ for hazardous and nonhazardous waste, respectively, and are in lb/yr. Additionally, the energy requirement, S and E, are added for the amount of energy produced by steam and electricity, respectively, in MJ/yr. The LCIs associated with the energy production are also included as LCI_S and LCI_E and are based on a 1 MJ basis.

The total avoided life cycle emissions can be calculated in Equation 25.

$$LCE_{avoided} = LCE_{base\ case} - LCE_{alternative\ process} \quad (25)$$

Equation 25 will be used to determine the extent of the reduced environmental impact from the alternative processes.

Operating Cost of the Nestlé Process

The current Nestlé soluble coffee manufacturing process and proposed water recovery processes were evaluated using economic metrics, in addition to the environmental metrics mentioned previously. The life cycle operating cost of the current process and water recovery processes were calculated to determine if operating costs were saved. The costs of water, wastewater discharge, and electricity have been provided by Nestlé. Nonhazardous wastewater discharge is charged at flat rate with additional surcharges for the disposal of BOD and TSS. As mentioned in the earlier section, BOD

and TSS are considered as "hazardous" wastes. To make the calculations to conform to the practices at Nestle, the surcharge rate is used as representative of "hazardous' waste costs and report as separate line items as BOD Surcharge and TSS Surcharge. These rates were provided by Nestlé and the Ocean County Utilities Authority; shown in Table 20 [33]. Water is drawn from on-site wells for the manufacturing process. According to Nestlé engineering management, approximately only 2% of water used in manufacturing is drawn from the municipality. Thus, the cost of water purchased through municipality is considered insignificant relative to all manufacturing costs.

Table 20

Unit operating costs of water, wastewater discharge, and utilities for the Nestlé plant

Water	0.0011 $/lb
Non-hazardous Wastewater Discharge	0.000475 $/lb
BOD Surcharge	0.4043 $/lb
TSS Surcharge	0.3862 $/lb
Electricity	0.025 $/MJ
High Pressure Steam	0.00665 $/lb

The cost of steam was estimated using Equation 26 [107]. Steam costs will only be associated with steam requirements for recovery processes. Any processes currently using steam in manufacturing will not be added to the cost assessment since these processes will not be altered. Currently, the proposed recovery process will not require steam for operation.

$$Cost_{HP,Steam} = Cost_{Fuel} \times \frac{dH_b}{\eta_b} \quad (26)$$

Where, $Cost_{HP\ Steam}$ is the cost of high pressure steam in $/Mlb, $Cost_{Fuel}$ is the cost of natural gas in $/MMBtu, dH_b is the heating rate in MMBtu/Mlb, and η_b is the boiler efficiency. The cost of fuel is 7.67 $/MMBtu, which is the average of available data for the industrial price of natural gas in New Jersey in 2017 [108]. Typical boiler efficiency is between 80 – 90%. The boiler efficiency will be assumed to be 85%. The heating rate can be calculated using Equation 27. Enthalpy values can be found using a steam table. High pressure steam is typically around 40 bar and condenses at a temperature of 250 °C [109].

$$dH_b = (h_s - h_e) \times \frac{1\ kg}{2.2046\ lb} \times \frac{1\ Btu}{1.055\ kJ} \times \frac{MMBtu}{1{,}000{,}000\ Btu} \times \frac{1{,}000\ lb}{Mlb} \qquad (27)$$

In Equation 27, h_s and h_e are the enthalpies of saturated steam and water, respectively, in kJ/kg. High pressure steam is 250ºC, so h_s and h_e are 2,800 kJ/kg and 1,087 kJ/kg, respectively. The heating rate was calculated to be 0.736 MMBtu/Mlb. The cost of high pressure steam was then calculated to be $6.65/Mlb.

The annual operating costs for the Nestlé coffee manufacturing base case (i.e. no water recovery) have been calculated corresponding to process information. The flowrates of water and wastewater discharge have been multiplied by their respective costs in $/lb. BOD and TSS concentrations vary by production; concentrations may be different depending on the product that is being manufactured at the plant on a given day. The surcharges for BOD and TSS are only processed for wastewater that is discharged above a concentration of 300 mg/L for each. For this reason, an average concentration of BOD and TSS has been estimated based on data received from Nestlé of wastewater

discharge. The average concentrations for BOD and TSS are 355 mg/L and 352 mg/L, respectively. Equations 28 and 29 are used to calculate the surcharges for BOD and TSS, respectively.

$$BOD\left(\frac{\$}{yr}\right) = Flow\left(\frac{gal}{day}\right) \times \left(BOD\left(\frac{mg}{L}\right) - 300\right) \times \frac{\$0.4043}{lb} \times \frac{3.785L}{gal} \times \frac{1\ kg}{10^6\ mg} \times \frac{2.0246\ lb}{1\ kg} \times \frac{365\ day}{yr} \quad (28)$$

$$TSS\left(\frac{\$}{yr}\right) = Flow\left(\frac{gal}{day}\right) \times \left(TSS\left(\frac{mg}{L}\right) - 300\right) \times \frac{\$0.3862}{lb} \times \frac{3.785L}{gal} \times \frac{1\ kg}{10^6\ mg} \times \frac{2.0246\ lb}{1\ kg} \times \frac{365\ day}{yr} \quad (29)$$

The operating costs of pumping water from the on-site wells at the plant have been estimated. The wells at the plant are roughly 565 ft deep according to Nestlé personnel. Up to three different well pumps may be used throughout the day. Two pumps have a power requirement of 150 hp, while the third is 75 hp. Equations 30 – 34 are used to estimate the operating costs of pumping the daily water requirement from the wells.

$$P_2 - P_1 = \Delta P = \rho g(h_2 - h_1) + friction\ losses = 1.15 \times [\rho g(h_2 - h_1)] \quad (30)$$

In Equation 30, the pressure drop is calculated as the static pressure difference from the well (h_1 = 0 ft) to surface (h_2 = 565 ft) . Frictional losses are assumed to be 15% of the pressure drop. The density, ρ, is assumed to be 1,000 kg/m^3. The gravitational acceleration constant, g, is 9.81 m/s^2. When calculated, the pressure drop, ΔP, is equal to 2x10^6 Pa.

$$Q_w = \frac{Power}{\Delta P} \cdot \eta \tag{31}$$

In Equation 31, Q_w is the operating flowrate of well water. The pump efficiency, η, is 85%, or 0.85.

$$t_{op} = \frac{Q_{req'd}}{Q_w} \times \frac{24\ hr}{day} \tag{32}$$

In Equation 32, t_{op}, is the operating time for a given pump in hrs per day. The required flowrate of water, $Q_{req'd}$ (470,000 GPD) is divided by the operating flowrate of well water by a given pump.

$$Energy = Power \times \eta \times t_{op} \tag{33}$$

In Equation 33, the energy requirement of a given pump is calculated.

$$Operating\ Cost = Energy \times 0.025 \frac{\$}{MJ} \tag{34}$$

In Equation 34, the operating cost is calculated using the cost of electricity per MJ for the Nestlé Freehold plant. A summary of the operation of the three well pumps can be seen in Table 21. To determine the final operating cost of the well pumps, a minimization function was used for determining the optimal operating times for each pump.

Table 21

Summary of operating parameters for the well pumps at the Nestlé plant

	Pump 1	Pump 2	Pump 3	**Total**
Run Time (hr/day)	3.46	3.46	6.93	-
Flowrate (GPD)	156,600	156,700	156,700	470,000
Energy Requirement (MJ/yr)	120,230	120,230	120,230	360,700
Operating Cost ($/yr)	10,800	10,800	10,800	32,400

The costs of the on-site wastewater pretreatment processes were estimated for Base Case 2. Operating costs would be the collective energy required to operate the sedimentation tanks and blowers in the aeration lagoon. It was anticipated that the bulk of the operating costs are associated with the motors for blowers in the aeration lagoon. After further discussion with staff at Nestlé, this was confirmed. There are two blowers, each with 200 hp motors, that operate continuously. Equations 35 and 36 were used to estimate the operating cost of the blowers.

$$Energy_{Blowers} = 2 \times P_{Blower} \times \eta \times run\ time \tag{35}$$

In Equation 35, the energy required to operate both blowers is calculated. The motor efficiency, η, is 85% or 0.85. The run time is 24 hrs per day.

$$Operating\ Cost_{Blowers} = Energy_{Blowers} \times 0.025 \frac{\$}{MJ} \tag{36}$$

In Equation 36, the operating cost of the blowers for the aeration lagoon is calculated using the cost of electricity per MJ for the Nestlé Freehold plant.

The annual operating costs for water use and wastewater discharge can be seen in Table 22. The costs shown are those that are within the LCA boundaries shown in Figure 17, as appropriate. As stated previously, the only utilities that will be considered in the base case cost assessment are those that will be altered by implementing a water recovery system. Thus, two different base case operating costs will be shown (BC1 and BC2). BC1 refers to the current process that will be altered when water recovery from the overall plant effluent is the alternative process. This assessment will not include the costs of the blowers as the wastewater pretreatment processes will not change. BC2 refers to the current process that will be altered if water recovery from wastewater that is directly from the factory processes (no on-site pretreatment) is the alternative process. This assessment will include the operating costs of the blowers in the aeration lagoon. By recovering water before the wastewater pretreatment processes, the volume of water to be treated will decrease. This results in less energy required for aeration in the lagoon.

Table 22

Operating costs of each Base Case of the current Nestlé process

	Cost ($/yr)	
	BC1	**BC2**
Freshwater	22,300	22,300
Non-hazardous Wastewater Discharge	505,900	505,900
BOD and TSS Discharge	45,000	45,000
Well Pumps	32,500	32,500
Blowers	N/A	199,900
Total	605,700	805,600

All other utilities are not included in this analysis since the electricity and steam requirements of the current processes will not be altered. The same rationale is used for other chemicals and consumable supplies. Only those impacted by using a recovery process are included. The total annual operating cost for BC1 was calculated using Equation 37. It can be seen that the cost of discharging wastewater to the municipality contributes to a majority of the total operating costs at 90%. This is caused by the large volume of wastewater discharged each day. The cost of electricity to operate the well pumps at the plant is about 6% of the total operating cost. The cost of freshwater makes up the balance at about only 4% of the total operating cost.

$$Cost_{BC1} = m_{water,BC} \cdot Cost_{water} + m_{NHWW,BC} \cdot Cost_{NHWW} + m_{BOD\&TSS} \cdot Cost_{BOD\&TSS} + E_{pumps,BC} \cdot Cost_E \quad (37)$$

The total annual operating cost for BC2 was calculated using Equation 38. The operating costs for the blowers contribute a significant portion of the operating costs at 26%. Nonhazardous wastewater discharge is still the majority of the operating costs at 67%. The costs to operate the well pumps and the cost of water are 4% and 3%, respectively. Table 22 shows that the operating costs of the blowers are considerable. Both the operating costs of the blowers and those associated with a decrease in wastewater discharge will be reduced upon the implementation of water recovery methods.

$$Cost_{BC2} = m_{water,BC} \cdot Cost_{water} + m_{NHWW,BC} \cdot Cost_{NHWW} + m_{BOD\&TSS} \cdot Cost_{BOD\&TSS} + (E_{pumps,BC} + E_{Blowers}) \cdot Cost_E \quad (38)$$

BOD and TSS disposal are included in the total annual operating cost. The current membrane recovery process reclaims water for reuse purposes while the contaminants of the wastewater stream (including the BOD and TSS constituents) are left in the retentate stream. The retentate stream will be discharged in the same manner as the nonhazardous waste is currently done. Thus, there is no reduction in the total mass of BOD and TSS from the base case to the recovery case and therefore no reduction in costs associated with BOD and TSS.

Recovery processes for water from the current Nestlé were designed to provide environmental benefit while reducing operating costs. The designs of recovery processes are detailed in the following sections. Reduction in environmental impact and cost can be achieved by reducing the amount of nonhazardous wastewater that is discharged. The operating costs of the Nestlé manufacturing process with water recovery is calculated as in Equation 39. Equation 39 is similar to Equations 37 and 38 except the mass amounts of certain terms have been reduced because of either the recovery of water or reduction in discharge. In each recovery case, Equation 39 also includes the utilities associated with the proposed recovery systems. For Case 2, the reduction in energy required for the on-site pretreatment process is also considered.

$$Cost_{Alternative\ Process} = (m_{water} - r_{water}) \cdot Cost_{water} + (m_{NHWW} - r_{NHWW}) \cdot Cost_{NHWW} + E \cdot Cost_E + S \cdot Cost_S \quad (39)$$

In Equation 39, r_{water} is the amount of water recovered. This term is subtracted since any recovered water will cause a reduction in freshwater that will be needed. The term r_{NHWW} represents the reduction amount of each nonhazardous wastewater that is

discharged from the plant. Terms for the utilities that may be required for the recovery process have been included; they are *E* for the required electricity in MJ and *S* for the required steam in MJ. $Cost_E$ and $Cost_S$ are the costs for each utility on a 1 MJ basis. Equation 40. shows the calculation for the avoided costs, of the Nestlé process with water recovery, or the alternative process. The avoided costs will then be used as a metric to determine if the alternative process has favorable economic benefits compared to the base case Nestlé process.

$$Cost_{avoided} = Cost_{Base\ Case} - Cost_{Alternative\ Process} \quad (40)$$

Economic Analysis Methods for Recovery Processes

Economic analyses were conducted to compare the current Nestlé coffee manufacturing process to the alternative processes based on both operating cost savings and recovery equipment capital costs. This was done to determine if the alternative processes would be economically favorable for Nestlé. Operating cost savings alone may not result in overall savings because capital equipment will also need to be purchased. To determine if alternative processes are profitable, various economic metrics will be assessed. Such metrics include: internal rate of return (IRR), return on investment (ROI), payback time after tax, net present value (NPV) after 5 years, and NPV after 10 years. Calculations for these metrics were carried out using the 7-year modified accelerated cost recovery system (MACRS) depreciation method, a 21% tax rate, and a 15% interest rate [107]. In these analyses, the capital cost of the recovery equipment was invested, and pretax cash flow was set equal to the negative of the capital cost in Year 0. Pretax cash flow was set equal to the operating cost savings in Years 1 – 10. Equations 41 – 49 were

used to calculate the IRR, ROI, payback time after tax, and NPV at 5 and 10 years for the alternative processes. All economic metrics are zero for the current Nestlé process because it does not have an investment for recovery equipment or operating savings via water recovery.

$$D_n = \frac{Investment \times DF_n}{100} \tag{41}$$

In Equation 41, D_n is the depreciation charge in year n, *investment* is the total capital cost, DF_n is the depreciation factor in year n specified by the MACRS depreciation method. D_n is zero for Year 0 and was calculated for Years 1 – 10 using Equation 41.

$$book\ value = investment - \sum_{n=1}^{n=t} D_n \tag{42}$$

In Equation 42, the *book value* is zero for Year 0 and *t* is the number of years of depreciation. The *book value* was calculated for Years 1 – 10 using Equation 42.

$$income = pretax\ cash\ flow - D_n \tag{43}$$

In Equation 43, the income is zero for Year 0 and the *pretax cash flow* is equal to the operating cost savings for Years 1 – 10. *Income* was calculated for Years 1 – 10 using Equation 43.

$$tax = tax\ rate \times income_{n-1} \tag{44}$$

In Equation 44, the *tax* is zero for Year 0, the *tax rate* is 0.21, and $income_{n-1}$ is the income in year n – 1. The *tax* was calculated for Years 1 – 10 using Equation 44.

$$cash\ flow = pretax\ cash\ flow - tax \tag{45}$$

In Equation 45, *pretax cash flow* is the negative of the capital investment for Year 0 and the operating savings for Years 1 – 10. The *cash flow* was calculated using Equation 45 for Years 0 – 10.

$$payback\ time\ after\ tax = \frac{investment}{average\ cash\ flow} \tag{46}$$

In Equation 46, the *average cash flow* is the average cash flow from Years 1 – 10.

$$ROI = \frac{average\ cash\ flow}{investment} \tag{47}$$

In Equation 47, *ROI* is the return on investment.

$$NPV = \sum_{n=1}^{n=t} cash\ flow \times (1+i)^{-n} \tag{48}$$

In Equation 48, *NPV* is the net present value, *i*, is the interest rate (15%), and *n* is the number of years (*t* = 5 or 10).

$$0 = \sum_{n=1}^{n=10} cash\ flow \times (1+i)^{-n} \quad (49)$$

In Equation 49, *i*, is the internal rate of return (IRR).

Chapter 6

The Nestlé Process

An experimental analysis was conducted for possible separation techniques to purify and recover water from wastewater at the Nestlé plant. As explained previously, there are two areas for water recovery in the Nestlé process. Figure 19 shows a flow diagram of the current Nestlé process, with mass flowrates. The direct factory wastewater is separated into two streams that enter two separate holding areas. Of these direct process wastewaters, one is more concentrated than the other in terms of major contaminants. The less concentrated wastewater stream is sent to the holding area "Pit #3," and is sourced from steam injectors from manufacturing. The Pit #3 wastewater has a slight concentration of organics and conductivity, has very low concentrations of suspended solids. The more concentrated wastewater stream is sent to the holding area "Pit #1," and is sourced from the other processes, such as, extraction, evaporation, and final drying. The Pit #1 wastewater is high in all major contaminants of COD, suspended solids, and conductivity. The only current process water that is recycled to the cooling tower is pump seal water.

Shown in Figure 19, not all of the well water used each day is sent to the factory processes for production. Based on wastewater discharge data and discussions with Nestlé staff, an estimate of the portion of the well water that is sent directly to the cooling tower was determined. It should be noted that wastewater flows may change from time to time caused by changes in production schedules or product manufactures at the Freehold factory. Therefore, the proposed green engineering solutions are based on

values presented herein, as they are representative of a typical soluble coffee manufacturing plant.

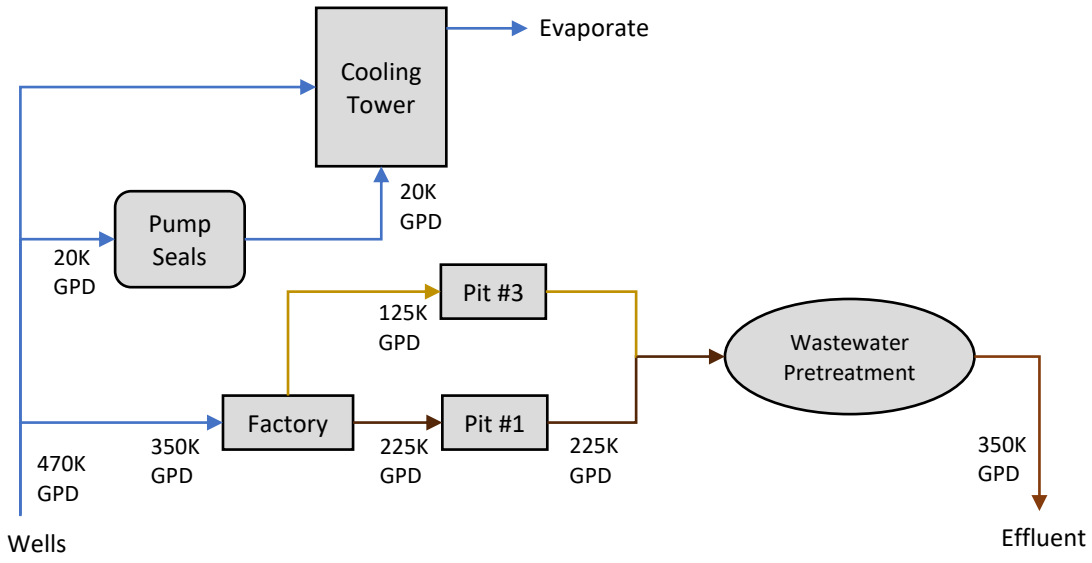

Figure 19. Simplified flow diagram of the current Nestlé process, including mass flowrates

Figure 20 shows the areas of process intervention for water recovery, with mass flowrates, that were evaluated. The systems, "Recov 1" and "Recov 2" are both designed to recover water that is suitable for use in the cooling tower. It has been proposed that successful intervention for water recovery will eliminate the need for daily well water draw for the cooling tower. Thus, to recover a sufficient volume of water for use in the cooling towers, only one recovery system may be required, or a combination of two smaller recovery systems. Overall, a total of 100,000 GPD of water will be recovered from either the overall plat effluent, the Pit #3 wastewater, or a combination of both. For example, if all water can be recovered effectively from the plant effluent, there will be no

implementation of a second recovery system for the Pit #3 wastewater. Further evaluation of each recovery system and assessments for possible recovery schemes are explained in detail in the design sections. With successful intervention, the amount of well water drawn will be reduced by 21%. The implementation of a recovery system(s) will also cut down approximately 29% of wastewater that is discharged to the county utilities authority each day.

An additional note on Figure 20: a greater flowrate than 100,000 GPD would be fed to each recovery system. The recovery systems will be designed to operate with a selected recovery goal (e.g. water recovery is 80-90% of the entering flow of wastewater). Thus, there will be a reject stream that returns to either the wastewater pretreatment processes or the to the wastewater effluent. This is shown for each recovery system in Figure 20; however, the feed and reject flowrates are not given for the recovery systems. They will be determined in the scale-up design calculations in later sections.

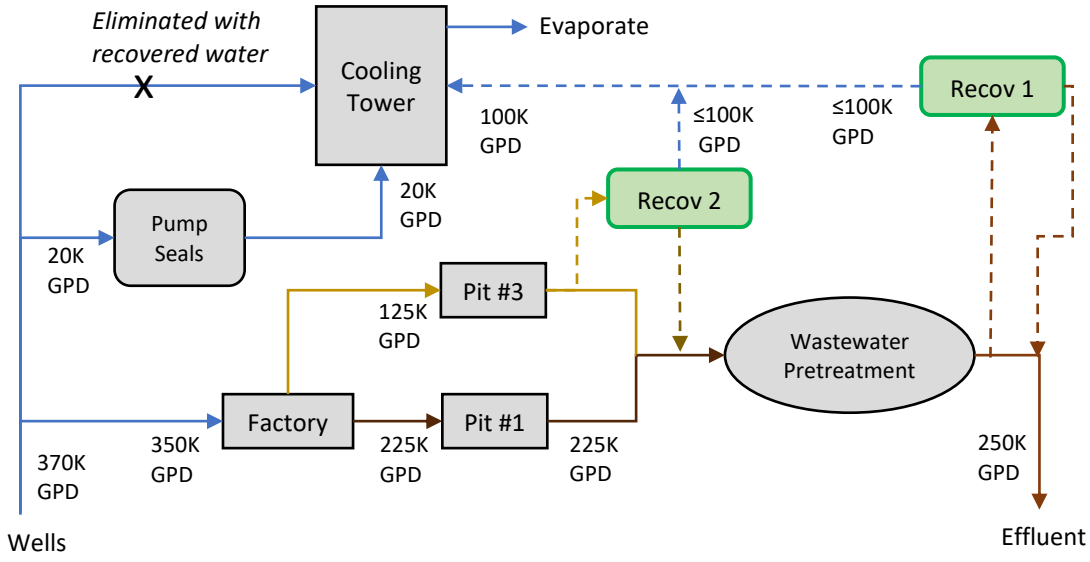

Figure 20. Flow diagram of the Nestlé process with proposed areas for intervention for water recovery

Chapter 7

Experimental Analysis of Water Recovery – Pit #3 Wastewater

Experimental analysis of recovering the Nestlé process wastewater began with evaluating separation techniques for the purification of the Pit #3 wastewater. The Pit #3 wastewater has lower concentrations of the major contaminants. Moderate COD concentrations can be caused by various organic aroma compounds in the wastewater. The concentrations of contaminants present in the wastewater are variable because of production; however, typical concentration ranges for the Pit #3 wastewater are shown in Table 23. Experimentation began with simpler separation methods – slow sand biofiltration and adsorption. Preliminary assessment of ozonation for purification has also been conducted. Actual concentrations of the Pit #3 wastewater are provided as necessary for the processes discussed.

Table 23

Typical concentrations of major contaminants in the Pit #3 wastewater

COD	510 – 1,200	mg/L
Turbidity	13 – 30	NTU
Conductivity	312 – 1,280	µS/cm

Slow Sand Biofiltration

This separation was selected for the Pit #3 wastewater because of its simplicity and cost-effectiveness. As shown in the background section, this process has been effective in reducing the COD, BOD, and TSS in food wastewater streams.

A laboratory-scale slow sand biofiltration system was assembled for experimentation. The system, shown in Figure 21, was designed based on industrial slow sand filtration rates. Typical filtration rates are between 0.04 to 0.10 GPM/ft^2 [50]. The bed diameter was selected so an appropriate flowrate could be used. An acrylic tube with an inner diameter of 4.03 in was used for the bed housing. Thus, a flowrate between 3.54×10^{-3} – 8.86×10^{-3} GPM (13.4 – 33.5 mL/min) would be used for the column. The column is composed of three sizes of gravel and fine grade sand that was washed. The gravel was sieved in the lab using 1.00 in, 0.75 in, No. 4 (about 3/16 in), and No. 10 (about 5/64 in) US standard size sieves. The three sizes of gravel that remained between the four sieves was used. Equal heights of about 1.5 in of each size of gravel were used to support the sand bed. The height of the sand bed was 19 cm. To wash the sand, a 5-gal bucket was filled with sand, and water was added and stirred. The sand settled, and the water was poured off. This process was repeated several times, each time the water getting clearer. Approximately 4 washings were required, with the water after a fourth washing being almost completely clear.

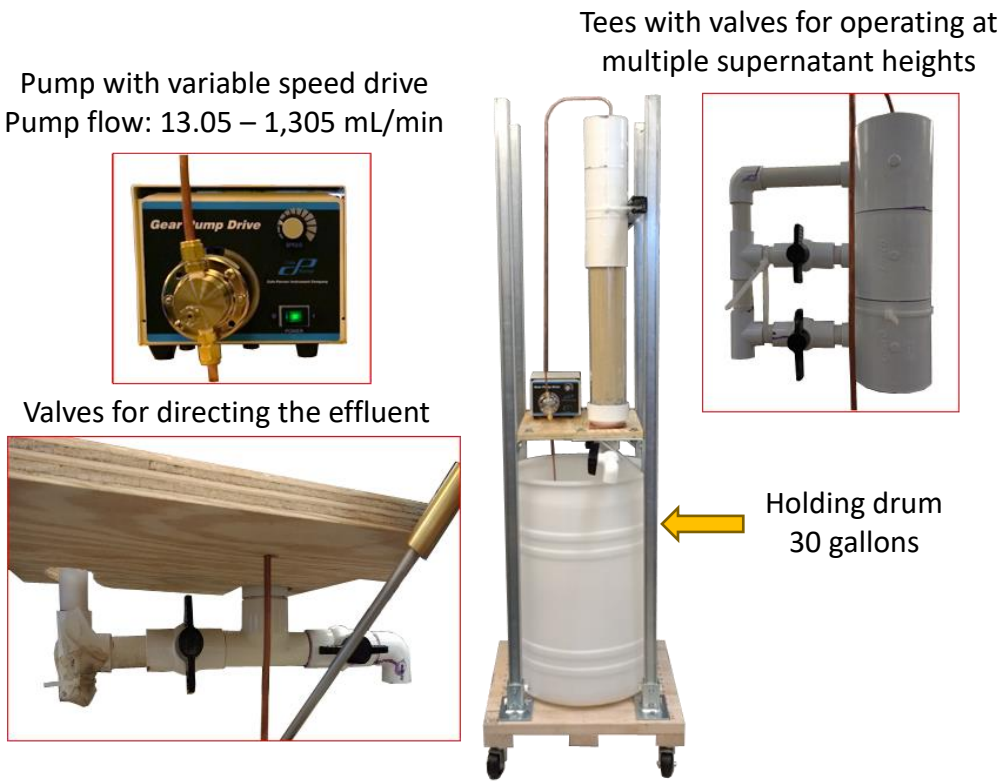

Figure 21. Photos of various parts of the fabricated slow sand biofiltration unit

The pump is a gear pump with a variable speed drive. The variable speed drive allows for operational flow rates between 13.05 and 1305 mL/min. Additionally, the tees were designed to allow for operation at supernatant heights of about 2, 4, or 6 in. Different supernatant heights were intended to control the effluent flowrate by supplying varying amounts of head. At the bottom of the column, there are two valves to direct the effluent. The effluent can be directed back into the 30 gal holding drum or out of the system for sampling.

Pit #3 wastewater was continuously fed to the slow sand biofiltration unit for 21 days. Samples were taken 2-3 times a day. A COD measurement was conducted for each sample following the closed reflux, colorimetric method (standard method 5220 D

in Standard Methods for the Examination of Water and Wastewater) [110]. The data were plotted as a function of time to determine the formation of the schmutzdecke (biologically-active layer), as shown in Figure 22. It is apparent the system is capable of reducing the COD of the coffee wastewater. The COD of the coffee wastewater feed was 1,900 mg/L. The COD slowly decreased for a period of approximately 11 days. After 11 days, a new steady state COD of 1,100 mg/L was reached. This indicated schmutzdecke formation, being that the schmutzdecke is responsible for most of the COD removal. Once the effluent reached a steady state minimum, the schmutzdecke had formed. It should be noted that this COD concentration is uncommonly high for the Pit #3 wastewater stream. The exact cause of this is unknown; however, it is expected that it is reflective of the particular production from the plant the day the sample was obtained.

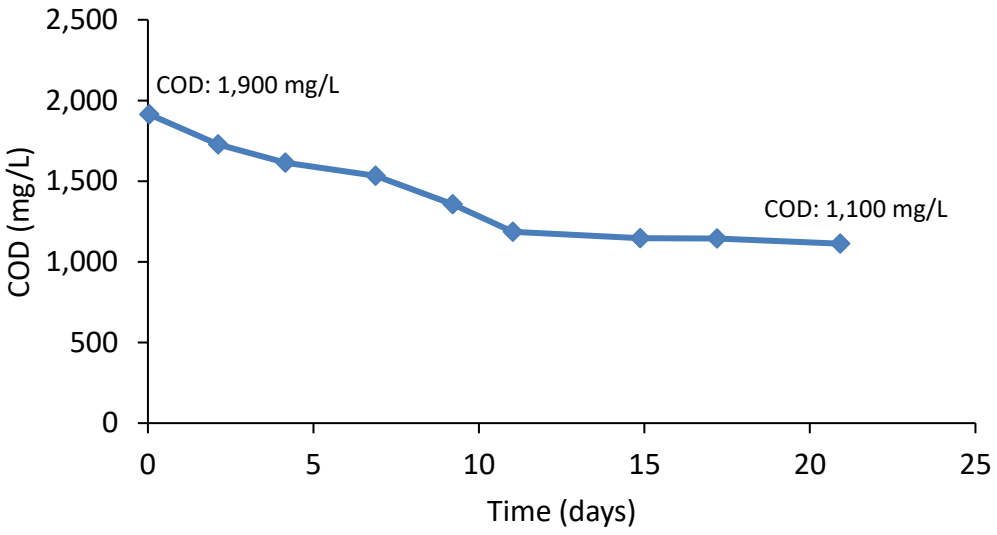

Figure 22. Plot of sample COD as a function of time for slow sand biofiltration

The rejection of COD was calculated as the amount of COD removed divided by the initial COD (shown in Equation 50). COD rejection in this system was approximately 42%. Thus, this separation process, on its own, has little potential for the purification of coffee wastewater to reuse standards for the cooling tower. Due to the limited removal of COD, further analysis of other performance metrics, e.g., turbidity and conductivity, were not undertaken. This process might be an appropriate pre-purification process to reduce the COD before more expensive or complex processes are used.

$$COD\ Rejection\ (\%) = \frac{Feed\ COD\ \left(\frac{mg}{L}\right) - Final\ COD\ \left(\frac{mg}{L}\right)}{Feed\ COD\ \left(\frac{mg}{L}\right)} \times 100\% \qquad (50)$$

Adsorption

Adsorption was selected for the Pit #3 wastewater stream since this technology is known to remove organic contaminants and this stream has a low concentration of suspended solids. Previous studies for coffee wastewater purification for reuse were conducted using adsorption with favorable results. More details on this study and information on adsorption can be found in the background section for adsorption.

An isotherm study was conducted to understand the capacity of the adsorbent for the contaminants in the Pit #3 wastewater. The adsorbent used in this study is activated carbon. The type of carbon used in these studies is untreated, granular, 8 – 20 mesh activated charcoal (available from Sigma-Aldrich, Inc.) [111]. To develop an isotherm, samples were prepared with various concentrations of activated carbon in the Pit #3 wastewater. Samples were prepared via one of two methods:

1. Dilute the coffee wastewater with deionized water and use a constant mass of activated carbon in each sample.
2. Use various masses of activated carbon in a specified volume of Pit #3 wastewater.

By diluting the coffee wastewater, additional concentrations of the wastewater can be studied. Therefore, data points on the low concentration end of the isotherm can be obtained. The second method allowed for obtaining data points for the actual wastewater, which were expected to be on the higher concentration end of the isotherm because deionized water was not added to the samples. The samples were continuously shaken for 48 hrs at room temperature. The samples were then filtered with a 0.45 µm syringe filter to remove any carbon in the sample. The COD of each sample was measured using standard method 5220 D [110].

The adsorptive capacity, q, represents the ability of the adsorbent (e.g. activated carbon) to remove contaminants in the coffee wastewater. In this case, the adsorptive capacity is determined for the COD in the coffee wastewater. To calculate the adsorptive capacity, Equation 51 is used.

$$q = \frac{COD\ Concentration\ Adsorbed}{Concentration\ of\ Activated\ Carbon} = \frac{C_{Adsorbed}}{C_{Adsorbent}} = \left[\frac{{}^{mg}/_{L}\ COD}{{}^{mg}/_{L}\ adsorbent}\right] \quad (51)$$

Where, the COD concentration that is adsorbed is calculated in Equation 52.

$$C_{Adsorbed} = C_{Feed} - C_{eq} = COD_{initial} - COD_{final} \quad (52)$$

And C_{eq} is calculated using Equation 53.

$$C_{eq} = Equilibrium\ Concentration = Final\ COD\ concentration \quad (53)$$

The isotherm curve is generated by plotting the adsorptive capacity (q) vs the equilibrium COD concentration (C_{eq}). Figure 23 shows this curve. From the isotherm, it can be determined that the activated carbon (AC) shows a moderate adsorptive capacity for the COD of the Pit #3 wastewater. The value, q_{max}, represents the maximum adsorptive capacity for the activated carbon. As can be observed, the q_{max} for this system trends towards 0.07 ((mg COD/L)/(mg AC/L)). Typically, the q_{max} value is around 0.10 ((mg COD/L)/(mg AC/L)) for systems which the adsorbent has a moderate to high adsorptive capacity [112]. Thus, it can be determined that for every mg COD/L removed, a loading of about 14 mg AC/L would be required.

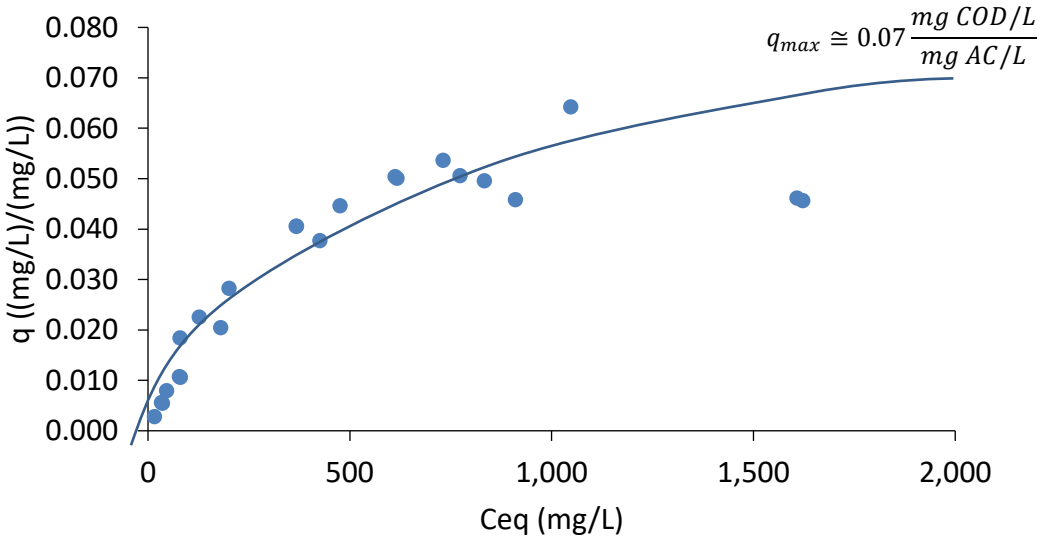

Figure 23. The isotherm curve for the Pit #3 wastewater with activated carbon as the adsorbent; AC – activated carbon

Further adsorption studies regarding continuous operation were conducted. It has been shown that activated carbon has a moderate adsorptive capacity for the COD in the Pit #3 wastewater stream. But there are limitations in this technology, as it does not typically remove ionic contaminants that comprise the conductivity, and its efficiency in continuous operation with traditional adsorbents can be greatly affected by turbidity in the feed. In addition, a continuous operation would either need to desorb the contaminants to reuse the carbon, or the implications of carbon waste and virgin carbon purchase would need to be considered.

Preliminary laboratory-scale continuous column operation was performed to determine when column breakthrough occurs. This study was hampered by several factors. First, the complex characteristics of the feed (colloidal and dissolved organic and inorganic impurities) make column adsorption with traditional granular activated carbon slightly challenging. Secondly, previous studies on wastes with these characteristics makes design, even for a laboratory-scale apparatus challenging. For instance, one cannot rely on readily available design protocols used in drinking water treatment. Initial column studies focused on flow dynamics.

Preliminary continuous column studies were conducted using activated carbon in a 2.1 in diameter glass column. Initially, a low-flow peristaltic pump was used to feed the Pit #3 wastewater to the top of the column. The column experienced issues of clogging, generating a build-up of wastewater above the activated carbon bed. The following trial was conducted by pouring the Pit #3 wastewater above the activated carbon, employing gravity to induce the flow of the Pit #3 wastewater through the column. The depth of the bed of activated carbon was 4.25 in. The removal of COD was

monitored during the testing. Clogging became an issue again, causing very low flowrates exiting the column. This caused an extensive period of time to be required for column breakthrough. It appears that the complex nature of the waste may not be conducive to using traditional packed bed adsorption.

The study was conducted for a period of 17 days, with a sample taken once, and sometimes twice a day. The study was ended because the flowrate of the column effluent decreased drastically. Figure 24 shows the results of the continuous column study. Breakthrough should occur once the column has become saturated with the COD from the Pit #3 wastewater, and the COD of the column effluent becomes equal to the feed concentration. It should be noted that the COD concentration of the Pit #3 wastewater is slightly higher than is typical, at 1,400 mg/L. The column effluent appears to trend to the feed concentration by the end of the study. Since breakthrough did not occur, it is expected that the clogging took place in the glass support plate at the bottom of the column, and not within the activated carbon bed. The flow was so low as to keep the column unsaturated for the period of the study.

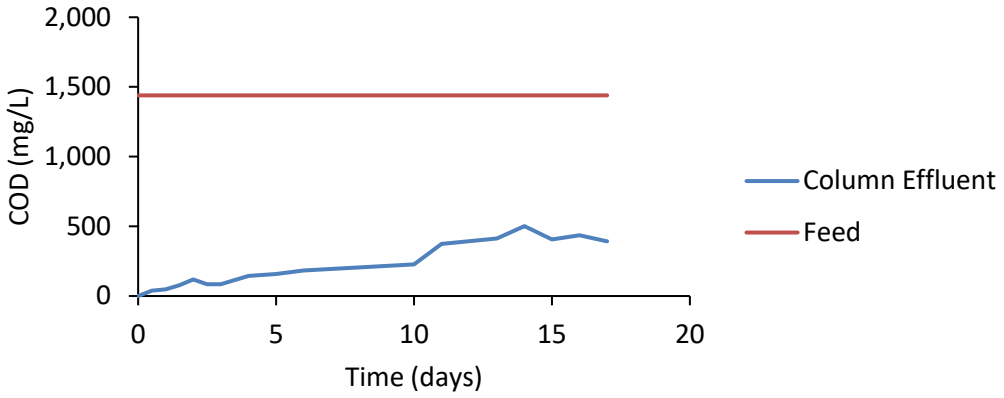

Figure 24. COD concentration results of the continuous adsorption column study

From Figure 24, it can be seen that the activated carbon column confirms a moderate capacity to adsorb to COD from the Pit #3 wastewater. This confirms the results from the isotherm study conducted prior. There were inconclusive results for the removal of conductivity, and it appears the column was successful in removing the turbidity, although that is at the expense of the column clogging.

Ozonation

Research for a laboratory-scale ozonation process was conducted and the apparatus was constructed. Research included a literature review of current laboratory ozonation experiments explained in research papers, as well as a review of vendors for possible equipment. A schematic of the constructed system is shown in Figure 25. The system is run in batch-mode and ozone is generated from air. Since experimentation in this process is preliminary, the results are limited. A full-scale set of experiments was not conducted for the Pit #3 wastewater; however, three experimental conditions were identified for consideration. They are: time, ozone concentration/feed rate, and initial wastewater concentration (mainly, COD).

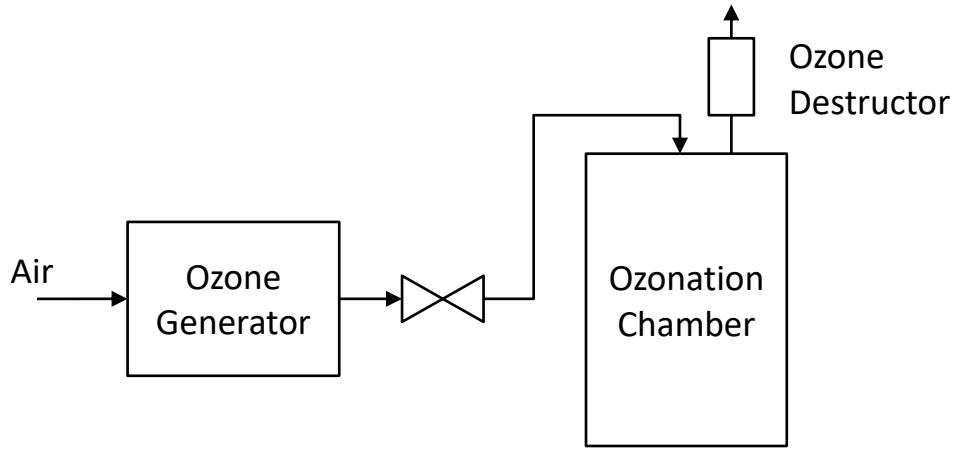

Figure 25. Schematic of the laboratory-scale ozonation system

The ozone generator used in the laboratory-scale system is an Enaly 1KNT-24, available from Oxidation Technologies, LLC (Inwood, IA). A picture of set-up is shown in Figure 26. The system is capable of producing ozone from a feed gas of pure oxygen or air. In this case, air is used as the ozone source since it is readily available. The maximum ozone production from air that the generator can achieve is 0.82g O_3/hr at an air feed flowrate of 4 L/min. The ozonation generator is connected to a glass ozonation chamber (also provided by Oxidation Technologies, LLC.). The chamber has a total capacity of 1.7 L. Ozone is distributed in the chamber via a diffuser stone. To ensure an adequate dispersion, a stir bar was placed in the chamber and the chamber was placed on stirring plate. Any ozone that did not react is destroyed by a carbon-based ozone destructor at the outlet of the chamber. As an additional safety precaution, all ozonation tests were conducted under a laminar flow hood.

Figure 26. Laboratory-scale set-up of the ozonation system

To test the ozonation system, a trial run using green dye was performed. One liter of deionized water was added to the ozonation chamber and green dye was added until a deep green color was present. After 7 minutes of run time, the water in the ozonation chamber was visually clear. This preliminary test shows that color removal can be achieved through ozonation, which also agrees with the literature. Ozonation has limitations in handling inorganic salts. Based on the principles of ozonation, the ozone molecules only destroy organics and biological components. The process may actually raise the conductivity of the recovered water since CO_2 and other intermediates are formed when the organics and biological components are broken down [113].

Chapter 8

Membrane Separation Assessment

Membrane separation processes were selected for the plant effluent since they provide a tunable technology – one that will be able to be adjusted for the performance required. This will enable the design of a system that can accommodate the variable concentrations of the plant effluent. The plant effluent is complex; it contains dissolved and suspended solids and organic and inorganic compounds. A typical composition range of contaminants is presented in Table 24; individual plant lots may vary depending on plant production. Reuse specifications of the water that is reclaimed must be met for use in the cooling tower. COD and suspended solids must be appreciably removed, and the conductivity must be below 300 µS/cm.

Table 24

Typical range of contaminants concentrations in the plant effluent

COD	1,400 – 2,000 mg/L
Turbidity	20.4 – 40 NTU
Conductivity	4,900 – 8,200 µS/cm

Membranes can be used for a spectrum of separation capacities, as described in the background information section. To fully understand the efficacy of membranes for the purification of this wastewater effluent, a range of membranes were tested in a screening study. This allows the matching of the specific membrane to the level of purity of the recovered water desired. Once it was determined which membranes produced the

best results (explained in the following section), process evaluations were performed using those membranes. Such studies include operating parameter studies and unsteady state process experiments.

The membrane separation system being used is the V-SEP L-101 from New Logic Research, Inc. A picture of the system and an enlarged diagram of the membrane housing are shown in Figure 27. The system is a laboratory-scale vibratory membrane unit capable of testing microfiltration, ultrafiltration, nanofiltration, and reverse osmosis membranes. It can be operated in standard cross-flow filtration and dynamic vibratory filtration. This laboratory-scale system is capable of testing one membrane with a surface area of 0.48 ft^2. Pilot-scale and commercial-scale units are capable of operating with multiple membranes for high flow systems. Performance results with individual membranes serve the basis for scale-up. Maximum operating temperature and pressure for this unit are 79 °C and 1,000 psig, respectively. When vibration is used, maximum shear rates range from 19,500 – 101,000 s^{-1}. Shear rates are selected by setting a specified vibrational displacement, *d* (as described in the background information section). Displacement values range from 0 in (no vibration) to 1.25 in by increments of 0.25 in. The greater the vibrational displacement, the greater the shear rate that can be achieved. Feed flowrates can range from 1 – 5 GPM.

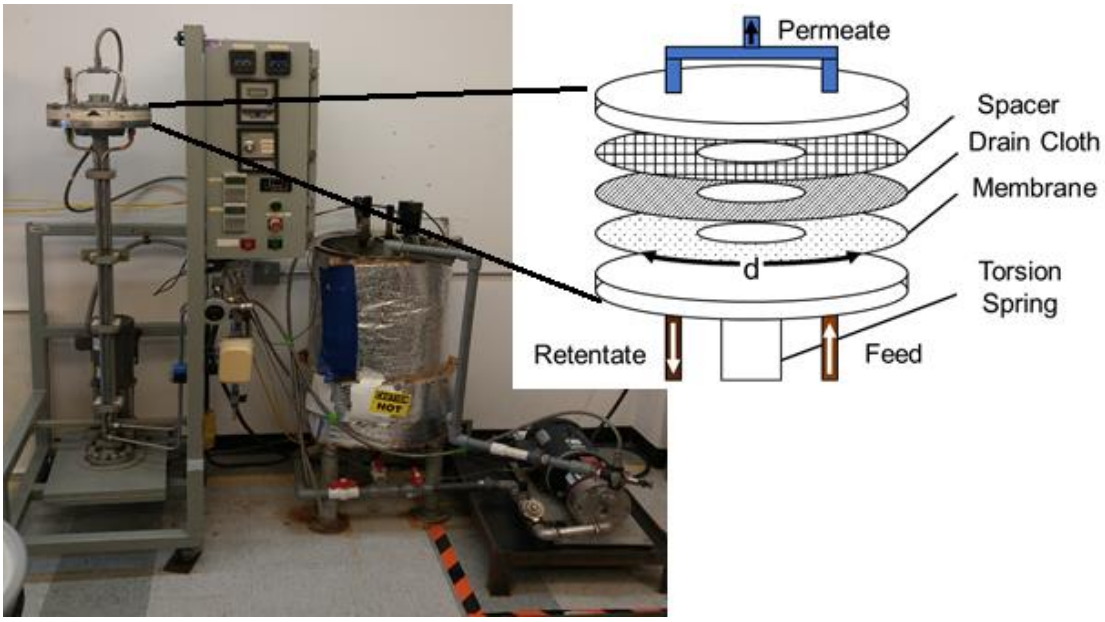

Figure 27. Photo of the V-SEP L-101 membrane system

Preliminary Membrane Separation Screening

The membrane screening study consisted of testing a range of membranes based on their separation capabilities. Screening study experiments were performed in standard cross-flow filtration (e.g. no vibration used). Experiments were run for 60 minutes. Temperature was maintained between 20 and 25 °C. Operating pressure varied among the membranes and was characteristic of the class of membrane they were; operating pressures can be observed in Table 25. A concentrate flowrate of 2 GPM was maintained in each run; the feed flowrate can be assumed at 2 GPM since the permeate flowrate is much smaller than the concentrate. A benchmark flux value was obtained and an analysis of the concentrations of the key contaminants was conducted. Flux values were compared, and higher values were favored. Those membranes that gave suitable contaminant rejections were also favored and considered for further testing.

Table 25

Operating pressure and membrane specifications for each type of membrane in the preliminary screening study

Membrane Type	**Manufacturer**	**Model**	**Operating Pressure (psig)**	**Pore Size / Molecular Weight Cut-off**
Microfiltration	Nadir	MP005	50	0.05 µm
Ultrafiltration	Ultura*	PES-5	150	7,000 Da
Nanofiltration	Ultura*	NF-4	350	225 Da
Reverse Osmosis	Hydranautics	LFC-3	350	30 Da

* Ultura was acquired by Nanostone Water in 2015 [114]

Table 26 provides a summary table of the results of the membrane screening study. As can be seen, the benchmark flux values at 60 minutes show similar results. The nanofiltration and reverse osmosis membranes achieved the highest flux values among all membranes. This would not typically be expected since these membranes are characterized by the smallest nominal pore sizes; however, a higher operating pressure was used in these runs. Thus, it can be expected that operating pressure contributes significantly to the flux that can be achieved.

Table 26

Comparison of flux values at 60 minutes and final permeate concentrations of major contaminants

Membrane Type	Flux (GFD)	COD (mg/L)	Conductivity (µS/cm)	Turbidity (NTU)
Microfiltration	12.4	441	3,585	1.42
Ultrafiltration	15.5	153	3,385	1.05
Nanofiltration	24.4	40	2,080	0.395
Reverse Osmosis	16.6	~0	63	0.164

Figure 28, Figure 29, and Figure 30 provide a graphical comparison of the degrees of contaminant removal among each type of membrane. Figure 28 shows clearly that COD removal increases from microfiltration to ultrafiltration. The nanofiltration and reverse osmosis membranes show almost complete removal of the COD from the wastewater. It was observed that all membranes provided sufficient turbidity removal, shown in Figure 29. The lowest turbidity removal from the plant effluent was 93%, with the microfiltration membrane. This shows that using a membrane process if effective in removing the suspended solids from the plant effluent. A different case is observed for the removal conductivity, seen in Figure 30. Both the microfiltration and ultrafiltration membranes only removed 27% and 31% of the wastewater conductivity, respectively. The nanofiltration membrane provided a conductivity removal of 58%. This is a greater removal than the microfiltration and ultrafiltration membranes; however, the nanofiltration membrane no longer provides a similar removal to the reverse osmosis membrane. The reverse osmosis membrane removes almost 99% of the plant effluent conductivity.

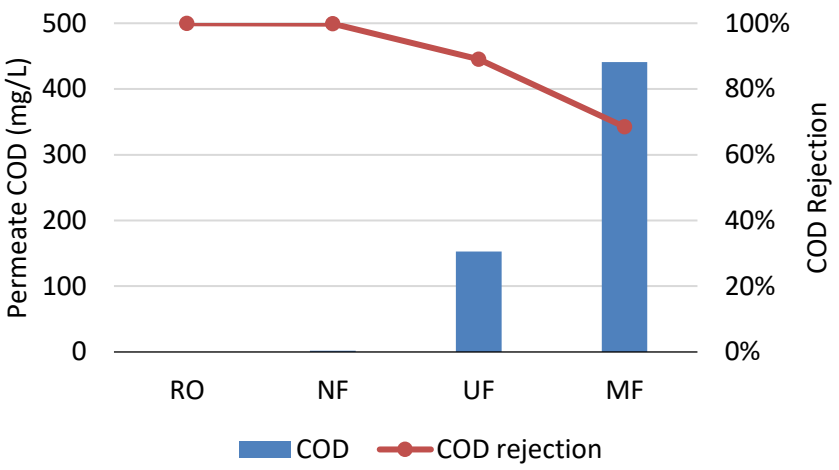

Figure 28. Membrane screening study results of COD removal from the plant effluent wastewater; MF – microfiltration, UF – ultrafiltration, NF – nanofiltration, RO – reverse osmosis

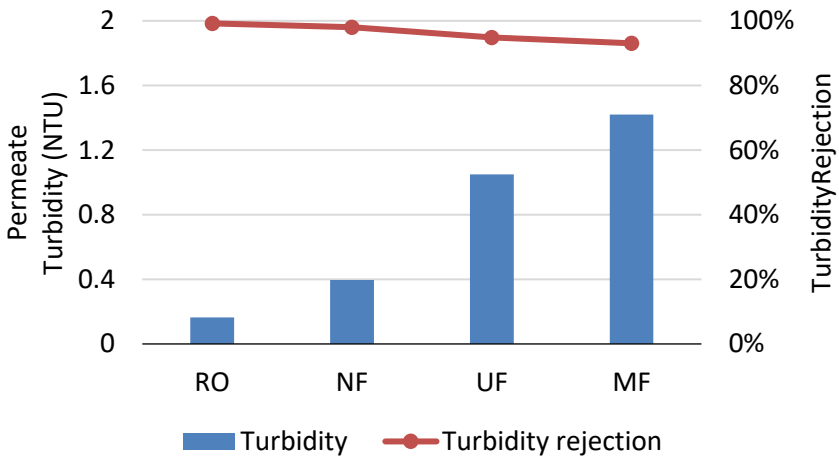

Figure 29. Membrane screening study results of turbidity removal from the plant effluent wastewater; MF – microfiltration, UF – ultrafiltration, NF – nanofiltration, RO – reverse osmosis

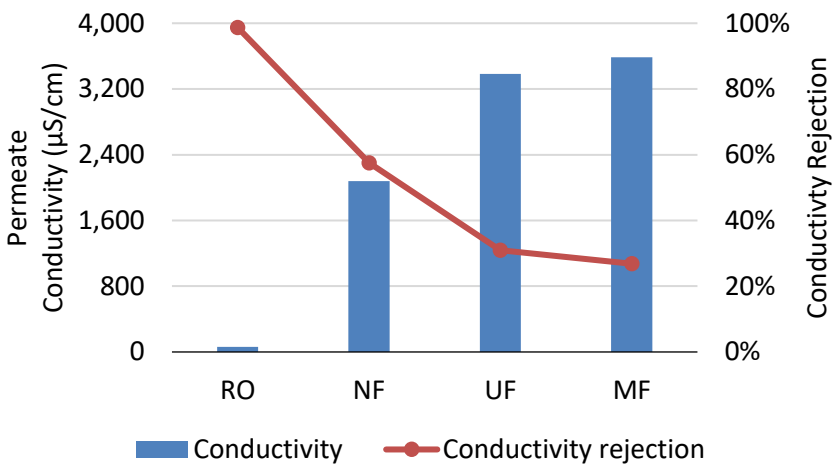

Figure 30. Membrane screening study results of conductivity removal from the plant effluent wastewater; MF – microfiltration, UF – ultrafiltration, NF – nanofiltration, RO – reverse osmosis

Since it was observed that similar benchmark flux values can be achieved for each membrane type, consideration on contaminant rejection was emphasized. The plant effluent is a complex waste stream with varying levels of fine particulates and colloidal matter as well as dissolved organics and inorganics, which are dependent on daily production. Degrees of rejection that were observed among the membranes were as expected. A summary table of the results comparing each membrane's capabilities is given in Table 27. Contaminant rejections were lowest with the microfiltration membrane and increased as the pore size/molecular weight cut-off decreased. The best rejection of contaminants was observed with the reverse osmosis membrane; however, the nanofiltration membrane provided excellent COD and turbidity rejections and moderate conductivity rejection. Water reused for utility generation at the Nestlé Freehold plant is required to have turbidity and COD removed to prevent potential scaling in the lines. While all membranes provide a good rejection of turbidity, it would

be recommended that the nanofiltration or reverse osmosis membranes would be more reliable to remove suspended solids from the wastewater. These membranes provided the highest turbidity rejection (Figure 29), and the wastewater is prone to changes in concentrations. Again, these membranes are the better options compared to the microfiltration and ultrafiltration as they provide very high and similar COD rejections (both above 97%). Water reused for utilities generation is also required to be at a conductivity of 300 µS/cm for appropriate cooling tower operations. The reverse osmosis membrane reduces the conductivity below the specification, while the nanofiltration membrane reduces the conductivity moderately, but is above the specification. It was determined that further studies would be conducted on both the nanofiltration and reverse osmosis membranes.

Table 27

Summary table of removal efficiencies for the membranes evaluated in the initial screening study

	Microfiltration	Ultrafiltration	Nanofiltration	Reverse Osmosis
Dissolved organics (COD)	L	M	H	H
Colloidal/fine particulates (turbidity)	M*	H*	H*	H*
Suspended large particulates (turbidity)	H*	H*	H*	H*
Dissolved inorganics (conductivity)	L	L	M	H

L = low removal efficiency
M = moderate removal efficiency
H = high removal efficiency
* would require vibratory membrane operation to prevent fouling

Vibratory Membrane Separation – Plant Effluent

As discussed in the background information section of this project, fouling is a key concern in membrane separation operations. This is especially true for complex waste streams, such as this one, where both surface fouling and inner pore fouling can occur from suspended solids and colloidal matter. Figure 31 shows a picture displaying the difference in membrane appearance when conventional cross-flow filtration (no vibration) is used and when vibration is introduced. The membrane shown in Figure 31 is a nanofiltration membrane. For the used membranes in Figure 31, process conditions were: an operating pressure of 350 psig, temperature between 20 – 25 °C, feed flow rate of 2 GPM, and a maximum shear rate of 80,500 s^{-1} when vibration was used. As can be seen, when there is no vibration, fouling occurs on the membrane surface. The fouling is mostly surface fouling, which the V-SEP is especially effective at reducing. Some inner pore fouling has occurred. Inner pore fouling can also be avoided by using vibration since the high shear zones prevent contaminants from being near the membrane surface. When vibration is used, the membrane had very minimal surface fouling.

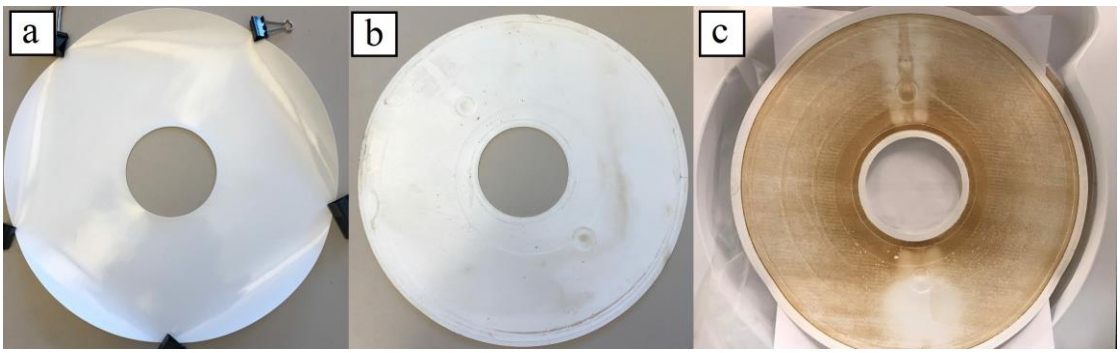

Figure 31. Comparison of membranes for the V-SEP L-101 system; (a) new membrane, (b) membrane after 2 hours of running with vibration, (c) membrane after two hours of processing without vibration

Fouling must be overcome in large scale industrial processes since flux decay quickly becomes an issue. As stated, the complex nature and magnitude of the coffee wastewater effluent present a prominent issue of fouling. Without the use of vibration, frequent cleaning cycles will be required to keep process performance adequate. This will accumulate to a significant amount of time and expenses to recover water from the wastewater effluent. In addition, a much larger membrane system – in terms of membrane area and plant footprint – will be required to achieve similar throughputs than will be needed by a commercial V-SEP unit. The results from the membrane screening study show that the recovery process will need to have a nanofiltration or reverse osmosis membrane to achieve desired levels of water purity. Thus, high pressures will be needed to operate the system. If the system is run in conventional cross flow filtration and is large, operating costs will be significant. However, a previous study using V-SEP in an industrial food wastewater effluent has shown that energy requirements are kept reasonable compared to cross-flow, even in high pressure systems such as nanofiltration [88].

The vibratory membrane process evaluation for the nanofiltration and reverse osmosis membranes consists of various process parameters. Process parameter studies include studying the effect of temperature, pressure, and vibration (shear) on flux and contaminant rejection performance. It is necessary to study the effect of all process parameters to design an optimized system. For example, it might be that the highest shear rate might only increase flux by only a few percent, but to attain that amount of shear, 20% more energy may be needed. Therefore, it is important to understand how all parameters effect flux and the rejection of the primary impurities (COD, turbidity,

conductivity). A study with varying feed concentration levels by an unsteady state concentration experiment has also been performed. This has simulated high feed concentrations that a commercial membrane system that would run with high recoveries.

The temperature study was conducted first to begin the process parameter studies. The main objective of the temperature study for each membrane is to normalize the flux data to one temperature. The temperature study was conducted for both the nanofiltration and reverse osmosis membranes. The temperature chosen is 25°C. To achieve elevated temperatures for the vibratory membrane system, a PID-controlled jacketed heater was used. Flux readings were recorded at each degree Celsius. The correlation between flux and temperature was found to be linear in the temperature range tested for the nanofiltration membrane (Figure 32). Since the linear correlation is strong, extrapolation of flux values for temperatures reasonably outside of the tested range are fair estimates.

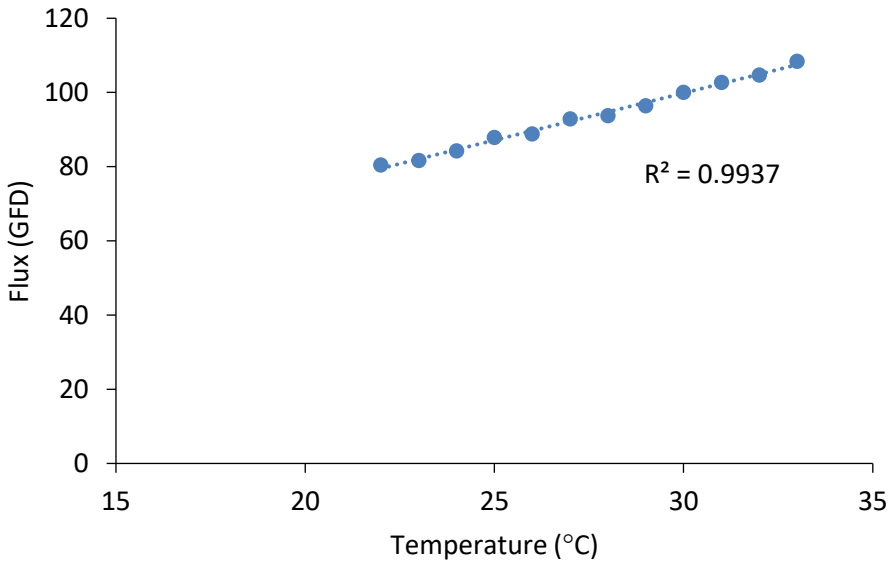

Figure 32. Permeate water flux as a function of temperature for the nanofiltration membrane, 350 psig

Figure 33 shows the relationship of flux with temperature for the reverse osmosis membrane. Again, there is a strong linear correlation for flux as a function of temperature, so flux values out of the data range can be feasibly predicted. The same methodology was used to obtain temperature study data for the reverse osmosis membrane as was used for the nanofiltration membrane.

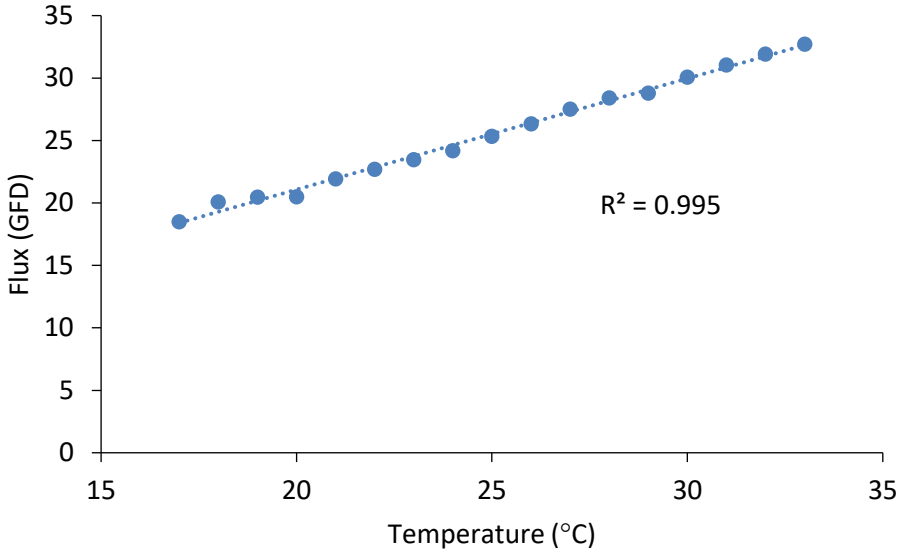

Figure 33. Permeate water flux as a function of temperature for the reverse osmosis membrane, 350 psig

This correlation was used to correct flux values recorded at different temperatures for the respective membranes. Equation 54 was used to correct the flux data.

$$Flux\ (GFD)_{T=25°C} = Flux\ (GFD)_{T(°C)} \times \frac{Water\ Flux\ (GFD)_{T=25°C}}{Water\ Flux\ (GFD)_{T\ (°C)}} \qquad (54)$$

Preliminary experiments pertained to observing the effect of vibration on flux and contaminant rejection performance. It was expected that the introduction of vibration would enhance flux, as described in the background section. Figure 34a and b show preliminary results for the effect of vibration on flux for the nanofiltration and reverse osmosis membranes. Both experiments were run at a pressure of 350 psig and temperatures were corrected to 25 °C using the respective membrane temperature correlation data. Runs were conducted for 120 minutes to achieve a steady state flux value. The maximum shear rate on the membrane surface was set to 80,500 s^{-1}. As can be seen, the flux is enhanced for both types of membranes. For the nanofiltration membrane, the steady state flux increased from 18.7 GFD to 85.2 GFD, or a factor of 4.56. For the reverse osmosis membrane, steady state flux increased from 15.9 GFD to 25.2 GFD, or a factor of about 1.58. These results agree with theory and background literature. A previous study for dairy wastewater purification by vibratory membrane separation has shown enhancements in flux by factors of 3 and 2 for nanofiltration and reverse osmosis membranes, respectively. Thus, it can be reliably expected that flux can be enhanced by introducing high shear zones by vibration.

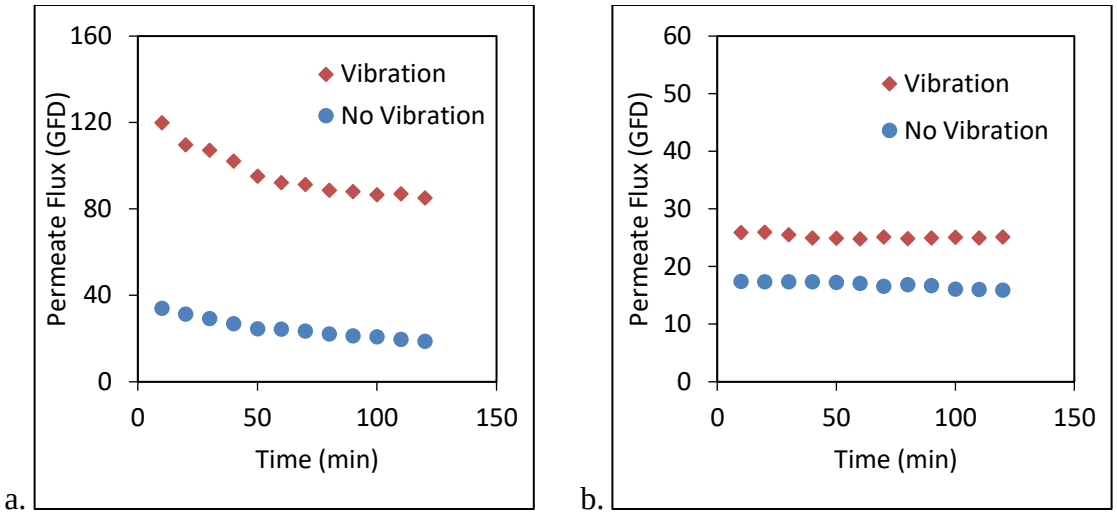

Figure 34. Flux as a function of time for the (a) nanofiltration membrane and the (b) reverse osmosis membrane

The pressure study consisted of observing the effect of pressure on flux performance both with and without vibration. The vibration for the pressure study was run with a set maximum shear rate of 80,500 s^{-1}, or, 1 in vibrational displacement. Figure 35a and b show the results of the pressure study, as well as the water flux for the nanofiltration and reverse osmosis membranes. Temperature was corrected to 25 °C for all flux values appropriately. It can be observed that the effect of pressure is nearly insignificant when vibration is not used. The steady state flux shows essentially no increase past 250 psig when processing with the nanofiltration membrane. Likewise, the flux does not show any significant increase after a pressure of 350 psig for the reverse osmosis membrane. This is caused by the gel layer resistance becoming the controlling factor for flux. At this point, increasing the pressure will have a negligible effect on increasing the flux. Conversely, with the introduction of vibration, the high shear rates combat the fouling formation of a gel layer resistance on the membrane surface. It can be

seen that the steady state flux continues to increase nearly linearly as the pressure is increased for both the nanofiltration and reverse osmosis membranes. Thus, there is no significant build-up of a gel layer on the membrane surface, and surface fouling is greatly reduced. This study indicates that when vibration is used, flux can be reliably increased and sustained as pressure is increased, following a direct pressure relationship transport model. While an increase is observed between pressures of 450 and 550 psig for the nanofiltration membrane, it is not significant. The best pressure for the nanofiltration membrane would be 450 psig since the increase in flux will most likely not economically justify the increase in pressure. This is not the case for the reverse osmosis membrane. The flux increases linearly up to 550 psig and may continue this trend at even greater pressures. An economic evaluation for the reverse osmosis membrane system would reveal the best operating pressure.

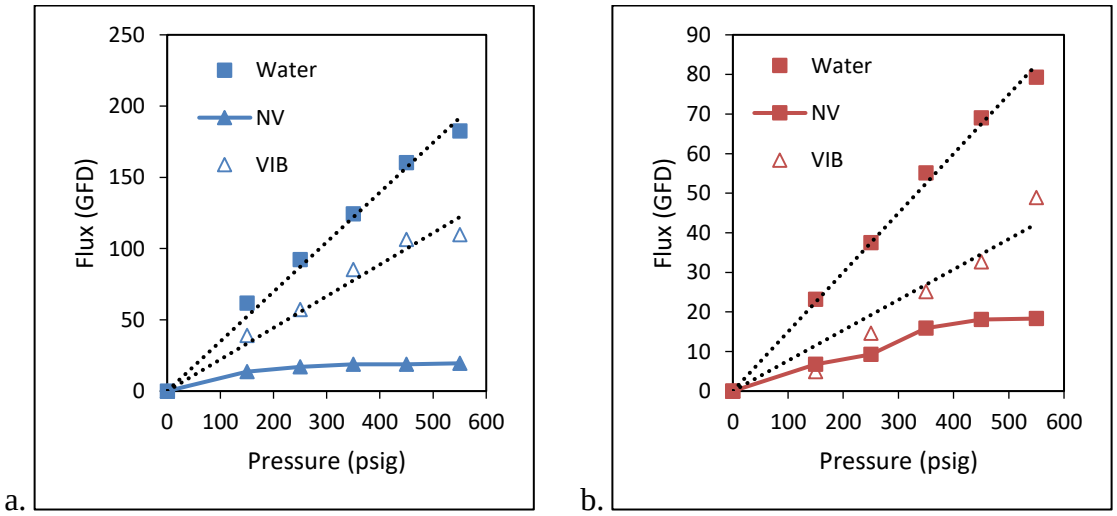

Figure 35. Permeate flux as a function of pressure for the (a) nanofiltration and (b) reverse osmosis membranes with no vibration (NV) and vibration (VIB)

Contaminant rejection is relatively unaffected when considering the change in pressure between runs. Table 28 shows a summary of the results of the pressure study, with and without vibration. As can be seen, rejections of COD and turbidity remained greater than 97% for both the nanofiltration and reverse osmosis membranes when vibration was introduced. As in the membrane screening study, conductivity rejection was the major difference in rejection performance between the membranes. Conductivity rejection remained above 98% for all tested pressures when using the reverse osmosis membrane with and without vibration. The nanofiltration membrane was only able to reject an average of 58% conductivity when vibration was not used. This average rejection was improved when vibration was used to 78%. A similar result was observed in a dairy wastewater vibratory membrane study [86]. Vibration increases the flux, thus, the volume of permeate that passes through the membrane increases. This effectively dilutes the permeate and reduces the concentration of contaminants like ions producing conductivity. Along with higher fluxes, the high shear rates are able to keep contaminants away from the membrane surface. The contaminants do not have the chance to leave in the permeate since they will be forced into the concentrate stream by shear.

Table 28

Summary table of the pressure study without and with vibration

	Nanofiltration					
	Without Vibration % Rejection			With Vibration % Rejection		
Pressure (psig)	COD Rejection	Turbidity Rejection	Conductivity Rejection	COD Rejection	Turbidity Rejection	Conductivity Rejection
150	97.3%	99.5%	54.5%	99.2%	99.7%	74.5%
250	97.6%	99.3%	54.4%	99.3%	99.8%	79.1%
350	97.3%	99.2%	56.7%	97.6%	99.7%	81.2%
450	97.5%	99.4%	59.2%	99.3%	99.4%	79.8%
550	97.5%	99.2%	60.6%	98.2%	99.7%	75.7%
	Reverse Osmosis					
	Without Vibration % Rejection			With Vibration % Rejection		
Pressure (psig)	COD Rejection	Turbidity Rejection	Conductivity Rejection	COD Rejection	Turbidity Rejection	Conductivity Rejection
150	99.9%	99.1%	98.6%	99.8%	98.1%	98.5%
250	99.6%	99.4%	99.0%	99.9%	99.3%	99.3%
350	99.9%	98.7%	99.1%	99.9%	99.5%	99.8%
450	99.8%	98.9%	99.0%	99.9%	99.6%	99.6%
550	99.9%	98.8%	99.2%	99.9%	98.0%	99.7%

The vibration study consisted of understanding how flux performance was affected by changing the maximum shear rate at the membrane surface. The maximum shear rate at the membrane surface can be calculated as shown in the background section on vibratory membrane separations. Shear rates are set by adjusting the frequency of the eccentric motor so that the membrane housing is vibrated at a set azimuthal displacement. The results of the vibration study are shown in Figure 36, given as flux as a function of the vibrational displacement (in). The results are also shown as flux as a function of the maximum shear rate in a semi-logarithmic plot in Figure 37. Operating pressure was set to 350 psig for all runs and temperature was corrected to 25°C. As can be seen, the steady state flux increases as the maximum shear rate increases for both membranes. The

increased shear rates decrease the chance of surface fouling on the membrane, and the permeate flux is increased.

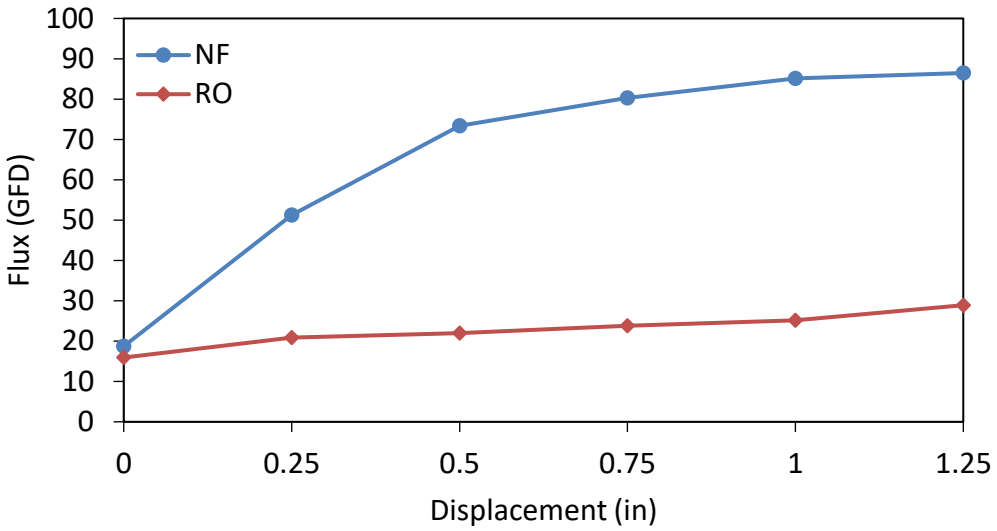

Figure 36. Steady state permeate flux as a function of the vibrational displacement; NF – nanofiltration, RO – reverse osmosis

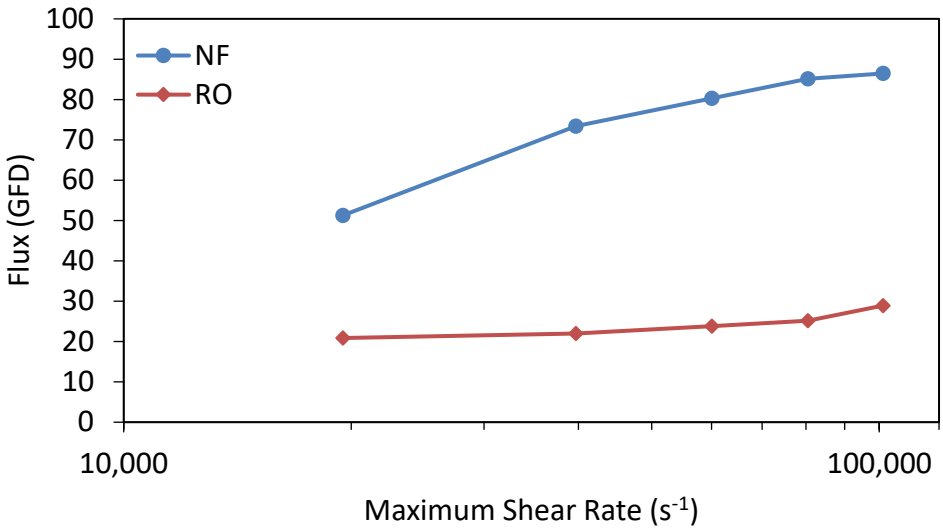

Figure 37. Steady state permeate flux as a function of the maximum shear rate at the membrane surface; NF – nanofiltration, RO – reverse osmosis

Flux performance is enhanced differently for each membrane. The nanofiltration membrane had a greater increase in flux when vibration was used. Flux increased sharply up to a vibrational displacement of 0.75 in and began to level off. At 0.75 in of displacement, the flux was increased by a factor of 4.30. At the maximum vibrational displacement of 1.25 in, the flux increased by 4.63. This is not an appreciable increase to warrant the additional energy required to vibrate the membrane. Therefore, it would be recommended to operate at a displacement of 0.75 in for a scaled-up process.

The reverse osmosis membrane showed a similar trend as in the time study. While vibration did provide an enhancement in flux, the effect was minor. In the vibration study, it was observed that the flux increased with an increase in the amount of vibration. The flux increased from a factor of 1.31 at 0.25 in of vibration (lowest setting) to 1.82 at 1.25 in of vibration (highest setting). It would still most likely be beneficial to have some

amount vibration to enhance the flux slightly. For example, at 0.75 in of vibrational displacement, the flux in is increased by 1.50.

Table 29 shows a summary of the results of the vibration study. The nanofiltration had favorable results for contaminant rejection. COD and turbidity rejection remained constantly high at above 97% and 99%, respectively. The introduction had a positive effect on conductivity rejection. This was observed in the pressure study and is confirmed here. Theoretically, a correlation between the degree of vibration and the rejection of conductivity (and other contaminants) should have been observed. Greater degrees of vibration result in higher shear rates at the membrane surface; higher shear rates would relate to more contaminants being kept away from the membrane surface. This was not observed in these studies; however, it can be concluded that any amount of shear via vibration reduces the amount of conductivity that permeates the membrane.

Table 29

Summary table of the nanofiltration and reverse osmosis vibration studies; all runs conducted with an operating pressure of 350 psig

Nanofiltration				
Vibrational Displacement (in)	Maximum Shear Rate (s^{-1})	COD Rejection	Turbidity Rejection	Conductivity Rejection
0	-	97.3%	99.2%	56.7%
0.25	19,500	97.2%	99.4%	72.2%
0.50	40,000	97.8%	99.7%	74.9%
0.75	60,000	97.0%	99.9%	70.0%
1.0	80,500	97.6%	99.7%	81.2%
1.25	101,000	97.6%	99.6%	75.2%
Reverse Osmosis				
Vibrational Displacement (in)	Maximum Shear Rate (s^{-1})	COD Rejection	Turbidity Rejection	Conductivity Rejection
0	-	99.9%	99.1%	99.1%
0.25	19,500	99.9%	99.5%	98.6%
0.50	40,000	99.9%	99.8%	99.7%
0.75	60,000	99.8%	99.6%	99.7%
1.0	80,500	99.9%	99.6%	99.8%
1.25	101,000	99.9%	99.8%	99.8%

Rejections of COD, turbidity, and conductivity were exceptionally high when using the reverse osmosis membrane with or without vibration. The membrane does very well in producing water of high quality. While minor, the biggest impact for processing with the reverse osmosis membrane is the enhancement in flux. It is important to note that for runs conducted with the reverse osmosis used a feed that differed in concentrations of contaminants. A new sample of wastewater was acquired for these runs. The concentrations are listed in Table 30. The greatest difference between feedstocks is the rise in conductivity. This increase is a result of attempting to match COD values to the original feed using concentrated plant effluent from the unsteady state concentration run. While there was a significant rise in conductivity, flux values and

contaminant rejections did not undergo a significant drawback. As stated earlier, there is lot-to-lot (day-to-day) variation in the waste samples depending on production schedules for the factory. It is almost impossible to have an exact feed composition each time, but all waste samples used have contaminant concentrations with an acceptable range.

Table 30

Concentrations of feed wastewaters used in the reverse osmosis vibration study

Vibrational Displacement (in)	Maximum Shear Rate (s^{-1})	COD (mg/L)	Turbidity (NTU)	Conductivity (µS/cm)
0	-	1,380	19.6	12,600
0.25	19,500	1,240	16.0	6,040
0.50	40,000	1,240	16.0	6,040
0.75	60,000	1,240	16.0	6,040
1.00	80,500	1,380	19.6	12,600
1.25	101,000	1,240	16.0	6,040

The V-SEP membrane process was run in an unsteady state mode to simulate high process recoveries. The process permeate was collected in a separate reserve tank while the process feed was concentrated. Throughout the run, the membrane was exposed to higher feed concentrations as more permeate was recovered. This allows one to observe the effect of higher feed concentrations on membrane performance – in terms of flux and contaminant removal. The operating pressure was maintained at 350 psig and the feed flowrate was held constant at 2 GPM. Flux values were corrected to 25°C using the temperature correlation. This study was conducted both in standard cross-flow filtration (i.e. no vibration) and vibratory filtration mode (1 in displacement). This study was also only conducted for the plant effluent with the nanofiltration membrane. Flux

performance was expected to be too poor if the reverse osmosis membrane was used. Figure 38 shows the instantaneous flux as a function of the percent recovery of the permeate. Percent recovery is defined in Equation 55.

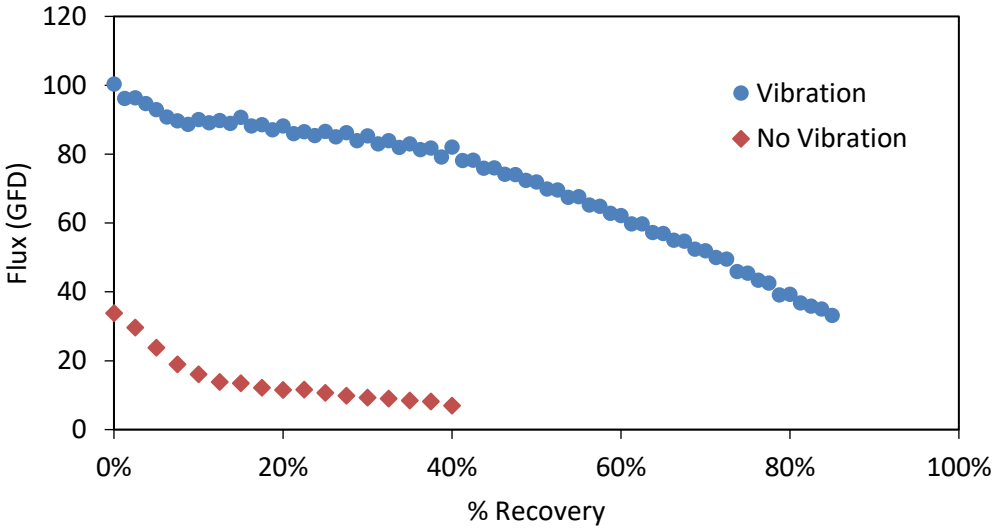

Figure 38. Instantaneous permeate flux as a function of percent recovery of permeate; nanofiltration, 350 psig

$$Percent\ Recovery\ (\%) = \frac{Total\ Permeate\ Volume\ Produced\ (L)}{Initial\ Feed\ Volume\ (L)} \times 100\% \quad (55)$$

It can easily be observed that the introduction of vibration gives a significant enhancement in flux performance for high recovery operations. When vibration is not used, the system becomes rapidly fouled. It can be estimated that value of flux will be nearly zero at approximately 65% recovery. Thus, no wastewater will be able to be processed, and the membrane will require cleaning. This is not the case when vibration is used. Viable flux values for industrial applications can still be observed for high

recovery operations. The study shows that permeate recoveries of 85% can realistically be efficiently achieved. It appears that even greater permeate recoveries – up to 95% recovery – could be managed. This is important from a commercialization standpoint since it is desired to produce the maximum amount of permeate and minimum retentate.

The concentration study was also evaluated in terms of a concentration factor. This allows one to predict the degree to which the feed wastewater can be concentrated until the permeate flux is diminished. In this case, the concentration factor will be represented as the volume reduction ratio, or VRR. The VRR is calculated as follows in Equation 56.

$$VRR = \frac{V_o}{V_c} \tag{56}$$

Where, V_o is the initial volume of feed wastewater and V_c is the volume of the concentrate remaining in the tank. The permeate flux was plotted as a function of VRR, shown in Figure 39. In the no vibration run, two distinct zones of the data can be seen. This has been observed and described in a previous membrane study in the food industry [86]. The point at which the data shift indicates the transition from the pressure-controlled region to the gel-layer controlled region. This phenomenon has been explained in the pressure study section of this project. The two distinct regions show when fouling takes control of the flux. When there is no vibration, this is apparent at a VRR of about 2.5. This indicates that the system is pressure-controlled for a very short period of operation before the gel layer is formed on the membrane surface. When vibration is used, the system appears to be in the pressure-controlled for all of operation.

This further confirms that vibration significantly reduces fouling on the membrane surface. This also shows that vibration can effectively reduce fouling at high feed concentrations and permeate recoveries.

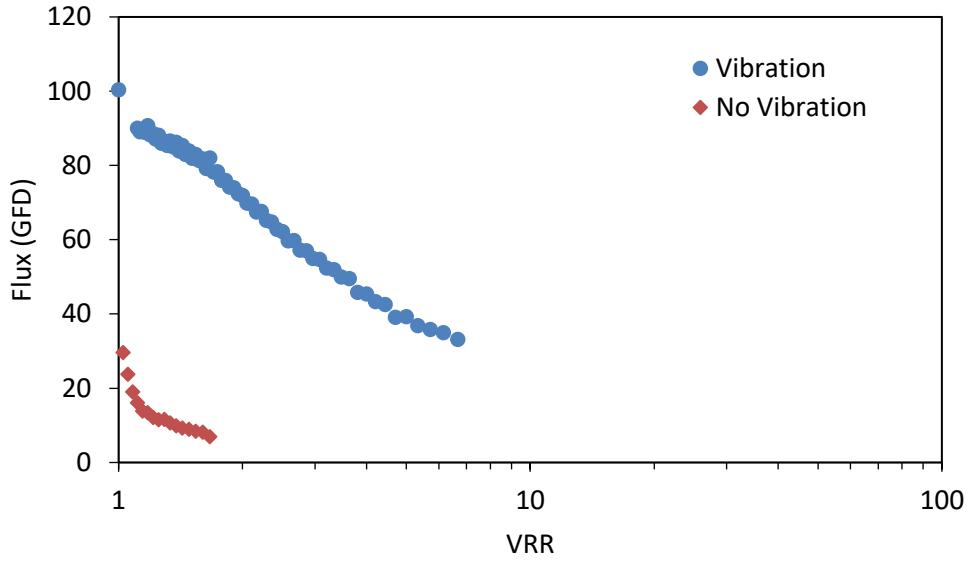

Figure 39. Permeate flux as a function of VRR for both no vibration and vibration modes of operation with the nanofiltration membrane; 350 psig

The instantaneous and average permeate concentrations of COD, turbidity, and conductivity have been recorded for the unsteady state concentrating run. The instantaneous permeate contaminant concentration is simply the permeate concentration at a given percent recovery. As the feed became more concentrated, the permeate concentrations also increased. Thus, the permeate concentrations that are found at higher recoveries are not representative of the total permeate that has been recovered. Concentrations for the permeate were taken every 10% recovery of permeate. Calculations for the average permeate conditions at a given percent recovery are shown

in Equations 57 and 58. Average permeate concentrations are what would be used to see if the permeate was within specifications for a particular water reuse application. It should be noted that these calculations are applied to the COD, turbidity, and conductivity concentrations of the permeate.

$$C_{permeate,X} = \frac{\sum_{x=0\%}^{X}\left[\left(\frac{C_{permeate,x} + C_{permeate,x+10\%}}{2}\right) \times (V_{x+10\%} - V_x)\right]}{\sum_{x=0\%}^{X}(V_{x+10\%} - V_x)} \quad (57)$$

$$x = 0\%, 10\%, 20\%, 30\%, 40\%, 50\%, 60\%, 70\%, 80\%$$

Equation 57 shows that calculation for a given percent recovery of permeate. The calculation takes into account an average permeate concentration over the span of a 10% recovery. This better represents the data in terms of permeates concentrations throughout testing. $C_{permeate,x}$ is the permeate concentration of COD, turbidity, or conductivity at x% recovery. V_x is the total volume of permeate collected at x% recovery, while $V_{x+10\%}$ is the total volume of permeate collected at x+10% recovery. Since there was no sample taken at 0% recovery of permeate, it is assumed that the concentrations of contaminants of the permeate at this point are those of the sample taken at 10% recovery. Equation 57 gives the average permeate concentrations up to 80% recovery. The equation is slightly modified to obtain the average concentration of contaminants in the permeate at 85% recovery (Equation 58).

$$C_{permeate,85\%} = \frac{1}{\sum_{x=0\%}^{X}(V_{x+10\%} - V_x) + (V_{85\%} - V_{80\%})}\left\{\sum_{x=0\%}^{X=80\%}\left[\left(\frac{C_{permeate,x} + C_{permeate,x+10\%}}{2}\right) \times (V_{x+10\%} - V_x)\right] + \left(\frac{C_{permeate,80\%} + C_{permeate,x+85\%}}{2}\right) \times (V_{85\%} - V_{80\%})\right\} \quad (58)$$

In Equation 58, the average permeate conditions from 80 to 85% recovery are added to the calculation for the average permeate contaminant concentrations at 80%.

The instantaneous and average permeate contaminant concentrations have been plotted vs percent permeate recovery – shown in Figure 40, Figure 41, and Figure 42. It can be seen that the average permeate concentrations at the highest recovery is lower than that of the instantaneous concentration at that recovery. The average concentration is the expected concentration that would result when operating at a given recovery. Thus, it can be seen that COD and turbidity concentration remain very low when operating at high recoveries. The concentrations of each would be acceptable for use in the cooling towers, as the organic contents and solids have been significantly reduced. The conductivity, however, would not meet the specification for feed to the cooling tower. It exceeds the limit of 300 µS/cm. Therefore, water recovered in this way would not be acceptable for feed to the cooling tower. There are still opportunities for the water recovered from the plant effluent. Some options are to use the water recovered for use as wash or landscaping water at the plant. Another consideration would be to further purify the recovered water in a reverse osmosis system to reduce the conductivity to be within the specification.

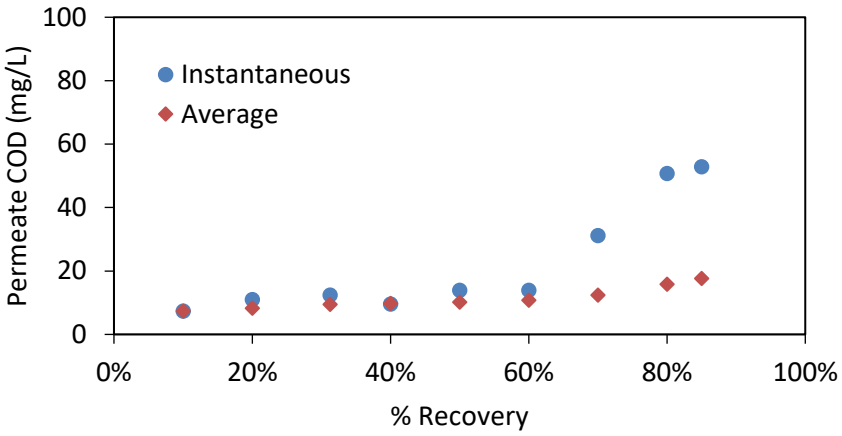

Figure 40. Instantaneous and average permeate COD concentration as a function of the percent permeate recovery; nanofiltration, 350 psig, 1" displacement, plant effluent

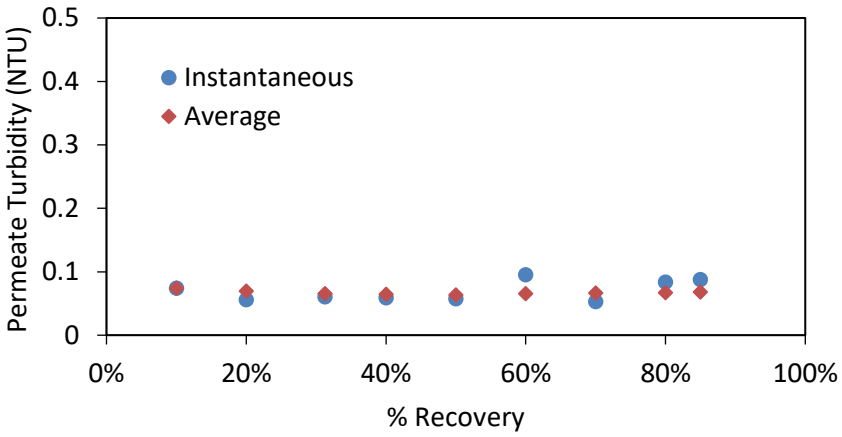

Figure 41. Instantaneous and average permeate turbidity as a function of the percent permeate recovery; nanofiltration, 350 psig, 1" displacement, plant effluent

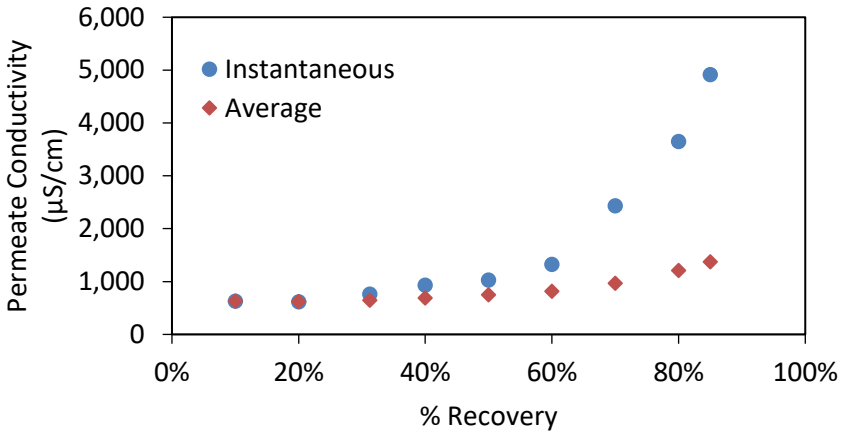

Figure 42. Instantaneous and average permeate conductivity as a function of the percent permeate recovery; nanofiltration, 350 psig, 1" displacement, plant effluent

The instantaneous and average permeate concentrations have been plotted vs percent permeate recovery for the run without vibration, as well – shown in *Figure 43*, *Figure 44*, and *Figure 45*. As with the run with vibration, it can be seen that the instantaneous and average COD concentration and turbidity remain low in the permeate. However, when vibration was used, rejections of each were greater. In addition, greater rejections were achievable even at permeate recovery percents that were not feasible to achieve in cross flow. When in crossflow membrane filtration with the nanofiltration, conductivity performance suffers. At 40% permeate recovery, the average conductivity of the permeate produced with cross flow was over four times as high as that achieved when vibration was used. This further confirms that vibration not only helps to enhance flux, but also the separation performance. Table 31 provides the average permeate concentrations achieved at the highest achieved recovery, in both vibratory and cross flow membrane filtration.

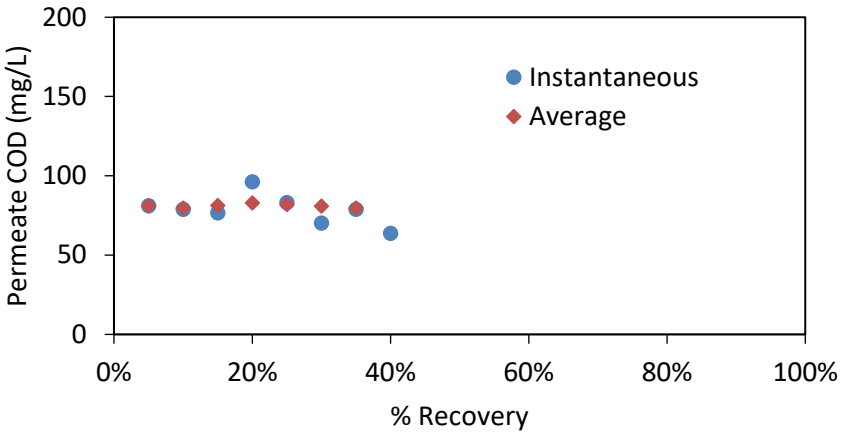

Figure 43. Instantaneous and average permeate COD concentration as a function of the percent recovery; nanofiltration, 350 psig, no vibration, plant effluent

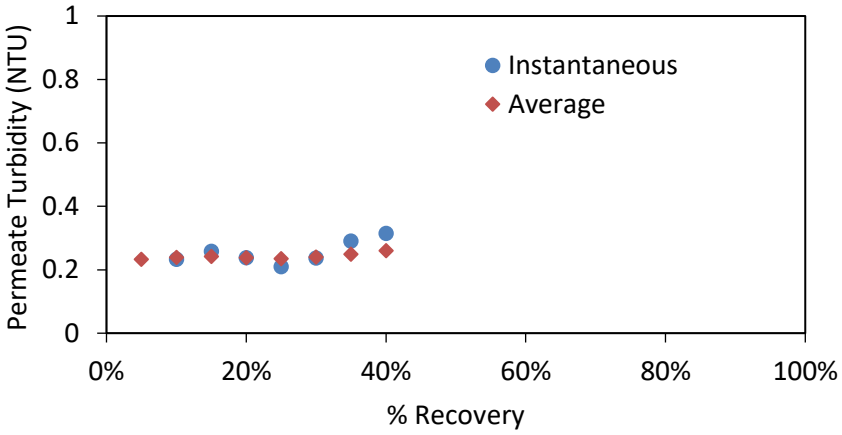

Figure 44. Instantaneous and average permeate turbidity as a function of the percent recovery; nanofiltration, 350 psig, no vibration, plant effluent

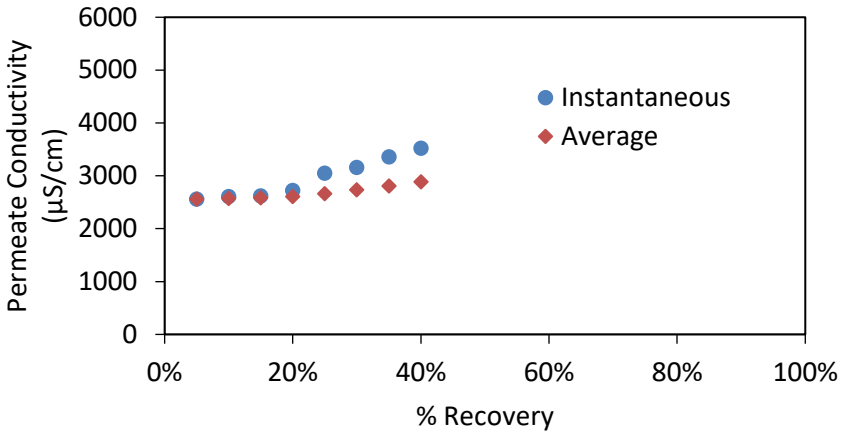

Figure 45. Instantaneous and average permeate conductivity as a function of the percent recovery; nanofiltration, 350 psig, no vibration, plant effluent

Table 31

Average permeate concentrations achieved in each mode of membrane filtration

	Vibratory Mode (85% permeate recovery)	Cross Flow (40% permeate recovery)
COD (mg/L)	18	80
Turbidity (NTU)	<<1	0.25
Conductivity (µS/cm)	1,370	2,890

The feed concentrations have also been plotted to show the effect of concentrating the wastewater during processing – these are shown in *Figure 46*, *Figure 47*, and *Figure 48*(vibratory mode) and *Figure 49*, *Figure 50*, and *Figure 51* (cross flow). In vibratory mode, it can be seen that each of the contaminant concentrations increase exponentially as more permeate is recovered. This is caused by the nanofiltration membrane rejecting the contaminants and leaving them in the feed. This increase in concentration occurs much more rapidly than compared to the rise in contaminant concentration for cross flow filtration. This is the result of fouling on the membrane surface. While a majority of

contaminants are rejected and remain in the retentate stream, a portion remains on the membrane surface. This can be observed minorly for the case of COD and conductivity. A portion of the organics and ions in the system become trapped on the membrane and the concentrations do not increase exponentially, as in the run with vibration. For the case of turbidity, operating in cross flow decreases the turbidity of the feed. Thus, more solids and other foulants that cause turbidity are actually remaining on surface of the membrane than are returning in the retentate stream. This further confirms that fouling by suspended solids is very probable when processing the plant effluent.

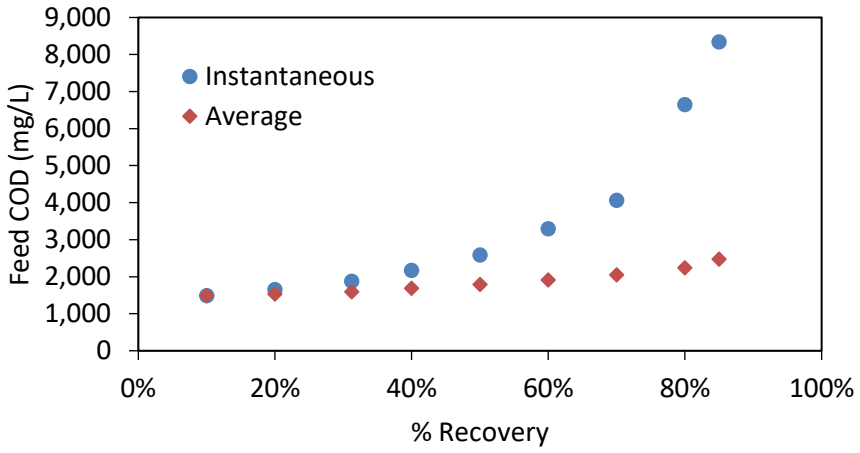

Figure 46. Instantaneous and average feed COD concentration as a function of the percent recovery; nanofiltration, 350 psig, 1" displacement, plant effluent

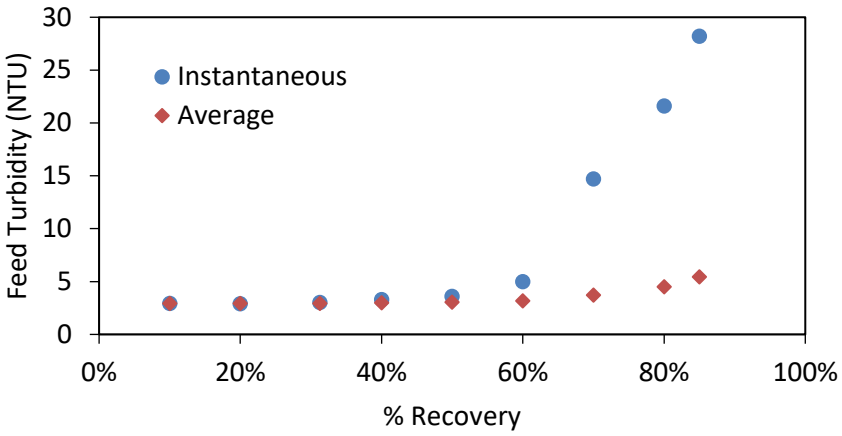

Figure 47. Instantaneous and average feed turbidity as a function of the percent recovery; nanofiltration, 350 psig, 1" displacement, plant effluent

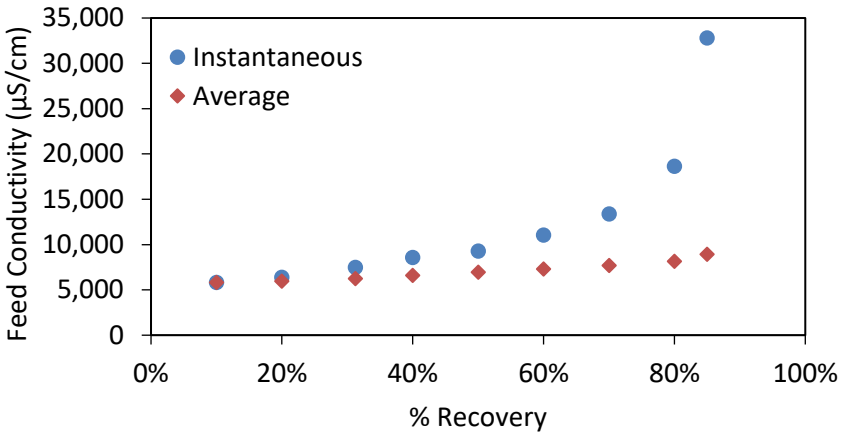

Figure 48. Instantaneous and average feed conductivity as a function of the percent recovery; nanofiltration, 350 psig, 1" displacement, plant effluent

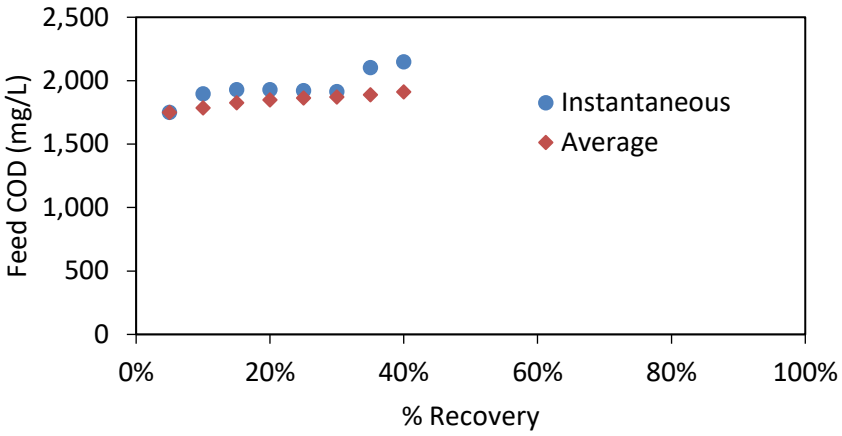

Figure 49. Instantaneous and average feed COD concentration as a function of the percent recovery; nanofiltration, 350 psig, no vibration, plant effluent

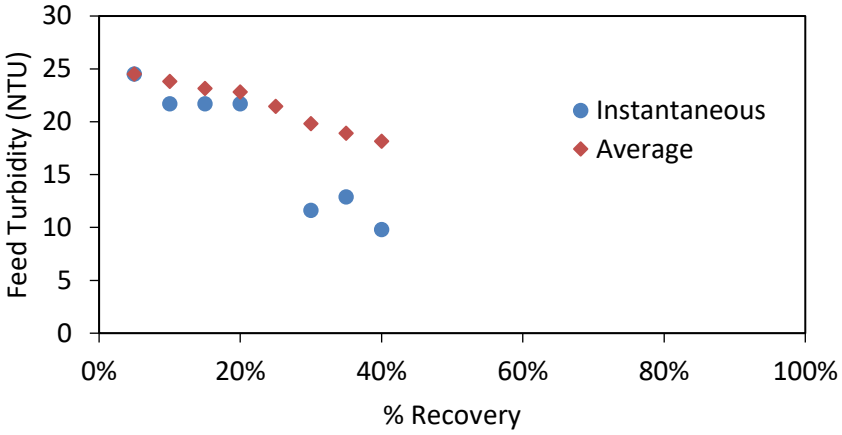

Figure 50. Instantaneous and average feed turbidity as a function of the percent recovery; nanofiltration, 350 psig, no vibration, plant effluent

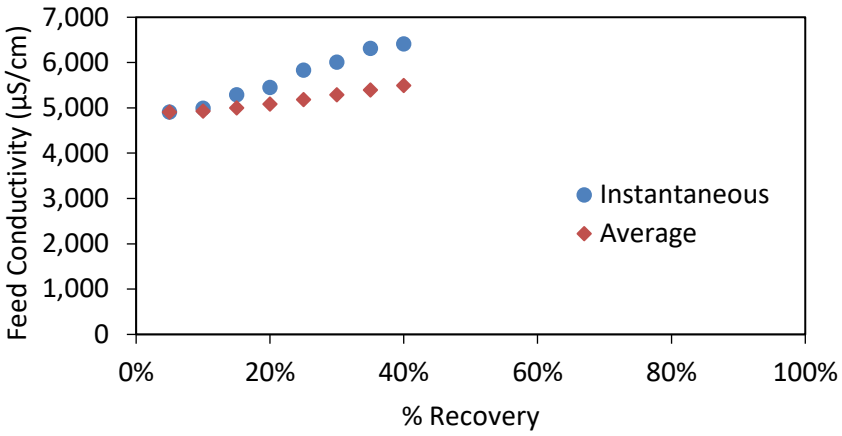

Figure 51. Instantaneous and average feed conductivity as a function of the percent recovery; nanofiltration, 350 psig, no vibration, plant effluent

A cleaning study was performed on a nanofiltration membrane after a vibratory, unsteady state concentration run using a standard membrane cleaning solution of 1% enzyme cleaner (Tergazyme ®) and 1% sodium hypochlorite for 30 minutes of processing. After cleaning, water flux performance of the membrane was tested at a suite of pressures to evaluate for comparison to water flux values at the same pressures of a new membrane, shown in *Figure 52*. Flux recovery was recorded at an average of 74% among all tested pressures.

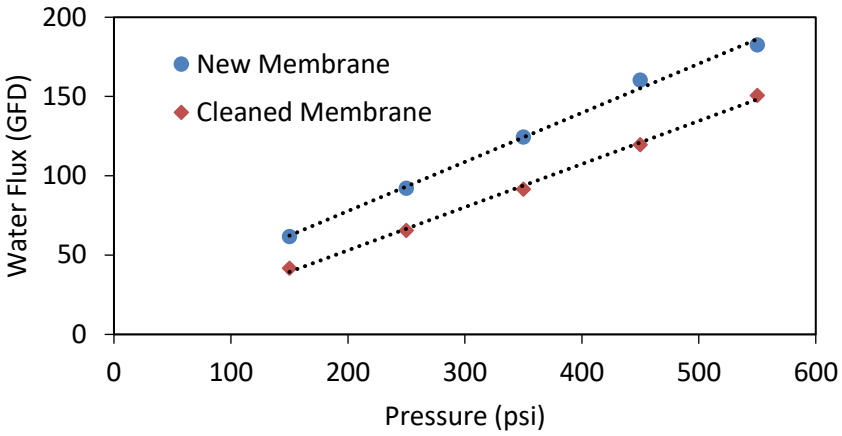

Figure 52. Flux recovery achieved during cleaning study for a nanofiltration membrane; 350 psig, plant effluent

Vibratory Membrane Separation – Pit #3 Wastewater

Processing the overall plant effluent with the vibratory membrane system gave favorable flux results as well as rejections of COD and turbidity. However, the process fell short of removing conductivity to the specification of the cooling tower. The system showed promise and scale-up experimentation (i.e. unsteady state high recovery study) was conducted for the Pit #3 wastewater. The membranes selected for these studies are the nanofiltration and reverse osmosis membranes, as they are the ones capable of producing a high quality permeate. To begin, the reverse osmosis membrane was tested, since the nanofiltration membrane could not reduce the conductivity to the cooling tower specification. The feed concentrations of the Pit #3 wastewater in this study are given in Table 32.

Table 32

Feed conditions of the Pit #3 wastewater for vibratory reverse osmosis and nanofiltration unsteady state concentration runs

COD (mg/L)	1,020
Turbidity (NTU)	13
Conductivity (µS/cm)	600

During the unsteady state concentrating run with the Pit #3 wastewater, the operating pressure was maintained at 550 psig and the feed flowrate was held constant at 2 GPM. The higher operating pressure was chosen to generate a reasonable flux value for reverse osmosis processing. Flux values were corrected to 25°C using the temperature correlation. This study was conducted only in vibratory mode, as fouling would occur too rapidly to obtain any appreciable data in cross-flow filtration. Figure 53 shows the instantaneous flux as a function of the percent recovery of the permeate. Average flux values used in design calculations are shown in a subsequent section. It can be seen that there is a slight flux decay during the unsteady state concentrating run. Flux can be achieved close to its initial value even at high recoveries. Although this value is low as compared to flux values that can be achieved using the nanofiltration membrane.

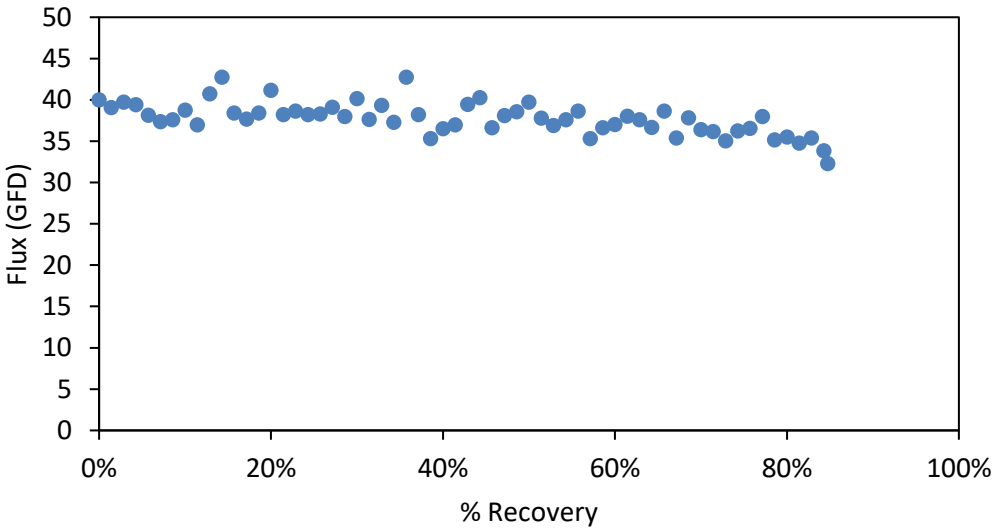

Figure 53. Instantaneous permeate flux as a function of percent recovery of permeate; reverse osmosis, 550 psig, 1" displacement, Pit #3 wastewater

The unsteady state concentration run for the Pit #3 wastewater using the reverse osmosis membrane has also been considered in terms of a VRR. Figure 54 shows the relationship of instantaneous permeate flux as a function of the VRR. As can be seen, the system appears to trend to a very high maximum VRR and would be able to be operated at high recoveries (>95%). This can be contributed the use of vibration and the characteristics of the wastewater. The Pit #3 wastewater has essentially no suspended solids. Therefore, there it is expected that there would not be any appreciable fouling on the membrane surface. Vibration is still necessary since the increased shear rates help to increase the flux through the membrane.

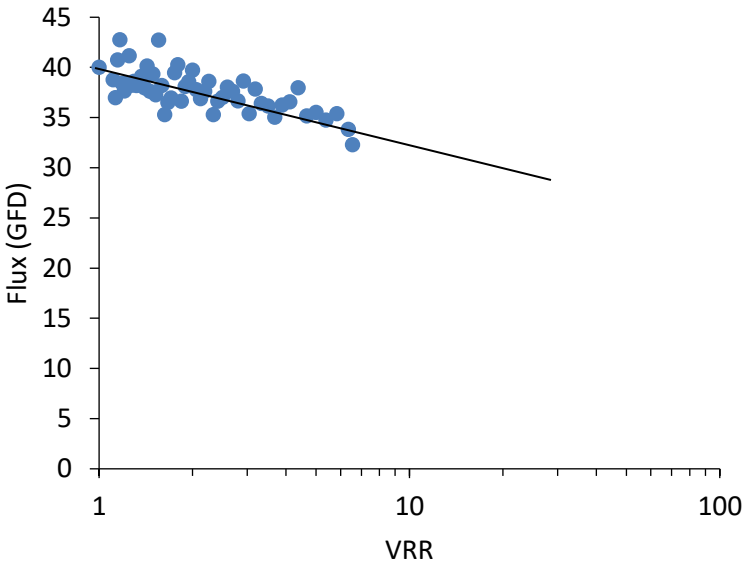

Figure 54. Instantaneous permeate flux as a function of VRR; reverse osmosis, 550 psig, 1" displacement, Pit #3 wastewater

As with the plant effluent unsteady state run, the average permeate contaminant concentrations have been calculated and plotted vs the percent recovery. Equations 57 and 58 have been used for such calculations. Figure 55, Figure 56, and Figure 57 show the instantaneous and average permeate concentrations of the COD, turbidity, and conductivity, respectively. As previously stated, the average concentration is the expected concentration that would result when operating at a given recovery. It can be seen that the concentrations of each major contaminant remain very low when operating at high recoveries. The concentrations of each would be acceptable for use in the cooling towers, as the organic contents, ions, and any potential suspended solids have been significantly reduced. Thus, the water recovered from the Pit #3 wastewater is acceptable for use in the cooling tower.

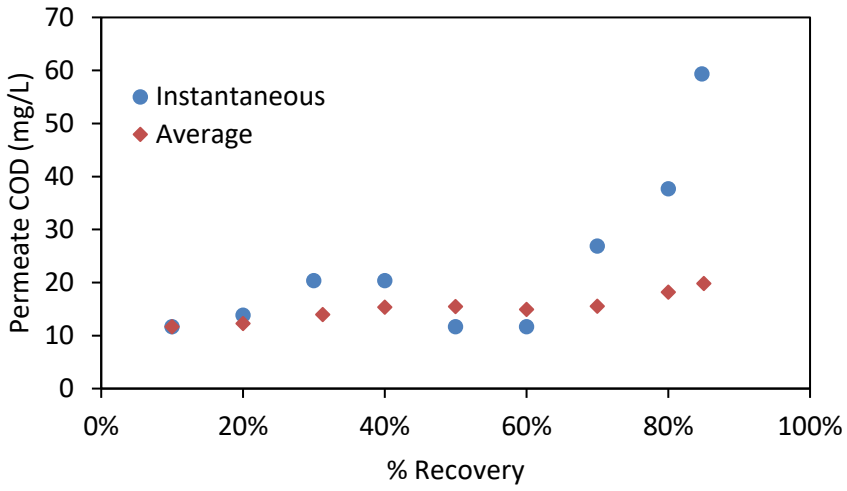

Figure 55. Instantaneous and average COD concentration as a function of the percent recovery of permeate; reverse osmosis, 550 psig, 1" displacement, Pit #3 wastewater

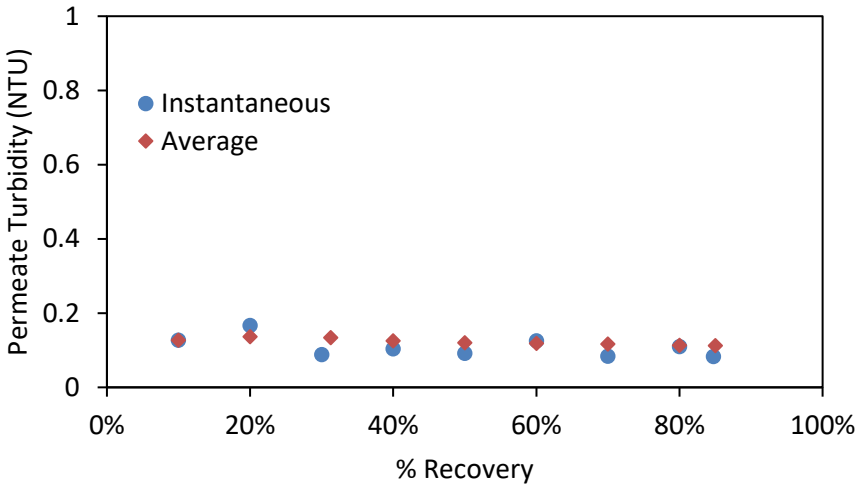

Figure 56. Instantaneous and average turbidity as a function of the percent recovery of permeate; reverse osmosis, 550 psig, 1" displacement, Pit #3 wastewater

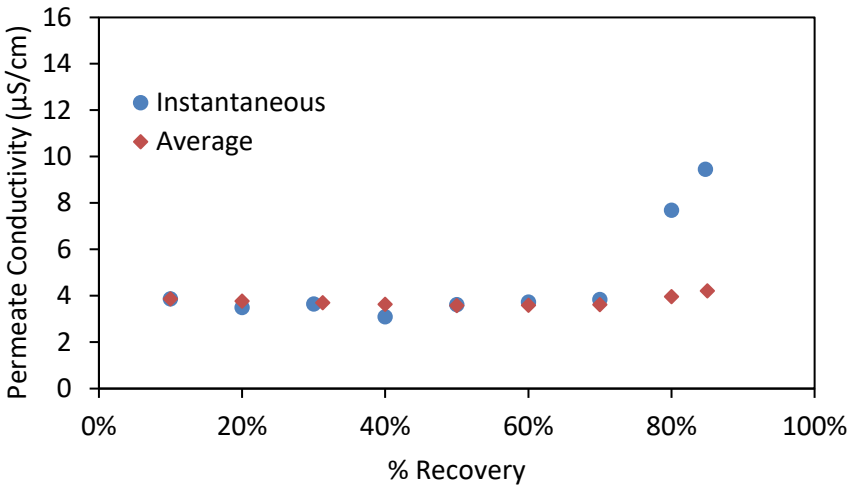

Figure 57. Instantaneous and average conductivity as a function of the percent recovery of permeate; reverse osmosis, 550 psig, 1" displacement, Pit #3 wastewater

The instantaneous and average feed concentrations during vibratory reverse osmosis have been plotted vs the percent permeate recovery – shown in *Figure 58*, *Figure 59*, and *Figure 60*. It can be seen that the instantaneous feed concentrations increased exponentially, as it occurred in vibratory nanofiltration. The majority of the contaminants are rejected by the membrane and are raised away from the surface to leave in the retentate stream.

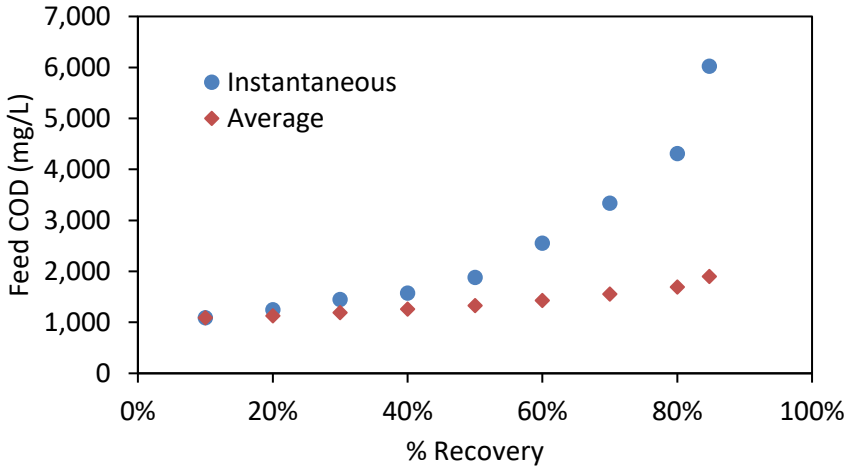

Figure 58. Instantaneous and average feed COD concentration as a function of the percent recovery; reverse osmosis, 550 psig, 1" displacement, Pit #3 wastewater

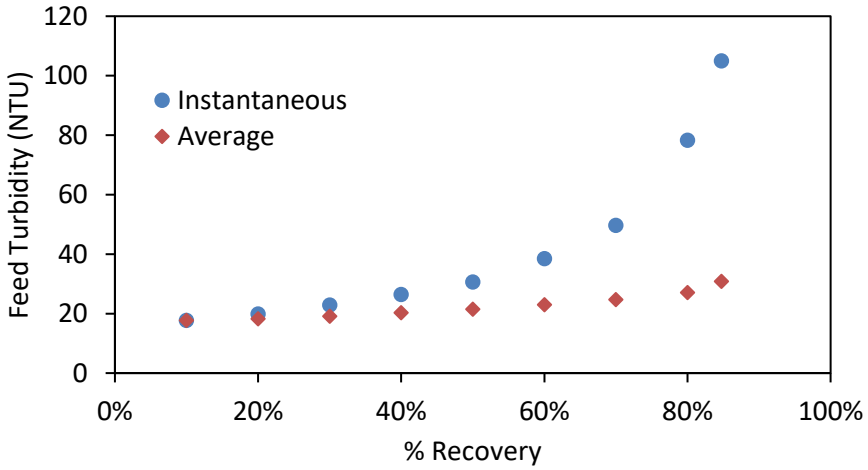

Figure 59. Instantaneous and average feed turbidity as a function of the percent recovery; reverse osmosis, 550 psig, 1" displacement, Pit #3 wastewater

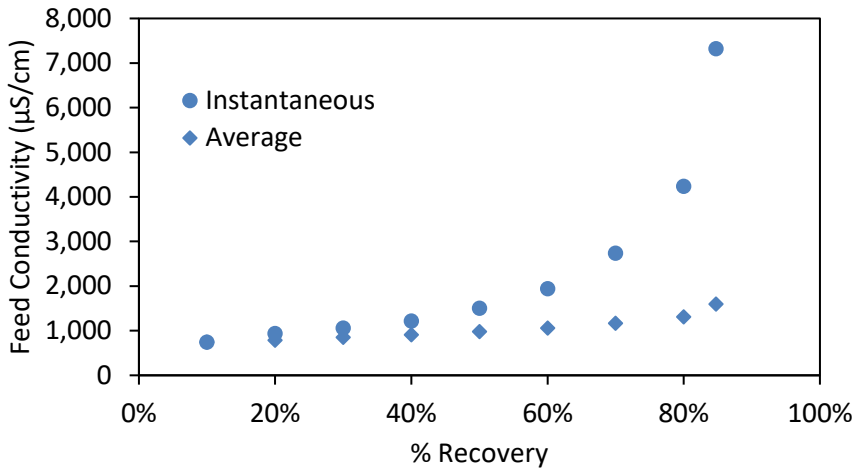

Figure 60. Instantaneous and average feed conductivity as a function of the percent recovery; reverse osmosis, 550 psig, 1" displacement, Pit #3 wastewater

Processing the Pit #3 wastewater with vibratory reverse osmosis reclaimed water with a high purity that meets the specifications for use in the cooling tower. The flux obtained with the vibratory reverse osmosis was fair but could be improved. The process was tested with a nanofiltration membrane. The initial conductivity of the Pit #3 wastewater is lower than that of the overall plant effluent. Thus, it was proposed that the vibratory nanofiltration process may reduce the conductivity sufficiently while providing a more favorable flux with lower operating pressure.

During the unsteady state concentrating run with the Pit #3 wastewater, the operating pressure was maintained at 350 psig and the feed flowrate was held constant at 2 GPM. Flux values were corrected to 25°C using the temperature correlation. The feed conditions of the Pit #3 wastewater are the same as those in the vibratory reverse osmosis unsteady state concentration study (Table 32). This study was conducted only in vibratory mode, as the effect of system fouling in the nanofiltration studies has been shown with the overall plant effluent study. Figure 61 shows the instantaneous flux as a

function of the percent recovery of the permeate. Average flux values used in design calculations are shown in the subsequent section. It can be seen that there is minimal flux decay when concentrating the feed and recovering 80% of the permeate.

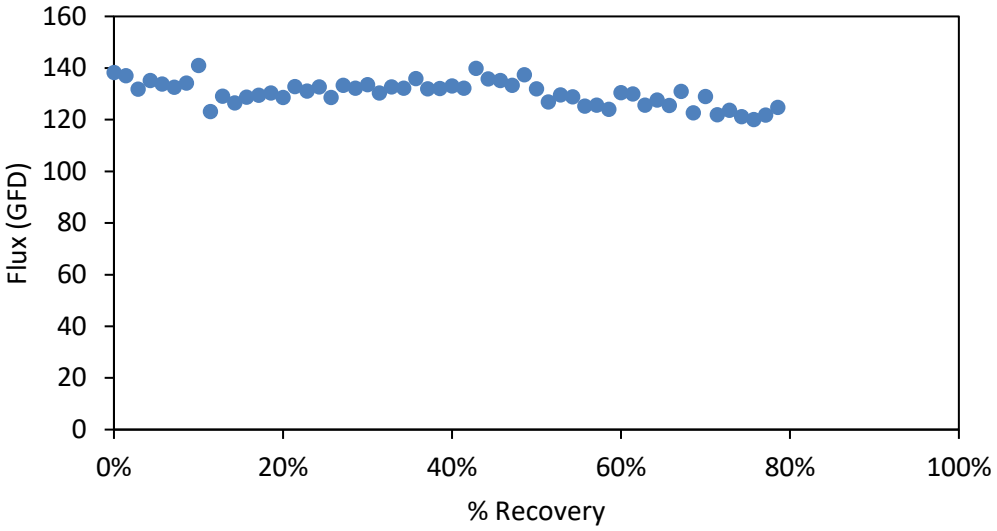

Figure 61. Instantaneous permeate flux as a function of percent permeate recovery; nanofiltration, 350 psig, 1" displacement, Pit #3 wastewater

The unsteady state concentration run for the Pit #3 wastewater using the reverse osmosis membrane has also been considered in terms of a VRR. Figure 62 shows the relationship of instantaneous permeate flux as a function of the VRR. As can be seen, the system appears to perform at a very high maximum VRR and would be able to be operated at high recoveries (>95%). A similar trend as processing with the reverse membrane can be seen; however, the flux achieved is appreciably greater. This can be contributed the use of vibration and the characteristics of the wastewater. The Pit #3 wastewater has essentially no suspended solids. Therefore, there it is expected that there

would not be any appreciable fouling on the membrane surface. Vibration is still necessary since the increased shear rates help to increase the flux through the membrane.

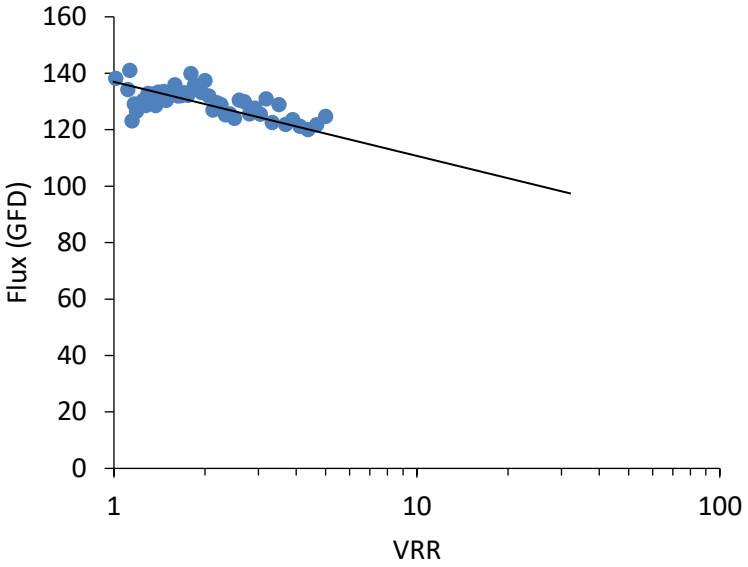

Figure 62. Instantaneous permeate flux as a function of VRR; nanofiltration, 350 psig, 1" displacement, Pit #3 wastewater

The average permeate contaminant concentrations have been calculated and plotted vs the percent recovery of permeate for the processing of the Pit #3 wastewater with the vibratory nanofiltration process. Figure 63, Figure 64, and Figure 65 show the instantaneous and average permeate concentrations of the COD, turbidity, and conductivity, respectively. As with processing with the overall plant effluent and reverse osmosis processing of the Pit #3 wastewater, turbidity is reduced to very minimal levels. The COD concentration of the permeate is higher than expected; however, after discussion with Nestlé, a greater concern for the permeate recovered is the absence of color. Color in the reuse water can interfere with the control systems of the cooling

tower. The permeate recovered by vibratory nanofiltration of the Pit #3 wastewater is clear in color. In contrast of the case of vibratory nanofiltration of the plant effluent, the permeate recovered from Pit #3 wastewater meets the conductivity specifications. The average conductivity at 80% recovery below the specification of 300 µS/cm at about 115 µS/cm. Thus, a scaled-up system can be designed to achieve reuse water purification goals using vibratory nanofiltration. The achievable flux greatly improves and will require less membrane area as compared to the vibratory reverse osmosis unit.

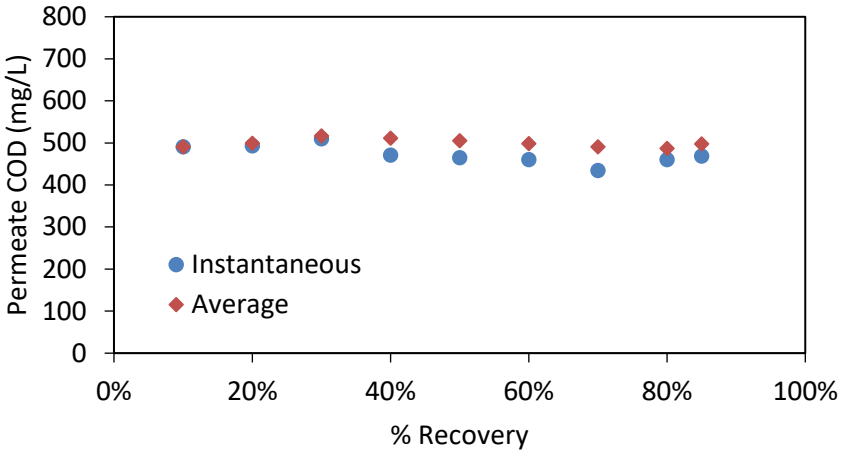

Figure 63. Instantaneous and average COD concentration as a function of the percent recovery of permeate; nanofiltration, 350 psig, 1" displacement, Pit #3 wastewater

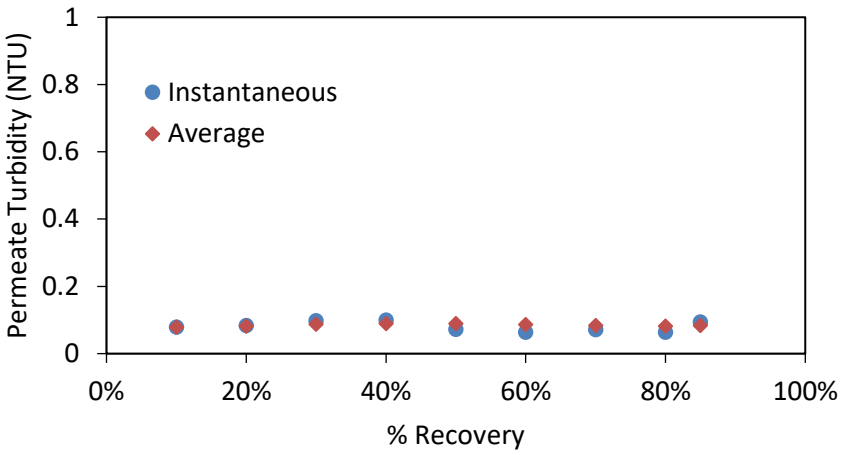

Figure 64. Instantaneous and average turbidity as a function of the percent recovery of permeate; nanofiltration, 350 psig, 1" displacement, Pit #3 wastewater

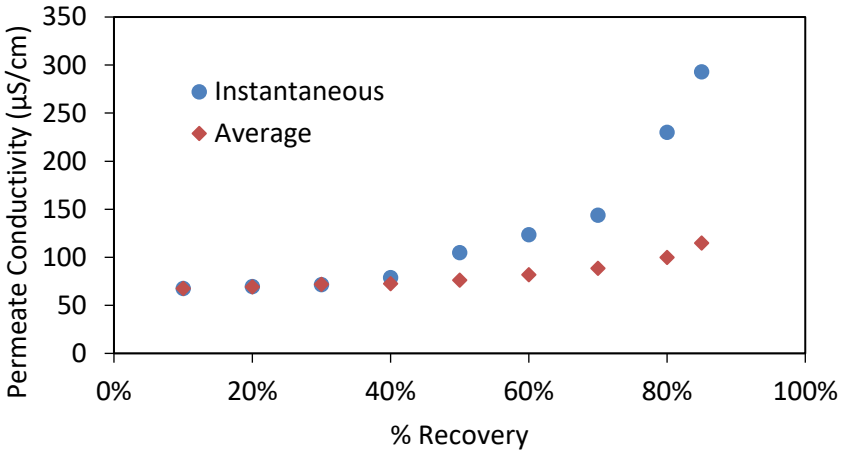

Figure 65. Instantaneous and average conductivity as a function of the percent recovery of permeate; nanofiltration, 350 psig, 1" displacement, Pit #3 wastewater

The instantaneous and average feed concentrations during vibratory nanofiltration have been plotted vs the percent permeate recovery – shown in *Figure 66*, *Figure 67*, and *Figure 68*. It can be seen that the instantaneous feed concentrations increased as more permeate was recovered, however, the increases were not highly exponential. The feed

COD did not increase significantly throughout the run. This is because COD was only moderately rejected in vibratory nanofiltration of the Pit #3 wastewater. Turbidity of the feed nearly doubled throughout the unsteady state concentration run. This conflicts with Figure 64, since turbidity was highly rejected in vibratory nanofiltration. It is expected that some of the organics that appear as COD also contribute to the turbidity of the feed. Conductivity of the feed had the greatest increase at a factor of 2.3.

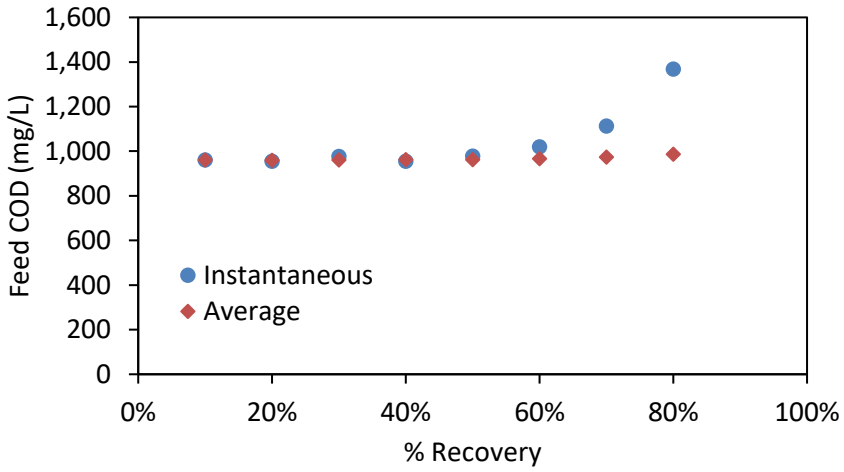

Figure 66. Instantaneous and average feed COD concentration as a function of the percent recovery; NF, 350 psig, 1" displacement, Pit #3 wastewater

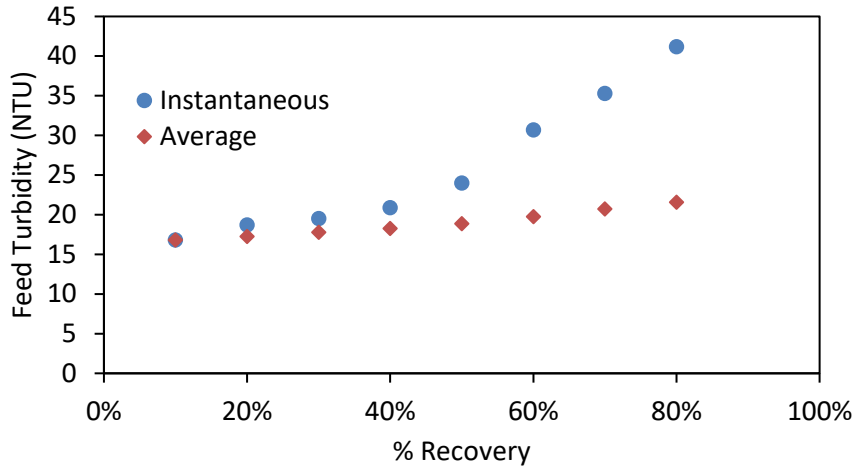

Figure 67. Instantaneous and average feed turbidity as a function of the percent recovery; NF, 350 psig, 1" displacement, Pit #3 wastewater

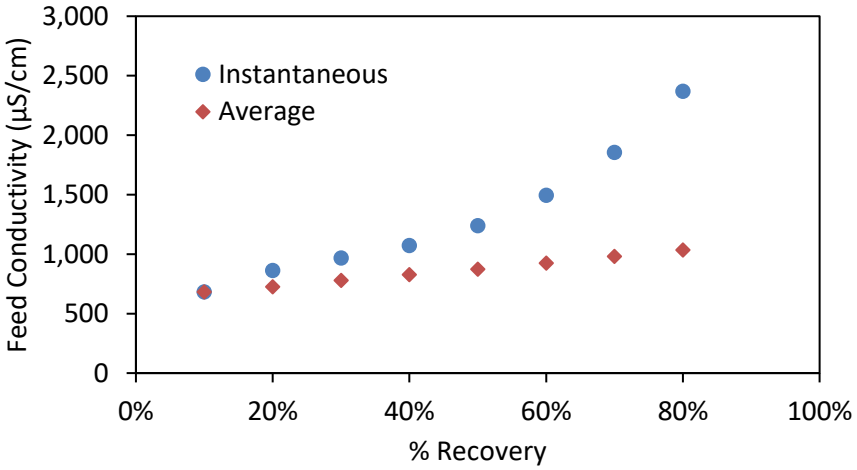

Figure 68. Instantaneous and average feed conductivity as a function of the percent recovery; NF, 350 psig, 1" displacement, Pit #3 wastewater

Chapter 9

Scale-up Design and Case Study Analysis

The full-scale design for each of the recovery cases uses a scaled up vibratory membrane (V-SEP) system based on the experimental data observed. This section details the calculations that have been used for such scale-up. An economic and environmental assessment (life cycle assessment) of each case is also provided.

Scale-up Calculations

Scale-up the V-SEP system incorporates data that is obtained during experimental runs. During experimentation, design factors such as operating transmembrane pressure (TMP), degree of vibration or shear rate, temperature, and, most importantly, a design flux. The design flux is the average observed flux found during an unsteady state concentration run. Figure 69 shows the average and instantaneous flux plotted vs recovery of the unsteady state concentration run for the plant effluent. The average recorded flux at a specified recovery is the design flux for scale-up calculations. The values for average flux have been calculated using Equations 59 and 60.

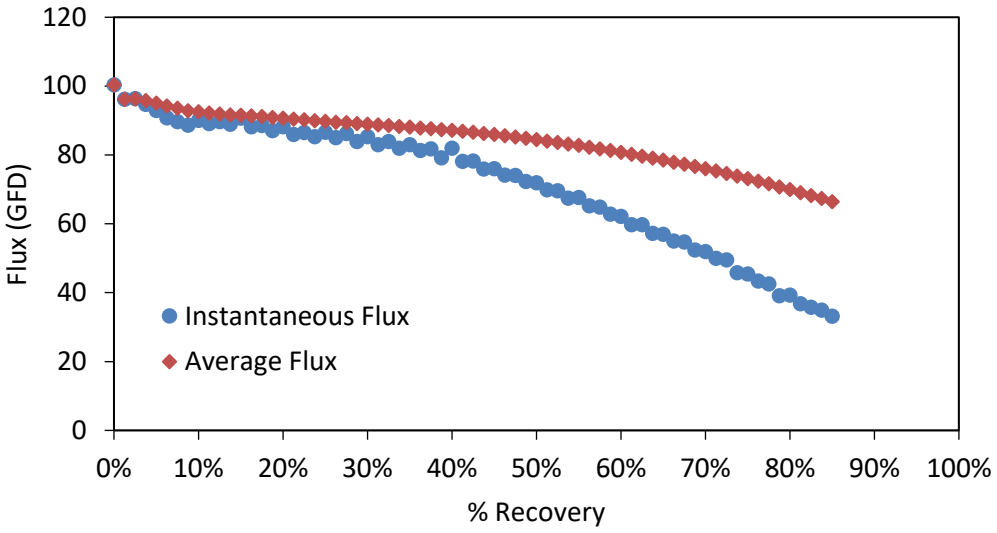

Figure 69. Instantaneous and average permeate flux as a function of the percent permeate recovery; nanofiltration, 350 psig, 1" displacement, plant effluent

$$J_{avg}(GFD) = \frac{\sum_{n=1}^{N} V_n}{(\sum_{n=1}^{N} t_n) \times membrane\ area} \times \frac{1\ gal}{3.785\ L} \times \frac{24\ hr}{1\ day} \quad (59)$$

$$V_n = 1\ L \times \frac{Water\ Flux\ (GFD)_{T=25°C}}{Water\ Flux\ (GFD)_{T_n\ (°C)}} \quad (60)$$

In Equation 59, *n* is the number of the nominal volume collected during the concentration study. V_n is the corrected collected volume for each sample taken, in L. Since samples were each taken at a nominal volume of 1 L, the temperature correlation shown in Equation 54 was used to correct the volume of permeate collected in the sample time (shown in Equation 60). The time required for each nominal liter of permeate collected is t_n, in hrs. The membrane area is constant throughout all calculations at 0.48 ft^2.

Once the average flux has been plotted vs the recovery of permeate, a value for the observed average flux can be determined at a specified recovery value. For the following sample calculations, the desired recovery will be 90%. From Figure 69, it can be seen that the data do reach 90% recovery; however, the average flux value at 90% can be accurately estimated following the trend of the data. In this case, the observed average flux at 90% recovery will be estimated at 65 GFD.

Equations 61 – 67 are used for the scale-up of a V-SEP membrane system. These equations will be used for Cases 1 and 2 to determine operating costs for the recovery system. The case study designations will be further described in detail in the following sections.

$$Design\ Flux = J_{avg} \times SB \tag{61}$$

In Equation 61, the *Design Flux* is the average observed flux at the desired recovery times a design safety buffer, *SB*. *SB* is set to 50%, or 0.50, for these calculations.

$$Q_F\ (GPD) = \frac{Permeate\ Rate\ (GPD)}{\%R} \tag{62}$$

In Equation 62, *Permeate Rate* is the amount of water that is desired to be recovered. This is divided by the desired recovery, *%R* to obtain the feed rate, Q_F, of wastewater to the recovery process.

$$\#modules = \frac{Permeate\ Rate}{J_{avg} \times A} \times \frac{1 + SB}{\frac{t_c - 120\ min}{t_c}} \quad (63)$$

Each V-SEP membrane module is capable of providing a set amount of membrane area available for purifying wastewater. In Equation 63, the number of modules is calculated. The result is then rounded up to the nearest whole number. The membrane area per module is *A*. In a full-scale V-SEP membrane system, the available membrane area options are 1,000, 1,200, or 1,400 ft^2. This can be altered by choosing the membrane spacing in the V-SEP unit per the required throughput [83]. The membrane area is chosen per application to reduce the amount of module required. Typically, the lowest amount of membrane area capable for a given application is selected to reduce the membrane replacement cost, so long as an additional module is not required. The time between membrane cleanings is t_c and is set to a specified value depending on the type of applications. Fouling is limited when vibration is used, so the time between cleanings is 40,320 minutes, or 4 weeks.

Each module consists of a number of membranes stacked vertically. A typical commercial module designation is an i84 Filtration System (Figure 70). This module is composed of 360, 432, or 504 membranes (each with an area of 2.78 ft^2) depending on the membrane surface area option needed. Commercial systems based on an i84 module would then have one or modules depending on the permeate flow required. Different membranes (RO, NF, UF, MF) would then be chosen based on individual laboratory performance results with actual waste. This is essentially how the case study was conducted. Each i84 module is 47 in (W) x 47 in (L) x 194 in (H). A standard system is accompanied with a controls skid, which includes pressure and temperature sensors,

conductivity and pH meters, vibration control, and a chemical metering station [83]. The controls skid also contains the feed pump and additional supports for piping. The controls skid with chemical metering station is 96 in (W) x 121 in (L) x 89 in (H). Custom configurations for the total plant footprint are available. The module(s) and skid can set up either inside or outside and have stainless steel piping for all high-pressure lines.

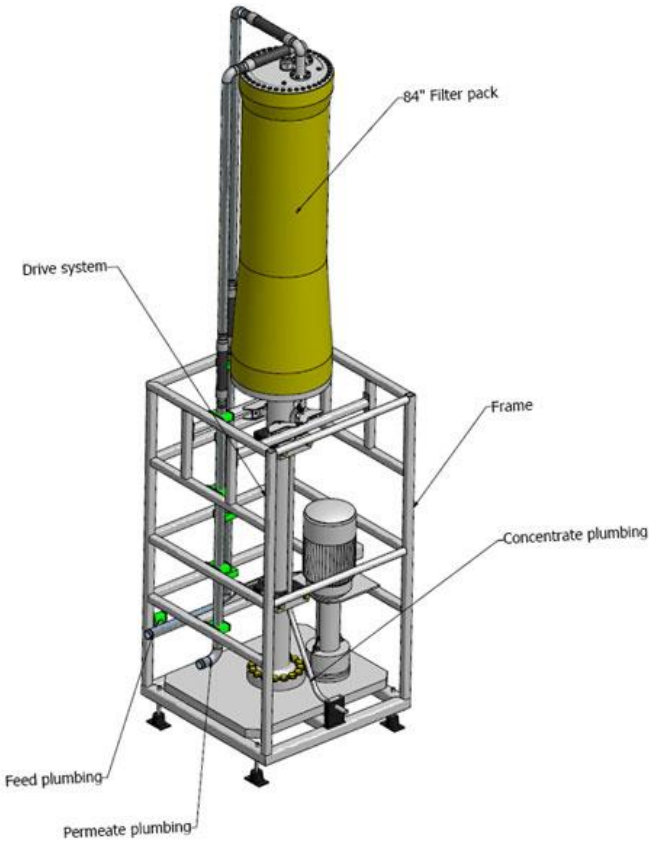

Figure 70. Technical drawing of one i84 V-SEP filtration system module; courtesy of New Logic Research, Inc. [83]

$$Feed\ pump\ power\ (hp) = \frac{Q_F \times P}{\eta} \times conversion\ factors \quad (64)$$

In Equation 64, P is the operating pressure of the feed pump for the V-SEP system. The pump efficiency is η and is assumed to be 85%, or 0.85.

$$Power\ Requirement = Feed\ Pump\ Power + (\#modules \times Vibration\ Motor\ Power) \quad (65)$$

In Equation 65, the total power requirement – by electricity – is the sum of the power requirements of the feed pump and the vibration motors. Each V-SEP module has one vibration motor and the power requirement per motor is assumed to be 10 hp.

$$Energy\ Requirement = Power\ Requirement \times Operating\ time \quad (66)$$

In Equation 66, the energy requirement of the V-SEP system is calculated. The operating time is assumed to be 22 hrs per day.

$$Cleaner\ consumption = V_c \times \frac{n_c}{t_c} \times \%c \times \#modules \quad (67)$$

In Equation 67, the amount of cleaner consumed is calculated using the volume of cleaner solution per module, V_c, the number of cleanings, n_c, the time between cleanings, t_c, the percent concentration of cleaner, $\%c$, and the number of modules. V_c is set to 70 gal, t_c is 40,320 minutes, and $\%c$ for all studies is set to 2%, or 0.02.

Case 1 – Recovery of Water from Plant Effluent

Case 1 involves the recovery of water from the plant effluent. The plant effluent is used as feed to the scaled-up V-SEP membrane system. Permeate recovered from this recovery process is intended to be used for feed water to the cooling towers. The plant

effluent will be split into two streams of 111,000 GPD and 239,000 GPD. The goal is to recover 100,000 GPD of water from the plant effluent, which will be 90% recover from the stream of 111,000 GPD. Figure 71 shows a flow diagram of the recovery scheme. By recovering 100,000 GPD of water from the plant effluent for the cooling tower, the water pumped directly from the wells to the cooling tower is eliminated. In addition, the amount of water discharged to the county utilities authority is reduced by 100,000 GPD to a total of 250,000 GPD. While the current design for water recovery does not produce water that is usable in the cooling tower (based on the conductivity specification), scale-up has been calculated as intended for Case 1. Water that is recovered could be reused for wash water or for other maintenance uses at the plant. In addition, the quality of the permeate required could be improved upon by using replacing some nanofiltration membranes in the i84 Filtration System with reverse osmosis membranes. In that case, the water produced could be used in the cooling towers. These are discussed in the prior section along with their calculations. Table 33 presents the mass and energy flows associated with the recovery processes proposed. Table 34 shows the actual feed conditions for the plant effluent wastewater in this study. Table 34 also shows the average permeate concentrations projected for 90% permeate recovery for Case 1. It can be seen that the average conductivity at 90% currently exceeds the specification of cooling tower water at 1,400 µS/cm.

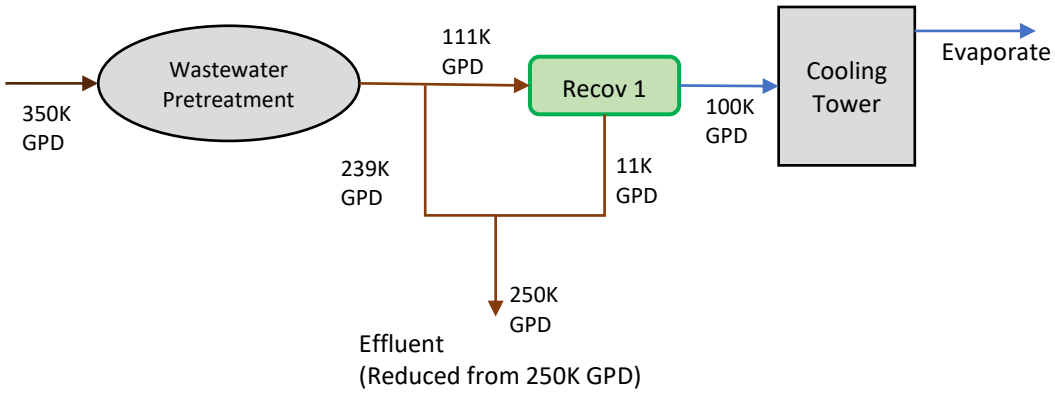

Figure 71. Case 1 water recovery scheme

Table 33

Mass and energy flows associated with Case 1 recovery

Flows	**Case 1 recovery**	
Freshwater	$1.35x10^8$	gal/yr
	$1.13x10^9$	lb/yr
Nonhazardous wastewater	$9.13x10^7$	gal/yr
	$7.60x10^8$	lb/yr
Hazardous wastewater	$1.14x10^5$	lb/yr
Electricity (pumps + recovery)	$1.02x10^6$	MJ/yr

Table 34

Feed conditions and average permeate concentrations at 90% recovery of the plant effluent wastewater used in the scale-up study

	Feed	Permeate at 90% Recovery
COD (mg/L)	2,000	20
Turbidity (NTU)	40	<<1
Conductivity (µS/cm)	5,730	1,400

The life cycle emissions associated with Case 1 recovery can be seen in Table 35. The total life cycle emissions are the sum of the emissions associated with water use,

nonhazardous (NHW) and hazardous (HW) wastewater disposal, and electricity for the well pumps and recovery system. This uses the flows in Table 33 along with the LCIs provided in Table 11 through Table 16, using Equation 24. As with the base case scenario, air emissions make up the majority of the total emissions at 98.6%. CO_2 emissions contribute to 97.9% of the total air emissions. Nonhazardous wastewater disposal is the greatest contributor to the total emissions of Case 1 at 94.7% of the total emissions.

Table 35

Life cycle emissions associated with Case 1 recovery

	Freshwater	NHW	HW	Electricity	Total
Total Air Emissions (lb/yr)	6.30E+05	2.11E+07	9.24E+03	4.24E+05	**2.21E+07**
CO_2 (lb/yr)	6.25E+05	2.09E+07	9.18E+03	4.17E+05	**2.20E+07**
CO (lb/yr)	1.03E+02	1.73E+03	7.47E-01	2.91E+02	**2.12E+03**
CH_4 (lb/yr)	6.85E+02	1.85E+04	8.04E+00	2.09E+03	**2.13E+04**
NO_X (lb/yr)	0.00E+00	4.36E+04	0.00E+00	3.33E+02	**4.40E+04**
NMVOC (lb/yr)	2.14E+01	5.81E+02	2.53E-01	1.32E+02	**7.35E+02**
Particulate (lb/yr)	1.94E+03	5.74E+02	2.45E-01	1.10E+02	**2.62E+03**
SO_2 (lb/yr)	6.81E+02	2.10E+04	9.05E+00	3.65E+03	**2.53E+04**
Total Water Emissions (lb/yr)	1.38E+04	2.73E+05	2.26E+02	6.08E+04	**3.48E+05**
VOCs (lb/yr)	2.34E-03	6.75E-02	2.94E-05	1.85E-01	**2.55E-01**
Total Soil Emissions (lb/yr)	7.73E+00	2.31E+02	1.01E-01	2.65E+00	**2.42E+02**
Total Emissions (lb/yr)	**6.44E+05**	**2.13E+07**	**9.46E+03**	**4.83E+05**	**2.24E+07**
CED (MJ/yr)	2.45E+06	5.93E+07	2.54E+04	7.32E+06	**6.91E+07**

Table 36 includes the mass and energy flows associated with Case 1 recovery and the reduction (the amount changed) of such flows with recovery implementation compared to Base Case 1. Note: a negative value indicates an increase of a flow. There

is an increase in the electricity (energy) required by using the Case 1 recovery. This is attributed to the electricity required to operate the V-SEP membrane recovery system. Further analysis of the implications (environmental and economic) of the increased energy requirement will follow.

Table 36

Flows of mass and energy associated with Case 1 recovery and the reductions of each as compared to Base Case 1

Flows	**Case 1 recovery**	**Flow Reduction**		**Reduction**
Freshwater	$1.35x10^8$	$3.65x10^7$	gal/yr	21.3%
	$1.13x10^9$	$3.04x10^8$	lb/yr	
Nonhazardous wastewater	$9.13x10^7$	$3.65x10^7$	gal/yr	28.6%
	$7.60x10^8$	$3.04x10^8$	lb/yr	
Hazardous wastewater	$1.14x10^5$	0	lb/yr	0%
Electricity (pumps + recovery)	$1.85x10^6$	$-5.54x10^5$	MJ/yr	-29.9%

Table 37 shows a comparison of the life cycle emissions associated with Base Case 1 and Case 1. As can be seen, there are varying amounts of reduction among the life cycle emissions. Most notably, the total emissions and CO_2 emissions are reduced by 28% when compared to the Base Case 1 scenario. The only increase in the life cycle emissions noted is in volatile organic compounds (VOCs). This is caused by the increased amount of electricity that is needed to operate the V-SEP membrane system. The life cycle inventory for electricity has a relatively high emission of VOCs when compared to the other inputs to the total life cycle emissions. The increase in VOCs is insignificant compared to all other emissions, however. The amount of VOCs emitted

per year does not exceed 1 lb and only increases by 0.03 lbs when comparing Case 1 to Base Case 1.

Table 37

Comparison of the total life cycle emissions of the current Nestlé process (Base Case 1) and Case 1

	Base Case 1	**Case 1**	**Reduction**
Total Air Emissions (lb/yr)	3.06E+07	2.21E+07	**27.7%**
CO_2 (lb/yr)	3.04E+07	2.20E+07	**27.7%**
CO (lb/yr)	2.75E+03	2.12E+03	**22.9%**
CH_4 (lb/yr)	2.82E+04	2.13E+04	**24.6%**
NO_X (lb/yr)	6.13E+04	4.40E+04	**28.3%**
NMVOC (lb/yr)	9.33E+02	7.35E+02	**21.3%**
Particulate (lb/yr)	3.34E+03	2.62E+03	**21.6%**
SO_2 (lb/yr)	3.28E+04	2.53E+04	**22.8%**
Total Water Emissions (lb/yr)	4.43E+05	3.48E+05	**21.4%**
VOCs (lb/yr)	2.27E-01	2.55E-01	**-12.2%**
Total Soil Emissions (lb/yr)	3.35E+02	2.42E+02	**28.0%**
Total Emissions (lb/yr)	**3.10E+07**	**2.24E+07**	**27.6%**
CED (MJ/yr)	9.13E+07	6.91E+07	**24.3%**

Table 38 shows the operating parameters of the V-SEP membrane system that will be used for the recovery water from the plant effluent. The design flux is calculated as shown in Equation 61, using the observed average flux of 65 GFD, shown in Figure 69. To recover 100,000 GPD of permeate when the system is operated at 90% recovery, a feed rate of 111,000 GPD wastewater is required. The cost of the membranes for the system are calculated based on an initial membrane estimate. Staff from New Logic Research estimate that the cost of membranes for a system that provides 1,400 ft^2 of membrane area would be $75,000 per module. The membrane area per module for the proposed system is 1,200 ft^2. From the initial estimate for membrane costs, a membrane

cost per area has been calculated at roughly $53.57/ft^2. Therefore, it is estimated that membrane cost per module for a system with 1,200 ft^2 is $64,300. New Logic Research has suggested that a typical lifespan of the membranes in the system would be 3 yrs; however, a 5-yr replacement cycle has been chosen, since the membranes are expected to be more durable. Thus, the annual membrane cost would result in about $12,850 per year per module. The recovery system for Case 1 requires 2 modules (Equation 68 shows a sample calculation of Equation 63). The annual cost of membranes for the Case 1 system would be $25,700. The cost of electricity is calculated using the rate for electricity at the Nestlé Freehold plant and the amount of energy needed to run the system. A sample calculation of the annual cleaner consumption is given in Equation 69. Sample calculations for determining the total energy consumption (corresponding to Equations 64 – 66) are given in Equations 70 – 72. The annual operating cost of the recovery system was calculated as in Equation 73. New Logic Research provided an initial estimate for the capital cost for a 3-module V-SEP membrane system at $880,000. This figure has been cross-verified with the capital cost of a commercial installation of a V-SEP membrane system at the Glassboro Water and Sewer Agency (Glassboro, NJ). It will be estimated that the capital cost of the 2-module system is $600,000.

Table 38

Operating parameters for the V-SEP membrane system for Case 1

Membrane Type	Nanofiltration (NF4)
Design Flux (GFD)	32.5
Pressure (psig)	350
Temperature (°C)	25
Feed Rate (GPD)	111,000
Recovery (%)	90%
Number of Modules	2
Membrane Area per Module (ft^2)	1,200
Cleaner Consumption (gal/yr)	73
Energy Consumption (MJ/yr)	829,900
Operating Cost ($/yr)	47,600
Capital Cost ($)	600,000

$$\#modules = \frac{100{,}000\,\frac{gal}{day}}{65\,\frac{gal}{ft^2 day}\cdot 1{,}200 ft^2}\cdot\frac{1+0.50}{\left(\frac{40{,}320\ min-120\ min}{40{,}320\ min}\right)} = 1.92 = 2\ modules \tag{68}$$

$$Cleaner\ consumption = \frac{70\ gal}{module}\cdot\frac{2}{40{,}320\ minutes}\cdot 0.02\cdot 2\ modules\cdot\frac{60\ min}{hr}\cdot\frac{24hr}{day}\cdot\frac{365day}{yr} = 73\,\frac{gal}{yr} \tag{69}$$

$$Feed\ pump\ power\ (hp) = \frac{77\ gal}{min}\cdot\frac{350\ lb_f}{in^2}\cdot\frac{ft^3}{7.48\ gal}\cdot\frac{(12\ in)^2}{ft^2}\cdot\frac{1\ hp\cdot min}{33{,}000\ lb_f\cdot ft}\cdot\frac{1}{0.85} = 18\ hp \tag{70}$$

$$Power\ Requirement = 18\ hp + (2\cdot 10\ hp) = 38\ hp \tag{71}$$

$$Energy\ Requirement = 38\ hp \cdot \frac{0.7457\ kW}{1\ hp} \cdot \frac{22\ hr}{day} \cdot \frac{365\ day}{yr} \cdot \frac{kJ}{kW \cdot s} \cdot \frac{MJ}{1{,}000\ kJ} \cdot \frac{3{,}600\ s}{hr} = \mathbf{829{,}900}\ \frac{MJ}{yr} \quad (72)$$

$$VSEP\ Operating\ Costs = Cost_E + Cost_{membrane} + Cost_{Cleaner}$$

$$VSEP\ Operating\ Costs = 20{,}800\ \frac{\$}{yr} + 25{,}700\ \frac{\$}{yr} + 1{,}200\ \frac{\$}{yr} = \mathbf{47{,}600}\ \frac{\$}{\boldsymbol{yr}} \quad (73)$$

A summary of the operating costs and savings compared to the Base Case scenario can be seen in Table 39. The greatest savings is in the nonhazardous wastewater discharge. This is a result of the decreased amount of wastewater sent to the county utilities authority for treatment. As stated earlier, there are no hazardous waste reductions since BOD and TSS discharges remain the same, due to retentate disposal from the V-SEP system. Implementation of the V-SEP membrane system for water recovery shows that savings to the overall operating cost exist. In total, successful intervention for water recovery yields a yearly operating costs savings of 17.9%. Calculations of operating costs of Base Case 1 and values presented in Table 39 are provided in the earlier section "Operating Cost of the Nestlé Process." Calculations of the Case 1 recovery are determined by using the recovery option mass and energy flows provided in Table 33 and multiplying be the unit costs values for those flows (on a per lb or MJ basis), as provided in Table 20 using Equation 39.

Table 39

Summary of the operating costs of Case 1 as compared to the current Nestlé process (Base Case 1)

	Base Case 1 ($/yr)	**Case 1 recovery ($/yr)**	**Savings ($/yr)**	**Savings (%)**
Freshwater	22,300	17,600	4,700	21.1
NHW Discharge	505,900	361,300	144,600	28.6
BOD Surcharge	22,400	22,400	0	0
TSS Surcharge	22,600	22,600	0	0
Well Pumps	32,500	25,600	6,900	21.2
Recovery System	N/A	47,600	-47,600	-
Total	605,700	497,100	108,600	17.9

An economic analysis was generated to evaluate Case 1 based on operating cost savings and the capital cost of the recovery equipment. Table 40 shows the economic metrics evaluated for the water recovery system. The economic assessment shows that it is not feasible to only recover reusable water from the plant effluent. The NPV after 10 years is a negative value, indicating the savings from the recovery system are not great enough to justify the capital cost. Likewise, the payback time after tax of 16.2 yrs is too high for implementation at the Nestlé Freehold plant.

Table 40

Economic metrics for the water recovery system in Case 1

Capital Cost ($)	600,000
Savings ($/yr)	108,600
IRR (%)	11.2
ROI (%)	16.8
Payback time after tax (yr)	16.2
10-yr NPV ($)	-81,000

While the recovery system does not appear to be economically feasible, the environmental assessment showed promising results. Thus, it is apparent that water recovery will provide an environmental benefit.

Case 2 – Recovery of Water from Pit #3 Wastewater

Case 2 involves the recovery of water from the Pit #3 wastewater. The Pit #3 wastewater stream is currently sent to the wastewater pretreatment processes at the plant and ends up in the plant effluent. The Pit #3 wastewater has relatively lower concentrations of contaminants when compared to the plant effluent. Water recovered from this stream will be used as feed to the cooling tower, as shown in Figure 72. Case 2 has the added benefit of introducing the intervention before the wastewater pretreatment processes. Thus, there will be a reduction in operating costs and life cycle emissions of the energy requirements of the pretreatment operation processes. Case 2 has been divided to four subcases: Case 2a, 2b, 2c and 2d. Case 2a will assess the recovery of water from the Pit #3 wastewater stream using vibratory reverse osmosis, while the remaining subcases will use vibratory nanofiltration. Case 2b assesses vibratory nanofiltration with the same Pit #3 wastewater sample as Case 2a. Case 2c also assesses water recovery from the Pit #3 wastewater stream; however, an alternate sample of Pit #3 wastewater is used in this case that has higher concentrations of major contaminants. Case 2d takes an average of the observed flux value from Cases 2b and 2c to use in scale-up calculations. Table 41 shows the actual feed concentrations of the major contaminants in the Pit #3 wastewater used in the studies for Case 2a and Case 2b. The contaminant concentrations for the Pit #3 wastewater in Case 2c are provided in the respective section.

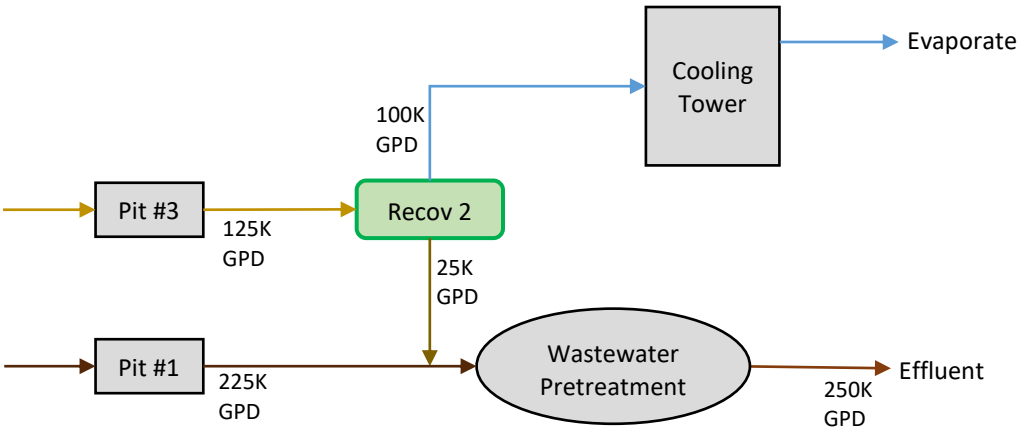

Figure 72. Case 2 water recovery scheme used for Cases 2a – 2d

Table 41

Feed conditions for the Pit #3 wastewater used in the scale-up studies for Case 2a and 2b

COD (mg/L)	1,020
Turbidity (NTU)	13
Conductivity (µS/cm)	600

Case 2a – Vibratory Reverse Osmosis

The design flux for the recovery system in Case 2a was determined the same way as in Case 1. Figure 73 shows the plot of the instantaneous and average flux values as a function of the percent permeate recovery. At 80% recovery, the average flux is observed at 38 GFD. There does not appear to be any appreciable degradation in the average flux from the start of the run to 80% recovery. The average permeate concentrations of contaminants at the design recovery of 80% can be seen in Table 42. It can be seen in Table 42 that all water specifications for use in the cooling tower have been met. The major difference is the removal of conductivity. While the initial conductivity is lower in Case 2a as compared to Case 1, the reverse osmosis membrane in

significantly removes the conductivity from the Pit #3 wastewater stream. This is at the cost of a lower flux value. Scale-up of the system will be performed as in "Scale-up Calculations" section. Table 43 shows the mass and energy flows associated with the Case 2a recovery scenario. The difference between this case and Case 1 is the blower electricity that is needed in the on-site wastewater pretreatment.

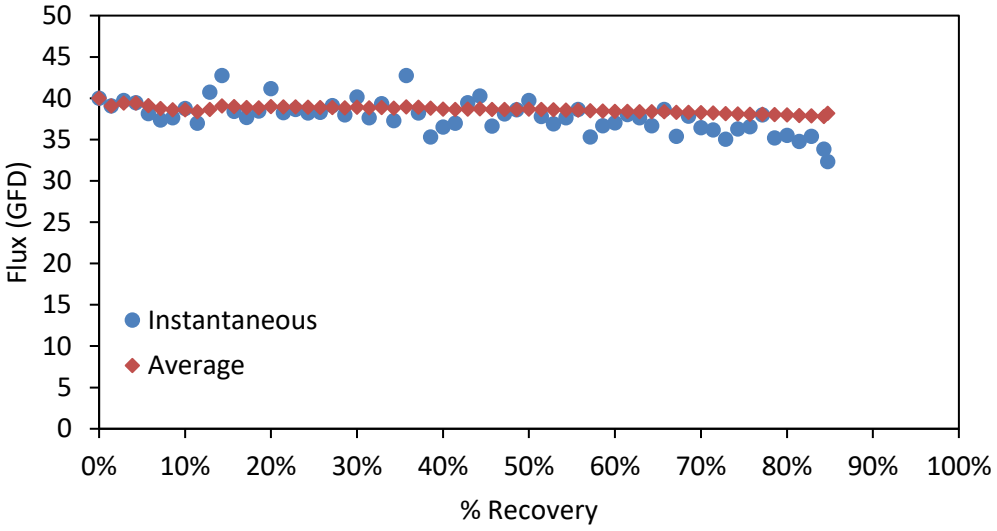

Figure 73. Instantaneous and average permeate flux as a function of the percent recovery of permeate; reverse osmosis, 550 psig, 1" displacement

Table 42

Average permeate concentrations at 80% recovery of permeate in Case 2a

COD (mg/L)	18
Turbidity (NTU)	<<1
Conductivity (µS/cm)	<10

Table 43

Mass and energy flow associated with Case 2a recovery

Flows		**Case 2a recovery**	
Freshwater		$1.35x10^8$	gal/yr
		$1.13x10^9$	lb/yr
Nonhazardous wastewater		$9.13x10^7$	gal/yr
		$7.60x10^8$	lb/yr
Hazardous wastewater		$1.14x10^5$	lb/yr
Electricity	-well pumps	$1.02x10^6$	MJ/yr
	-blowers	$5.71x10^6$	MJ/yr
	-recovery	$1.35x10^6$	MJ/yr
Total Electricity		$8.09x10^9$	MJ/yr

The life cycle emissions associated with Case 2a can be seen in Table 44. Air emissions are the dominant type of emissions in Case 2a, contributing to 97.9% of the total emissions. Furthermore, the total CO_2 emissions make up over 99% of the total air emissions. Nonhazardous wastewater disposal accounts for 89.4% of the total air emissions and 88.4% of the total emissions.

Table 44

Life cycle emissions associated with Case 2a

	Freshwater	NHW	HW	Electricity	Total
Total Air Emissions (lb/yr)	6.30E+05	2.11E+07	9.24E+03	1.85E+06	**2.36E+07**
CO_2 (lb/yr)	6.25E+05	2.09E+07	9.18E+03	1.82E+06	**2.34E+07**
CO (lb/yr)	1.03E+02	1.73E+03	7.47E-01	1.27E+03	**3.10E+03**
CH_4 (lb/yr)	6.85E+02	1.85E+04	8.04E+00	9.14E+03	**2.83E+04**
NO_X (lb/yr)	0.00E+00	4.36E+04	0.00E+00	1.46E+03	**4.51E+04**
NMVOC (lb/yr)	2.14E+01	5.81E+02	2.53E-01	5.77E+02	**1.18E+03**
Particulate (lb/yr)	1.94E+03	5.74E+02	2.45E-01	4.81E+02	**2.99E+03**
SO_2 (lb/yr)	6.81E+02	2.10E+04	9.05E+00	1.59E+04	**3.76E+04**
Total Water Emissions (lb/yr)	1.38E+04	2.73E+05	2.26E+02	2.65E+05	**5.52E+05**
VOCs (lb/yr)	2.34E-03	6.75E-02	2.94E-05	8.09E-01	**8.79E-01**
Total Soil Emissions (lb/yr)	7.73E+00	2.31E+02	1.01E-01	1.16E+01	**2.51E+02**
Total Emissions (lb/yr)	**6.44E+05**	**2.13E+07**	**9.46E+03**	**2.11E+06**	**2.41E+07**
CED (MJ/yr)	2.45E+06	5.93E+07	2.54E+04	3.19E+07	**9.37E+07**

Table 45 includes the mass and energy flows associated with Case 2a recovery and the reduction (the amount changed) of such flows with recovery implementation compared to Base Case 2. Note: a negative value indicates an increase of a flow. There is a decrease in the total electricity (energy) required in the Case 2a scenario, despite the required energy by the recovery system. The reduction in total electricity required is a cause of reducing the duty required by the blowers in the wastewater pretreatment. It can be seen that an overall reduction of 1,210,000 MJ/yr is achieved, which appears to be significant. Further analysis of the implications (environmental and economic) of the increased energy requirement will follow.

Table 45

Flows of mass and energy associated with Case 2a recovery and the reductions of each as compared to Base Case 2

Flows	**Case 2a Recovery**	**Flow Reduction**		Reduction
Freshwater	$1.35x10^8$	$3.65x10^7$	gal/yr	21.3%
	$1.13x10^9$	$3.04x10^8$	lb/yr	
Nonhazardous wastewater	$9.13x10^7$	$3.65x10^7$	gal/yr	28.6%
	$7.60x10^8$	$3.04x10^8$	lb/yr	
Hazardous wastewater	$1.14x10^5$	0	lb/yr	0%
Electricity -well pumps	$1.02x10^6$	$2.76x10^5$	MJ/yr	21.3%
-blowers	$5.71x10^6$	$2.28x10^6$	MJ/yr	28.6%
-recovery	$1.35x10^6$	$-1.35x10^6$	MJ/yr	-
Total Electricity	$8.09x10^6$	$1.21x10^6$	MJ/yr	13.0%

Table 46 shows a comparison of the life cycle emissions associated with the Base Case 2 scenario and Case 2a. As can be seen, there are varying amounts of reduction among the life cycle emissions. Most notably, the total emissions and CO_2 emissions are reduced by 27.2% and 27.4%, respectively, when compared to Base Case 2.

Table 46

Comparison of the total life cycle emissions of the current Nestlé process (Base Case 2) and Case 2a

	Base Case 2	Case 2a	Reduction
Total Air Emissions (lb/yr)	3.24E+07	2.36E+07	**27.4%**
CO_2 (lb/yr)	3.22E+07	2.34E+07	**27.4%**
CO (lb/yr)	4.01E+03	3.10E+03	**22.6%**
CH_4 (lb/yr)	3.73E+04	2.83E+04	**24.0%**
NO_X (lb/yr)	6.28E+04	4.51E+04	**28.2%**
NMVOC (lb/yr)	1.50E+03	1.18E+03	**21.6%**
Particulate (lb/yr)	3.82E+03	2.99E+03	**21.6%**
SO_2 (lb/yr)	4.86E+04	3.76E+04	**22.6%**
Total Water Emissions (lb/yr)	7.05E+05	5.52E+05	**21.6%**
VOCs (lb/yr)	1.03E+00	8.79E-01	**14.4%**
Total Soil Emissions (lb/yr)	3.47E+02	2.51E+02	**27.8%**
Total Emissions (lb/yr)	**3.31E+07**	**2.41E+07**	**27.2%**
CED (MJ/yr)	1.23E+08	9.37E+07	**23.7%**

Table 47 shows the operating parameters of the V-SEP membrane system that will be used for the recovery of water from the Pit #3 wastewater. The design flux is calculated from the observed average flux of 38 GFD, shown in Figure 73. The low flux shown is characteristic of a reverse osmosis system; however, it creates a drawback in that a larger overall V-SEP system is required. This drives the capital cost to a high value for the recovery system. The recovery system for Case 2a requires 3 modules. The membrane area per module is greater for Case 2a than in Case 1 at 1,400 ft^2. The membrane replacement cost per module will be $75,000 and will be assumed to need replacement every 5 yrs. Therefore, the total annual cost for membranes for the system needed for Case 2a would be $45,000. This is obtained by dividing the replacement cost by 5 yrs to obtain $15,000 per year, and then multiplying this by 3 modules. It should be noted that the V-SEP recovery system in Case 2a requires an operating pressure of 550

psig, which further raises the electricity requirement of the recovery equipment. All other calculations have been carried out similarly to Equations 68 – 72, with changes to specified constants. The annual operating cost of the recovery system was calculated as in Equation 73. New Logic Research provided an initial estimate for the capital cost for a 3-module V-SEP membrane system at $880,000. For consistency, a capital cost of $900,000 has been used for the 3-module system.

Table 47

Operating parameters for the scaled-up V-SEP membrane (RO) system for Case 2a

Membrane Type	Reverse Osmosis (LFC3)
Design Flux (GFD)	19
Pressure (psig)	550
Temperature (°C)	25
Feed Rate (GPD)	125,000
Recovery (%)	80%
Number of Modules	3
Membrane Area per Module (ft^2)	1,400
Cleaner Consumption (gal/yr)	110
Energy Consumption (MJ/yr)	1,355,000
Operating Cost ($/yr)	80,600
Capital Cost ($)	900,000

A summary of the operating costs and savings as compared to Base Case 2 can be seen in Table 48. The greatest savings is in the nonhazardous wastewater discharge and the reduced energy required by the blowers of the aeration lagoon. Since the retentate stream of the membrane process is sent for discharge, there is no reduction in BOD and TSS. The recovery of water before the on-site pretreatment processes results in a greater amount of annual savings. A successful intervention results in $132,700 in savings per

year, which is about 16.5% compared to Base Case 2. Calculations of the operating costs of Base Case 2 were done as shown in the section "Operating Cost of the Nestlé Process." Case 2 recovery operating costs have been determined using the mass and energy flows provided in Table 43 and multiplying by the unit cost values for those flows (on a per lb or MJ basis), as provided in Table 20.

Table 48

Summary of the operating costs of Case 2a as compared to the current Nestlé process (Base Case 2)

	Base Case 2 ($/yr)	**Case 2a recovery ($/yr)**	**Savings ($/yr)**	**Savings (%)**
Freshwater	22,300	17,600	4,700	21.1
NHW Discharge	505,900	361,300	144,600	28.6
BOD Surcharge	22,400	22,400	0	0
TSS Surcharge	22,600	22,600	0	0
Well Pumps	32,500	25,600	6,900	21.2
Blowers	199,900	142,800	57,100	28.6
Recovery System	N/A	80,600	-80,600	-
Total	805,600	672,900	132,700	16.5

An economic analysis was generated to evaluate Case 2a based on operating cost savings and the capital cost of the recovery equipment. Table 49 shows the economic metrics evaluated for the water recovery system in Case 2a. The economic assessment shows that the recovery system proposed in Case 2a is not feasible. The NPV after 10 years is a negative value, which indicates that the savings from the recovery system are not significant enough to justify the capital cost of the recovery system. Likewise, the payback period of 27.1 is not feasible for use in the Nestlé process. It can be determined that the economic assessment of the recovery system is limited by the capital cost of the

system, since the savings generated present a reasonable value. The main reason the Case 2a recovery is not economically feasible is because the larger 3-module V-SEP membrane system is required to accommodate the low flux value obtained. Thus, there is room for improvement for the economic metrics for the design of a recovery system.

Table 49

Economic metrics for the water recovery system designed for Case 2a

Capital Cost ($)	900,000
Savings ($/yr)	132,700
IRR (%)	7.0
ROI (%)	14.1
Payback time after tax (yr)	27.1
10-yr NPV ($)	-246,700

Case 2b – Vibratory Nanofiltration

The recovery Case 2a was not economically feasible since the flux achieved in the reverse osmosis system was limited to a low value. Thus, Case 2b has been conducted to evaluate the recovery of water from the Pit #3 wastewater using vibratory nanofiltration. Figure 74 shows the plot of the instantaneous and average flux values as a function of the percent permeate recovery. At 80% recovery, the average flux is observed at 130 GFD. There does not appear to be any appreciable degradation in the observed average flux from the start of the run to 80% recovery. The average permeate concentrations at the design recovery of 80% can be seen in Table 50. Concentrations are not as low as those achieved in Case 2a; however, the concentrations meet the specifications for use in the cooling tower. The COD concentration is higher than expected and even greater than

achieved in Case 1. As previously stated, this has been discussed with the staff at the Nestlé Freehold plant, and the absence of color is mores significant. Color has been removed in the permeate in Case 2b. Scale-up of the system will be performed as in Scale-up Calculations section. Table 51 shows the mass and energy flow associated with Case 2b recovery. All mass flows associated with Case 2b are identical to Case 2a; however, the electricity required by the designed recovery system is less than that of Case 2a. This will be explained in greater detail in this section. Since the average observed flux is much greater than that achieved in Case 2a, the scaled-up V-SEP system requires less modules.

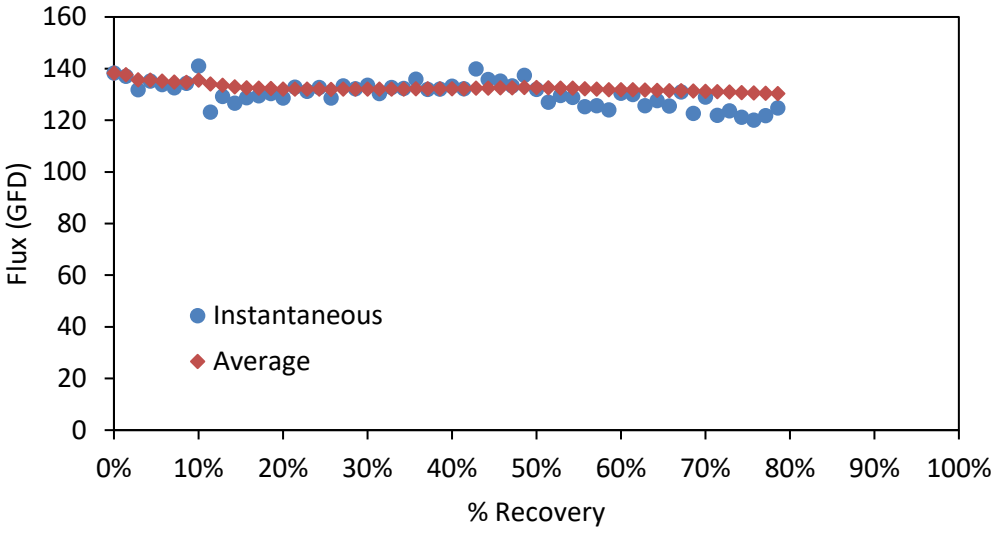

Figure 74. Instantaneous and average permeate flux as a function of the percent recovery of permeate; nanofiltration, 350 psig, 1" displacement

Table 50

Average permeate concentration at 80% recovery of permeate in Case 2b

COD (mg/L)	490
Turbidity (NTU)	<<1
Conductivity (µS/cm)	100

Table 51

Mass and energy flows associated with Case 2b recovery

Flows	**Case 2b recovery**	
Freshwater	$1.35x10^8$	gal/yr
	$1.13x10^9$	lb/yr
Nonhazardous wastewater	$9.13x10^7$	gal/yr
	$7.60x10^8$	lb/yr
Hazardous wastewater	$1.14x10^5$	lb/yr
Electricity -well pumps	$1.02x10^6$	MJ/yr
-blowers	$5.71x10^6$	MJ/yr
-recovery	$6.66x10^5$	MJ/yr
Total Electricity	$7.40x10^9$	MJ/yr

The life cycle emissions associated with Case 2b recovery can be seen in Table 52. As with the previous cases, it can be seen that air emissions make up the majority of the total emissions at 98.0%. Of all air emissions, CO_2 emissions contribute to 99.2%. Again, similar to previous cases, the emissions associated with nonhazardous wastewater discharge contribute to most of the total life cycle emissions at 89.1%.

Table 52

Life cycle emissions associated with Case 2b

	Freshwater	NHW	HW	Electricity	Total
Total Air Emissions (lb/yr)	6.30E+05	2.11E+07	9.24E+03	1.69E+06	**2.34E+07**
CO_2 (lb/yr)	6.25E+05	2.09E+07	9.18E+03	1.66E+06	**2.32E+07**
CO (lb/yr)	1.03E+02	1.73E+03	7.47E-01	1.16E+03	**2.99E+03**
CH_4 (lb/yr)	6.85E+02	1.85E+04	8.04E+00	8.36E+03	**2.75E+04**
NO_X (lb/yr)	0.00E+00	4.36E+04	0.00E+00	1.33E+03	**4.50E+04**
NMVOC (lb/yr)	2.14E+01	5.81E+02	2.53E-01	5.28E+02	**1.13E+03**
Particulate (lb/yr)	1.94E+03	5.74E+02	2.45E-01	4.40E+02	**2.95E+03**
SO_2 (lb/yr)	6.81E+02	2.10E+04	9.05E+00	1.46E+04	**3.63E+04**
Total Water Emissions (lb/yr)	1.38E+04	2.73E+05	2.26E+02	2.43E+05	**5.30E+05**
VOCs (lb/yr)	2.34E-03	6.75E-02	2.94E-05	7.40E-01	**8.10E-01**
Total Soil Emissions (lb/yr)	7.73E+00	2.31E+02	1.01E-01	1.06E+01	**2.50E+02**
Total Emissions (lb/yr)	**6.44E+05**	**2.13E+07**	**9.46E+03**	**1.93E+06**	**2.39E+07**
CED (MJ/yr)	2.45E+06	5.93E+07	2.54E+04	2.92E+07	**9.10E+07**

Table 53 includes the mass and energy flows associated with Case 2b recovery and the reduction (the amount changed) of such flows with recovery implementation compared to Base Case 2. Note: a negative value indicates an increase of a flow. As with Case 2a, an overall reduction in electricity required is observed, despite the energy requirement of the recovery system. Since the electricity required by the recovery system has been reduced for Case 2b, the overall electricity reduction increases to 20.4%. Further analysis of the implications (environmental and economic) of the increased energy requirement will follow.

Table 53

Flows of mass and energy associated with Case 2b recovery and the reduction of each as compared to Base Case 2

Flows	**Case 2b Recovery**	**Flow Reduction**		Reduction
Freshwater	$1.35x10^8$	$3.65x10^7$	gal/yr	21.3%
	$1.13x10^9$	$3.04x10^8$	lb/yr	
Nonhazardous wastewater	$9.13x10^7$	$3.65x10^7$	gal/yr	28.6%
	$7.60x10^8$	$3.04x10^8$	lb/yr	
Hazardous wastewater	$1.14x10^5$	0	lb/yr	0%
Electricity -well pumps	$1.02x10^6$	$2.76x10^5$	MJ/yr	21.3%
-blowers	$5.71x10^6$	$2.28x10^6$	MJ/yr	28.6%
-recovery	$6.66x10^5$	$-6.66x10^5$	MJ/yr	-
Total Electricity	$7.40x10^6$	$1.89x10^6$	MJ/yr	20.4%

Table 54 shows a comparison of the life cycle emissions associated with Base Case 2 and Case 2b recovery. Similar reductions in emissions can be seen as compared to Case 2a recovery (shown in Table 46). This is because the nonhazardous wastewater discharge and disposal controls such a significant portion of the total life cycle emissions. Case 2a and Case 2b recover the same mass of water from processing which explains the similar reductions in emissions. Case 2b provides slightly higher reductions in each category, as less electricity is required to operate the water recovery equipment.

Table 54

Comparison of the total life cycle emissions of Base Case 2 and Case 2b

	Base Case 2	Case 2b	Reduction
Total Air Emissions (lb/yr)	3.24E+07	2.34E+07	**27.8%**
CO_2 (lb/yr)	3.22E+07	2.32E+07	**27.9%**
CO (lb/yr)	4.01E+03	2.99E+03	**25.3%**
CH_4 (lb/yr)	3.73E+04	2.75E+04	**26.1%**
NO_X (lb/yr)	6.28E+04	4.50E+04	**28.4%**
NMVOC (lb/yr)	1.50E+03	1.13E+03	**24.8%**
Particulate (lb/yr)	3.82E+03	2.95E+03	**22.7%**
SO_2 (lb/yr)	4.86E+04	3.63E+04	**25.4%**
Total Water Emissions (lb/yr)	7.05E+05	5.30E+05	**24.8%**
VOCs (lb/yr)	1.03E+00	8.10E-01	**21.1%**
Total Soil Emissions (lb/yr)	3.47E+02	2.50E+02	**28.0%**
Total Emissions (lb/yr)	**3.31E+07**	**2.39E+07**	**27.8%**
CED (MJ/yr)	1.23E+08	9.10E+07	**25.9%**

Table 55 shows the operating parameters of the V-SEP membrane system that will be used for the recovery of water from the Pit #3 wastewater. The design flux has been calculated from the average observed flux at 80% recovery, which is 130 GFD (shown in Figure 74). All other calculations have been carried out similarly to Equations 68 – 72, with changes for specified constants. The most significant difference for Case 2b as compared to the previous cases is the V-SEP system is a 1-module system. This provides great reductions in operating costs and energy requirement as compared to the previous cases. The membrane area for the single module is 1,200 ft^2. The cost for membrane replacement is $64,300, which results in $12,850 per year assuming a 5 yr period between membrane replacement. The annual operating cost of the V-SEP recovery system needed for Case 2 is $30,100. The annual operating cost of the recovery system was calculated as in Equation 73. The capital cost of the equipment has been estimated at $300,000.

Table 55

Operating Parameters for the V-SEP membrane system for Case 2b

Membrane Type	Nanofiltration (NF4)
Design Flux (GFD)	65
Pressure (psig)	350
Temperature (°C)	25
Feed Rate (GPD)	125,000
Recovery (%)	80%
Number of Modules	1
Membrane Area per Module (ft^2)	1,200
Cleaner Consumption (gal/yr)	37
Energy Consumption (MJ/yr)	666,100
Operating Cost ($/yr)	30,100
Capital Cost ($)	300,000

A summary of the operating costs and savings as compared to Base Case 2 are provided in Table 56. The greatest amount of savings is represented in the nonhazardous wastewater discharge and the blowers of the on-site pretreatment processes. An appreciable amount of total savings is seen at 22.7% as compared to Base Case 2. Calculations of operating costs of Base Case 2 are provided in the former section "Operating Cost of the Nestlé Process." Calculations for Case 2b recovery are determined using Case 2b mass and energy flows shown in Table 51 and multiplying them by the unit cost values for each flow (on a per lb or MJ basis), as shown in Table 20.

Table 56

Summary of the operating costs of Case 2b as compared to Base Case 2

	Base Case 2 ($/yr)	**Case 2b recovery ($/yr)**	**Savings ($/yr)**	**Savings (%)**
Freshwater	22,300	17,600	4,700	21.1
NHW Discharge	505,900	361,300	144,600	28.6
BOD Surcharge	22,400	22,400	0	0
TSS Surcharge	22,600	22,600	0	0
Well Pumps	32,500	25,600	6,900	21.2
Blowers	199,900	142,800	57,100	28.6
Recovery System	N/A	30,100	-30,100	-
Total	805,600	622,400	183,200	22.7

An economic analysis was generated to evaluate Case 2b based on operating cost savings and the capital cost of recovery equipment. Table 57 shows the economic metrics evaluated for the water recovery system in Case 2b. The economic assessment shows that this system is feasible for water recovery from the Pit #3 wastewater stream. The NPV after 10 years is positive and a greater value than the capital cost of the equipment, indicating a favorable investment. In addition, the payback time is below 3 years, which is also favorable. The most significant contributing factor to the economics is the smaller (1-module) V-SEP system used. Again, this highlights the importance of the capital cost in system design. Thus, Case 2b provides an effective recovery method of water from an environmental and economic standpoint.

Table 57

Economic metrics for the water recovery system in Case 2b

Capital Cost ($)	300,000
Savings ($/yr)	183,200
IRR (%)	54.2
ROI (%)	51.6
Payback time after tax (yr)	2.6
10-yr NPV ($)	494,200

Case 2c – Vibratory Nanofiltration, Alternate Sample

Since it has been found that recovery of the Pit #3 wastewater is feasible economically and environmentally in Case 2b, an additional test was conducted for an alternative sample of the Pit #3 wastewater. Table 58 shows the feed conditions of the alternate Pit #3 wastewater sample as compared to the original Pit #3 wastewater sample. As can be seen, the alternate sample has higher concentrations of the major contaminants than the original sample. This will provide a good analysis of the recovery system's capacity to handle variations in the wastewater that would be expected as production varies at the Nestlé plant.

Table 58

Feed conditions of the original (Case 2b) and alternate samples (Case 2c) of the Pit #3 wastewater

	Case 2b	Case 2c
COD (mg/L)	1,020	1,260
Turbidity (NTU)	13	30
Conductivity (µS/cm)	600	1,280

Figure 75 shows the average and instantaneous flux values as a function of the percent permeate recovery. At 80% recovery, the observed average flux is observed at 82 GFD. There appears to be a slight decay in flux as compared to the original Pit #3 wastewater sample (Figure 74) from the start of the run to 80% recovery. This is most likely caused by the increased conductivity in the alternate sample. The flux that has been achieved using the alternate Pit #3 wastewater sample is 37% lower than that achieved in the original Pit #3 wastewater sample; however, it is over double the flux achieved when using a reverse osmosis membrane. Scale-up of the system will be performed as in Scale-up Calculations section.

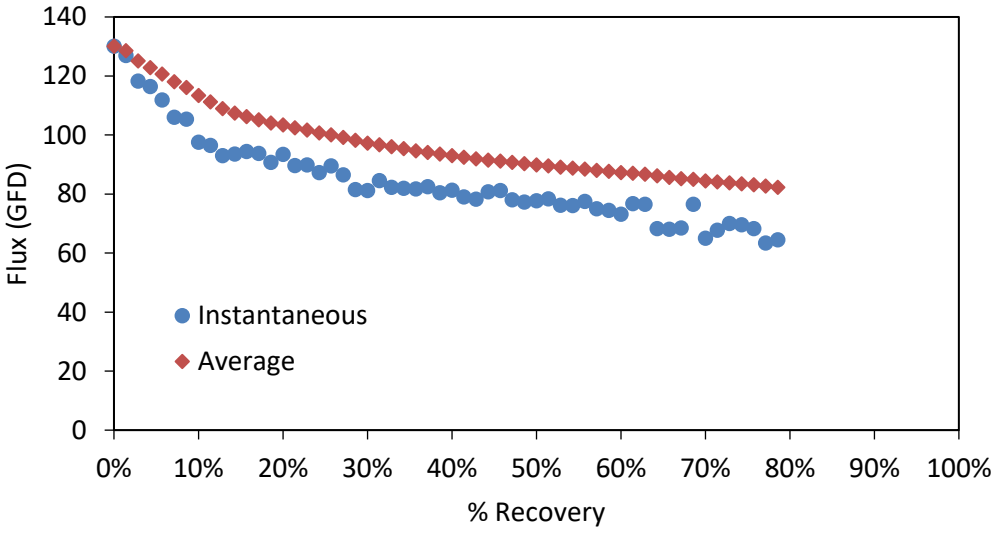

Figure 75. Instantaneous and average permeate flux as a function of the percent recovery of permeate from the alternate Pit #3 wastewater sample; nanofiltration, 350 psig, 1" displacement

The instantaneous flux has also been plotted as a function of VRR, shown in Figure 76. Again, it can be seen that there is greater amount of decay in flux as compared

to processing with the original Pit #3 wastewater sample (Figure 62). However, the system appears to trend to a high VRR that would be practical for water recovery. Thus, it can be considered that the fouling in the system with alternate sample is effectively controlled by using vibration.

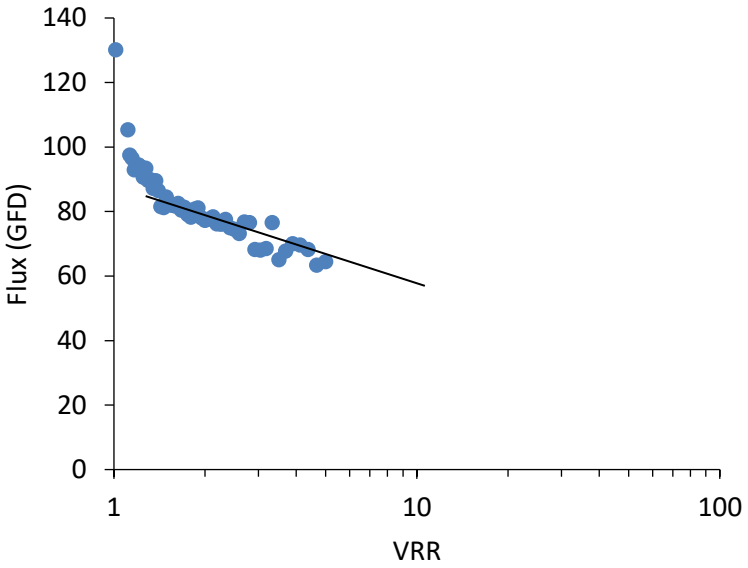

Figure 76. Instantaneous permeate flux as a function of VRR for the alternate Pit #3 wastewater sample; nanofiltration, 350 psig, 1" displacement

The average permeate contaminant concentrations have been calculated for the permeate produced from the alternate Pit #3 wastewater sample and are shown in Figure 77, Figure 78, and Figure 79. The average permeate concentrations of COD and turbidity are similar to those achieved when processing with the original sample. The permeate samples are again clear and will not cause issues with the controls systems of the Nestlé plant cooling tower. Table 59 shows the average permeate concentrations at 80% permeate recovery. The average permeate conductivity is greater than that achieved for

the original sample and is slightly above the specification for the cooling tower. However, it can be considered the alternate sample is on the higher end of contaminant concentrations of what is normally expected. Thus, the permeate conductivity achieved with the alternate Pit #3 wastewater sample can be considered within reason for reuse.

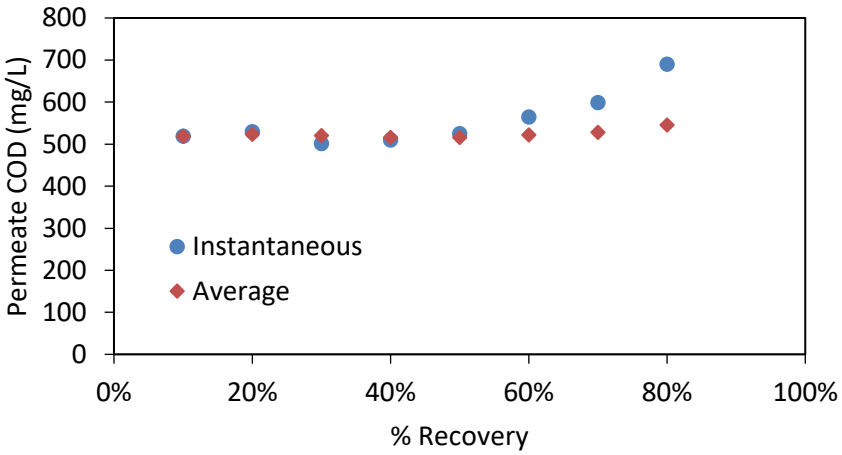

Figure 77. Instantaneous and average permeate COD concentration as a function of the percent permeate recovery when processing the alternate Pit #3 wastewater; nanofiltration, 350 psig 1" displacement

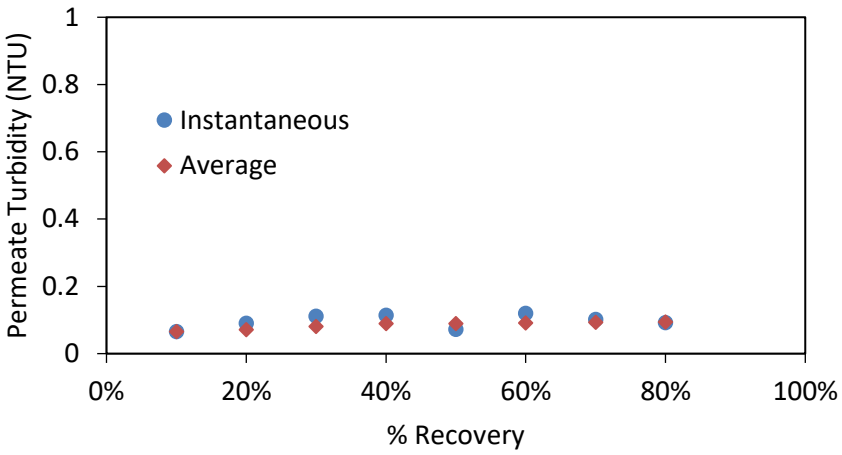

Figure 78. Instantaneous and average permeate turbidity as a function of the percent permeate recovery when processing the alternate Pit #3 wastewater; nanofiltration, 350 psig 1" displacement

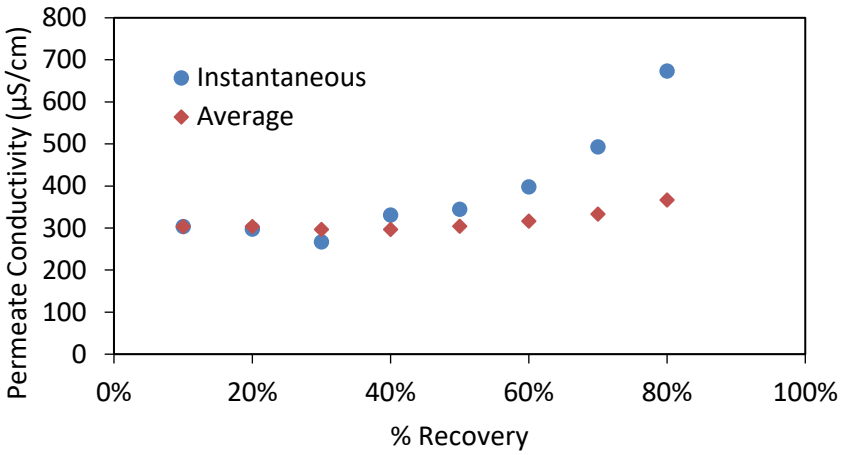

Figure 79. Instantaneous and average permeate conductivity as a function of the percent permeate recovery when processing the alternate Pit #3 wastewater; nanofiltration, 350 psig 1" displacement

Table 59

Average permeate concentration at 80% recovery of permeate in Case 2c

COD (mg/L)	545
Turbidity (NTU)	<<1
Conductivity (µS/cm)	367

The instantaneous and average feed concentrations for Case 2c have been plotted vs the percent permeate recovery – shown in *Figure 80*, *Figure 81*, and *Figure 82*. A similar scenario has occurred as with the initial studies for vibratory nanofiltration that accompanied Case 2b. The feed COD concentration dos not exponentially increase since COD is only moderately rejected. Feed turbidity and conductivity have a greater increase when compared to the COD concentration, and the respective increases behave exponentially.

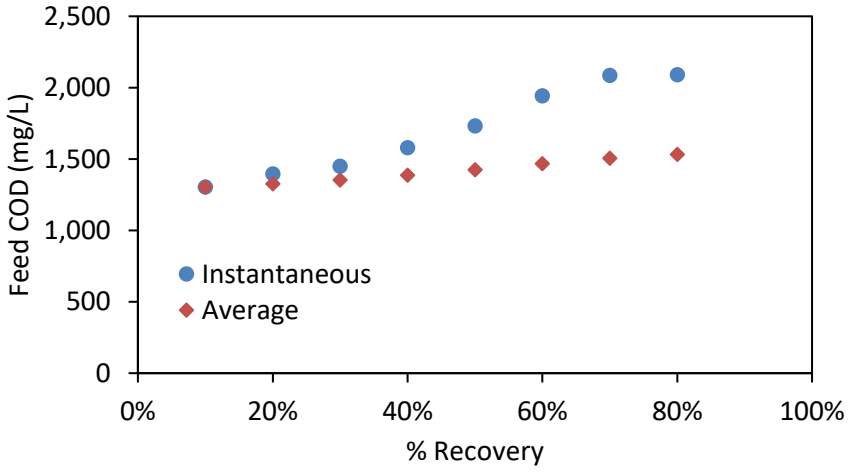

Figure 80. Instantaneous and average feed COD concentration as a function of the percent recovery; nanofiltration, 350 psig, 1" displacement, Pit #3 wastewater – Case 2c

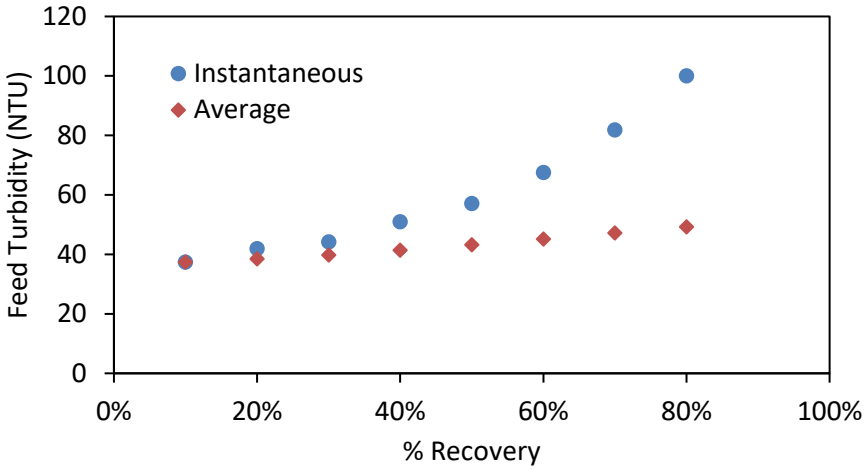

Figure 81. Instantaneous and average feed turbidity as a function of the percent recovery; nanofiltration, 350 psig, 1" displacement, Pit #3 wastewater – Case 2c

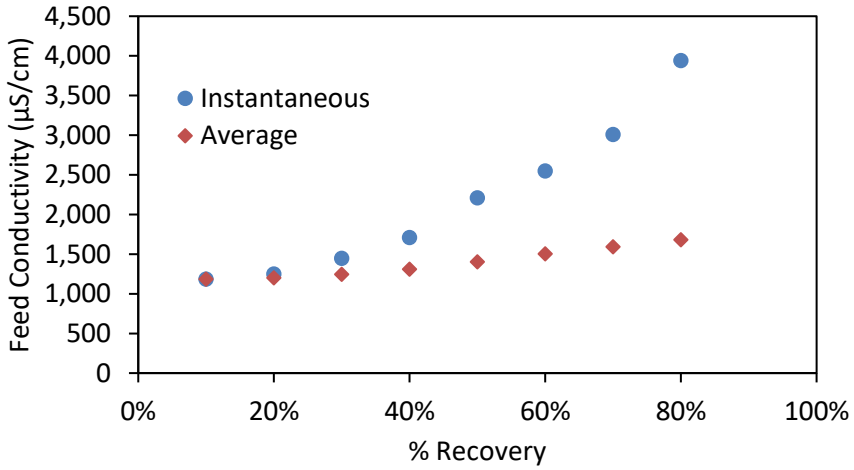

Figure 82. Instantaneous and average feed conductivity as a function of the percent recovery; nanofiltration, 350 psig, 1" displacement, Pit #3 wastewater – Case 2c

The mass flows in Case 2c and the electricity requirements for the pumps and the blowers for the wastewater pre-treatment are the same as those of Case 2b and can be seen in Table 51. The electricity required for the recovery system is increased, and a comparison between the electricity requirements for Case 2b and 2c can be seen in Table

60. This increase is caused by the need of a larger recovery system. The flux achieved in Case 2c is not high enough to provide enough permeate via a 1-module V-SEP system. There is a 32.4% increase in the amount of electricity required when processing the alternate Pit #3 wastewater sample.

Table 60

Comparison of the electricity required for a scaled-up system with the Case 2b and Case 2c Pit #3 wastewater samples

	Case 2b	Case 2c		Increase
Electricity (recovery)	6.66×10^5	8.82×10^5	MJ/yr	32.4%

The life cycle emissions associated with Case 2b can be seen in Table 61. Similar to Case 2b, air emissions are the majority of the total life cycle emissions at 98.0%. Of the air emissions, CO_2 emissions make up over 99%. There is no significant difference in the total life cycle emissions when comparing Case 2b and 2c. This is expected because the majority of life cycle emissions are generated from the disposal of nonhazardous wastewater; there is no change in the mass of nonhazardous wastewater that is disposed when considering with sample.

Table 61

Life cycle emissions associated with Case 2c recovery

	Freshwater	NHW	HW	Electricity	Total
Total Air Emissions (lb/yr)	6.30E+05	2.11E+07	9.24E+03	1.74E+06	**2.34E+07**
CO_2 (lb/yr)	6.25E+05	2.09E+07	9.18E+03	1.71E+06	**2.33E+07**
CO (lb/yr)	1.03E+02	1.73E+03	7.47E-01	1.20E+03	**3.03E+03**
CH_4 (lb/yr)	6.85E+02	1.85E+04	8.04E+00	8.61E+03	**2.78E+04**
NO_X (lb/yr)	0.00E+00	4.36E+04	0.00E+00	1.37E+03	**4.50E+04**
NMVOC (lb/yr)	2.14E+01	5.81E+02	2.53E-01	5.43E+02	**1.15E+03**
Particulate (lb/yr)	1.94E+03	5.74E+02	2.45E-01	4.53E+02	**2.96E+03**
SO_2 (lb/yr)	6.81E+02	2.10E+04	9.05E+00	1.50E+04	**3.67E+04**
Total Water Emissions (lb/yr)	1.38E+04	2.73E+05	2.26E+02	2.50E+05	**5.37E+05**
VOCs (lb/yr)	2.34E-03	6.75E-02	2.94E-05	7.62E-01	**8.31E-01**
Total Soil Emissions (lb/yr)	7.73E+00	2.31E+02	1.01E-01	1.09E+01	**2.50E+02**
Total Emissions (lb/yr)	**6.44E+05**	**2.13E+07**	**9.46E+03**	**1.99E+06**	**2.39E+07**
CED (MJ/yr)	2.45E+06	5.93E+07	2.54E+04	3.01E+07	**9.19E+07**

Since the mass flow rates are the same as Case 2b with the original sample, there is no additional reduction in mass as compared to Base Case 2 for Case 2c. The reduction in electricity required has changed, however. Table 62 shows the reduction in total electricity achieved in Case 2c as compared to Base Case 2. It can be seen that the total electricity required has been reduced by 18.1%. This reduction is the result of less electricity required for the blowers of the wastewater pre-treatment processes.

Table 62

Flow of total electricity associated with Case 2c as compared to Base Case 2

	Case 2c Recovery	**Flow Reduction**		**Reduction**
Total Electricity	$7.62x10^6$	$1.68x10^6$	MJ/yr	18.1%

Table 63 shows the comparison of the total life cycle emissions associated with Base Case 2 and Case 2c. As can be seen, the increased amount of electricity required – as compared to processing Case 2b – has a minimal effect on the total life cycle emissions reductions. CO_2 and total emissions reductions remain at nearly 28%. This further shows that the reduction in life cycle emissions that are possible is directly related to amount of nonhazardous wastewater disposal is avoided.

Table 63

Comparison of the total life cycle emissions of Base Case 2 and Case 2c

	Base Case 2	**Case 2c**	**Reduction**
Total Air Emissions (lb/yr)	3.24E+07	2.34E+07	**27.7%**
CO_2 (lb/yr)	3.22E+07	2.33E+07	**27.7%**
CO (lb/yr)	4.01E+03	3.03E+03	**24.5%**
CH_4 (lb/yr)	3.73E+04	2.78E+04	**25.4%**
NO_X (lb/yr)	6.28E+04	4.50E+04	**28.3%**
NMVOC (lb/yr)	1.50E+03	1.15E+03	**23.8%**
Particulate (lb/yr)	3.82E+03	2.96E+03	**22.3%**
SO_2 (lb/yr)	4.86E+04	3.67E+04	**24.5%**
Total Water Emissions (lb/yr)	7.05E+05	5.37E+05	**23.8%**
VOCs (lb/yr)	1.03E+00	8.31E-01	**19.0%**
Total Soil Emissions (lb/yr)	3.47E+02	2.50E+02	**28.0%**
Total Emissions (lb/yr)	**3.31E+07**	**2.39E+07**	**27.6%**
CED (MJ/yr)	1.23E+08	9.19E+07	**25.2%**

Table 64 provides the operating parameters of the scaled-up V-SEP membrane system that has been design for Case 2c. The design flux is calculated from the observed average flux of 82 GFD, shown in Figure 75. All other calculations have been carried out similarly to Equations 68 – 72. Case 2c requires a 2-module V-SEP system, but the membrane area per module is 1,000 ft^2. This causes an increase in capital cost, as well as additional operating costs related to membrane replacement and electricity. Membrane replacement per module is $53,500, with the total membrane replacement cost every 5 yrs is $107,000. This results in a yearly cost of $21,400 contributing to membrane replacement. The annual operating cost of the recovery system was calculated as in Equation 73. The annual operating cost of the V-SEP recovery system needed for Case 2c is $44,600. The capital cost of the equipment has been estimated at $600,000.

Table 64

Operating parameters for the V-SEP membrane system for Case 2c

Membrane Type	Nanofiltration (NF4)
Design Flux (GFD)	41
Pressure (psig)	350
Temperature (°C)	25
Feed Rate (GPD)	125,000
Recovery (%)	80%
Number of Modules	2
Membrane Area per Module (ft^2)	1,000
Cleaner Consumption (gal/yr)	73
Energy Consumption (MJ/yr)	881,600
Operating Cost ($/yr)	44,600
Capital Cost ($)	600,000

A summary of the operating costs and savings of Case 2c as compared to Base Case 2 can be seen in Table 65. An appreciable amount of annual savings in operating costs can be seen for Case 2c at 20.9%. The high amount of savings is the result of the considerable mass of nonhazardous wastewater disposal avoided. Thus, the increased electricity does not have a significant effect on the total operating cost savings. Calculations of operating costs of Base Case 2 are provided in the former section "Operating Cost of the Nestlé Process." Calculations for Case 2c recovery are determined using Case 2b mass flows of Table 51 and total electricity flow shown in Table 62 for Case 2c. The flows are multiplied by the respective unit costs (on a per lb or MJ basis) provided in Table 20.

Table 65

Summary of the operating costs of Case 2c as compared to those of Base Case 2

	Base Case 2 ($/yr)	**Case 2c ($/yr)**	**Savings ($/yr)**	**Savings (%)**
Freshwater	22,300	17,600	4,700	21.1
NHW Discharge	505,900	361,300	144,600	28.6
BOD Surcharge	22,400	22,400	0	0
TSS Surcharge	22,600	22,600	0	0
Well Pumps	32,500	25,600	6,900	21.2
Blowers	199,900	142,800	57,100	28.6
Recovery System	N/A	44,600	-44,600	-
Total	805,600	636,900	168,700	20.9

An economic analysis of Case 2c was conducted based on operating cost savings and the capital cost of the recovery equipment. Table 66 shows the economic metrics evaluated for the V-SEP water recovery system for Case 2c. Most notably as compared

to processing the original sample, the capital cost is doubled since a 2-module V-SEP system is required. This has an adverse effect on the economic metrics of the recovery system; however, the metrics remain reasonable. The NPV after 10 years is positive, indicating the recovery process is feasible. The payback time of 7.4 years is reasonable, especially when compared to the 25.4 yr payback time found for Case 2a.

Table 66

Economic metrics for the water recovery system in Case 2c

Capital Cost ($)	600,000
Savings ($/yr)	168,700
IRR (%)	22.3
ROI (%)	24.9
Payback time after tax (yr)	7.4
10-yr NPV ($)	168,200

Case 2d – Vibratory Nanofiltration, Average Flux

For a more accurate scenario of the wastewater that may be processed for recovery on a given day at the Nestlé Freehold plant, an average of the observed fluxes achieved for Case 2b and 2c has been found. With this data, a scaled-up V-SEP system was designed that would represent the recovery of an average Pit #3 wastewater that is produced at the plant. Thus, the observed average flux used for this design is 108 GFD. The feed conditions and the permeate concentrations at 80% recovery have been estimated based on the results of Cases 2b and 2c, shown in Table 67. Note: these are not actual results, just estimations from previous data. It can be seen in Table 67 that the permeate concentrations at 80% permeate recovery are within the specifications for use in

the cooling tower. The mass flows associated with this process are the same as those shown in Table 51; the electricity requirement of the recovery equipment is shown in Table 68, as compared to the electricity requirements of the systems designed for Cases 2b and 2c. It can be seen that the electricity requirement needed for the averaged system is the same as that needed for the original Pit #3 wastewater sample (Case 2b). Thus, the life cycle emissions of this system will be identical to those presented for the original sample in Table 52. Similarly, the flow and life cycle emissions reductions compared to Base Case 2 will be the same as those shown in Table 53 and Table 54.

Table 67

Feed conditions and permeate concentrations of Cases 2b, 2c, and 2d, where Case 2d shows the projected conditions based on the average of Cases 2b and 2c

	Case 2b		Case 2c		Case 2d	
	Feed	Permeate*	Feed	Permeate*	Feed	Permeate*
COD (mg/L)	1,020	490	1,260	545	1,140	524
Turbidity (NTU)	13	<<1	30	<<1	22	<<1
Conductivity (µS/cm)	600	100	1,280	367	940	241

* Permeate concentrations at 80% permeate recovery

Table 68

Comparison of the electricity required by the recovery system when comparing Cases 2b, 2c, and 2d

	Case 2b	Case 2c	Case 2d	
Electricity (recovery)	6.66×10^5	8.82×10^5	6.66×10^5	MJ/yr

While the life cycle emissions and the reductions in mass and energy flows are the same for Case 2d as they are for Case 2b, the operating parameters of the scaled-up V-

SEP system differ. Since the observed average flux has decreased, the V-SEP system requires more membrane area to remain a 1-module V-SEP system. Thus, the membrane area in the 1-module system is increased to 1,400 ft^2. All other calculations have been carried out similarly to Equations 68 – 72, with changes to specified constants. As a result, the annual operating cost of the system is increased to account for the increase in price of membrane replacement. The membrane replacement cost increases to $75,000; resulting in an annual cost of $15,000 for membrane replacement. This is an increase of $2,150 per year when compared to Case 2b. Table 69 shows the full operating parameters of the V-SEP system designed for Case 2d. The design flux has been calculated from the flux value of 108 GFD. As in Case 2b, the capital cost of the water recovery system has been estimated at $300,000.

Table 69

Operating parameters for the V-SEP membrane system for Case 2d

Membrane Type	Nanofiltration (NF4)
Design Flux (GFD)	54
Pressure (psig)	350
Temperature (°C)	25
Feed Rate (GPD)	125,000
Recovery (%)	80%
Number of Modules	1
Membrane Area per Module (ft^2)	1,400
Cleaner Consumption (gal/yr)	37
Energy Consumption (MJ/yr)	666,100
Operating Cost ($/yr)	32,200
Capital Cost ($)	300,000

A summary of the operating costs and savings of Case 2d as compared to Base Case 2 can be seen in Table 70. The savings shown are similar to those of Case 2b. There is a small increase in the operating costs of the recovery system; this is the result of the additional membrane area required for the system. Similar to all scenarios of Case 2, the greatest cost savings are found from the reductions of nonhazardous wastewater disposal and electricity required by the aeration lagoon blowers. Calculations of operating costs of Base Case 2 are provided in the former section "Operating Cost of the Nestlé Process." Calculations for Case 2d recovery are determined using Case 2b mass and energy flows shown in Table 51, and multiplying them by the unit cost values for each flow (on a per lb or MJ basis), as shown in Table 20.

Table 70

Summary of the operating costs of Case 2d as compared to Base Case 2

	Base Case 2 ($/yr)	**Case 2d ($/yr)**	**Savings ($/yr)**	**Savings (%)**
Freshwater	22,300	17,600	4,700	21.1
NHW Discharge	505,900	361,300	144,600	28.6
BOD Surcharge	22,400	22,400	0	0
TSS Surcharge	22,600	22,600	0	0
Well Pumps	32,500	25,600	6,900	21.2
Blowers	199,900	142,800	57,100	28.6
Recovery System	N/A	32,200	-32,200	-
Total	805,600	624,500	181,100	22.5

An economic assessment was conducted to evaluate Case 2d based on operating cost savings and capital cost of the recovery equipment. Table 71 shows the economic metrics evaluated from the water recovery system in this case. As can be seen, similar

metrics as Case 2b are obtained, shown in Table 57. The payback time shows a marginal increase while the NPV after 10 years shows a small decrease. The economic metrics of Case 2d are similar to Case 2b because the capital cost of the equipment is the same. When considering Case 2c, the annual savings are only 7% lower than Case 2d, but the capital cost is double. This resulted in a payback time for Case 2c that is nearly three times greater than Case 2d. Thus, it can be determined that the economic metrics are significantly affected by the capital cost of the equipment.

Table 71

Economic metrics for the water recovery system in Case 2d

Capital Cost ($)	300,000
Savings ($/yr)	181,100
IRR (%)	53.6
ROI (%)	51.0
Payback time after tax (yr)	2.7
10-yr NPV ($)	485,300

In the event that the proposed V-SEP system for water recovery requires additional costs for installation to meet plant requirements, an economic assessment for Case 2d with twice the capital cost has been conducted. This will account for any potential expenses associated with the equipment. Table 72 shows the updated economic metrics associated with doubling the capital cost of the recovery equipment in Case 2d. It can be seen that the economic metrics are affected adversely; however, they are still within reason. The NPV after 10 years is approximately 45% of the value when the original capital cost is used (Table 71). Likewise, the ROI and IRR are also reduced to

nearly half of the original values, while the payback time is increased by a factor of 2.4. These values are still potentially feasible and represent a scenario in which installation costs are equal to the capital cost of the equipment. Further discussion with the staff at the Nestlé Freehold plant would be required to fully realize the feasibility of this project.

Table 72

Economic metrics for the water recovery system in Case 2d, with twice the capital cost

Capital Cost ($)	600,000
Savings ($/yr)	181,100
IRR (%)	24.5
ROI (%)	26.6
Payback time after tax (yr)	6.6
10-yr NPV ($)	219,700

Case 2 Comparison

A comparison based on the environmental and economic assessments of all Case 2 scenarios has been conducted. Figure 83 shows the comparison of the total emissions of each Case 2 scenario as compared to Base Case 2. As can be seen, the total life cycle emissions of each recovery case are similar to each other and show a similar reduction as compared to Base Case 2. This result was expected since each recovery case showed that the major reduction of life cycle emissions was through avoiding nonhazardous wastewater disposal. Each case recovers the same amount of water (100,000 gal/yr) and reduces the same amount of nonhazardous wastewater disposal (304 MMlb/yr). Therefore, the life cycle emissions associated with those flows are the same for each case. The difference among the recovery cases is a result of the varying amounts of electricity

required to operate the recovery equipment. Each case presents approximately a 27 – 28% reduction in total life cycle emissions over Base Case 2. Thus, it can be concluded that each Case 2 recovery scenario provides the same environmental impact reduction.

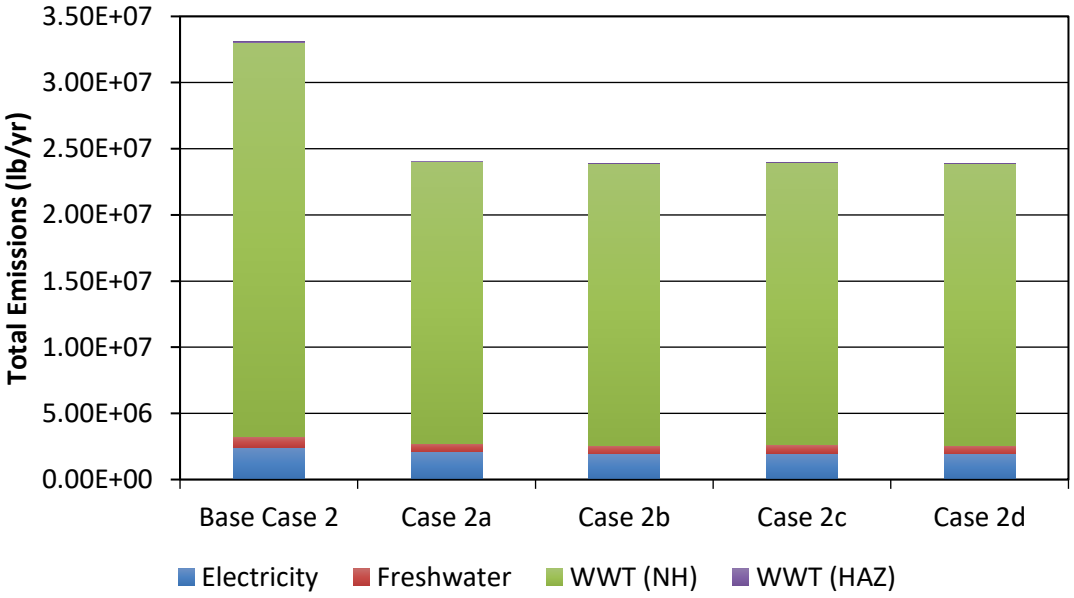

Figure 83. Comparison of the total life cycle emissions of each Case 2 scenario

A comparison of the economic assessments of each Case 2 recovery scenario has also been conducted to determine which is the most economically viable. Figure 84 shows the annual operating costs and savings of each proposed recovery system for the Case 2 scenarios, as well as the annual operating costs of Base Case 2. Each Case 2 recovery scenario presents savings as compared to Base Case 2. It can be seen that Case 2b and 2d present the best savings among the Case 2 recovery scenarios. They are nearly identical in terms of savings; however, the operating costs are slightly higher for Case 2d to account for the increase in membrane replacement costs. This is caused by the minor

increase in membrane area required in Case 2d (1,400 ft^2) as compared to Case 2b (1,200 ft^2).

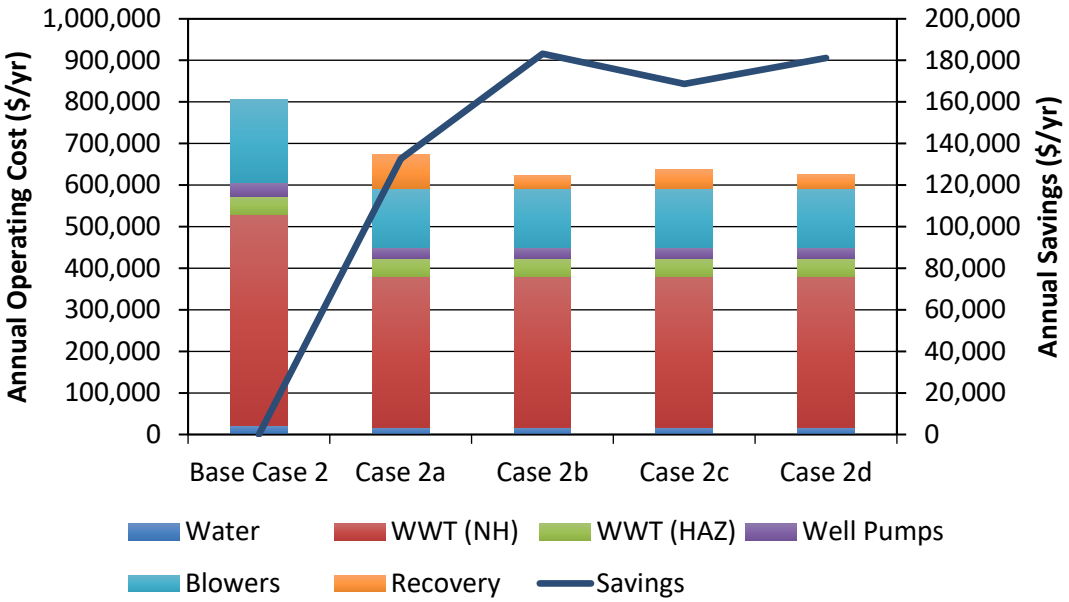

Figure 84. Comparison of the annual operating costs of Base Case 2 and the Case 2 recovery scenarios, as well as the annual savings presented from each Case 2 recovery scenario

In addition to annual operating costs and savings, the Case 2 recovery scenarios were evaluated based on the capital cost and economic metrics they present. A comparison of the payback time and return on investment (ROI) of each Case 2 recovery scenario are shown in Figure 85. It can be seen that the payback time for Case 2b and 2d are the most feasible, with Case 2c being reasonable. The payback time required for Case 2a is well out of feasibility. The case is similar for the ROI of each Case 2 recovery scenario. Case 2b and Case 2d are both feasible, while Case 2c may be acceptable. The ROI for Case 2a is too low to be a practical proposal. Again, the economic metrics of

each recovery case hinge significantly on the capital cost of the system. For instance, the capital cost in Case 2a is three times that of Case 2b and 2d to add two V-SEP modules. Thus, if a larger system is required as in Case 2a, the capital cost will rise and have a significant impact on metrics such as the payback time and ROI.

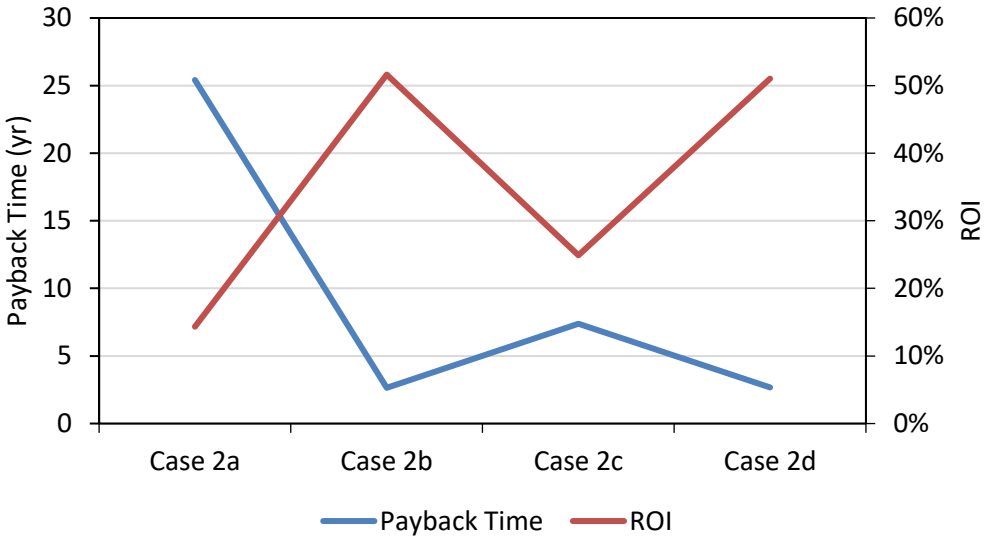

Figure 85. Comparison of the payback time and ROI of each Case 2 recovery scenario

Table 73 shows a summary of the environmental and economic comparison of the Case 2 recovery scenarios. From Table 73, the significant effect of the capital cost of the recovery equipment on the payback time and ROI can be observed. The increased capital cost for Case 2a results in a very high payback time and low ROI. The total emissions reductions are nearly the same for all Case 2 recovery scenarios. To further improve the reduction in total life cycle emissions, further assessment of additional water recovery would be required.

Table 73

Summary of the comparison of the Case 2 recovery scenarios

	Total Emissions Reduction (%)	Annual Savings ($/yr)	Annual Savings (% reduction)	Capital Cost ($)	Payback Time (yr)	ROI (%)
Case 2a	27.2	132,700	16.5	900,000	25.4	14.3
Case 2b	27.8	183,200	22.7	300,000	2.6	51.6
Case 2c	27.6	168,700	20.9	600,000	7.4	24.9
Case 2d	27.8	181,100	22.5	300,000	2.7	51.0

It can be concluded that vibratory nanofiltration of the Pit #3 wastewater provides a feasible recovery system in terms of environmental and economic analyses. Vibratory reverse osmosis (Case 2a) is not economically feasible as the payback time is too high. Cases 2b, 2c, and 2d are the same vibratory nanofiltration recovery scenario with varying concentrations of contaminants in the wastewater. Case 2b presents a low concentration of contaminants while Case 2c presents higher concentrations. Case 2d presents the most accurate scenario for water recovery in the Nestlé process, since an average flux was determined based on the results of Cases 2b and 2c. Thus, Case 2d has been determined the as the most accurate and best option of the Case 2 recovery scenarios.

References

[1] Food and Agriculture Organization of the United Nations, "The State of the World's Land and Water Resources for Food and Agriculture," Earthscan, Abington, 2011.

[2] Food and Agriculture Organization of the United Nations, "AQUASTAT Database," 2016. [Online]. Available: http://www.fao.org/nr/water/aquastat/data/query/results.html?regionQuery=true&yearGrouping=SURVEY&showCodes=false&yearRange.fromYear=1958&yearRange.toYear=2017&varGrpIds=4250%2C4251%2C4252%2C4253%2C4257&cntIds=&regIds=9805%2C9806%2C9807%2C9808%2C9809&edit. [Accessed 29 November 2016].

[3] W. Lee and M. R. Okos, "Sustainable food processing systems - Path to zero liquid discharge: reduction of water, waste and energy," *Procedia Food Science,* vol. 1, pp. 1768-1777, 2011.

[4] H. K. Jeswani, R. Burkinshaw and A. Azapagic, "Environmental sustainability issues in the food-energy-water nexus: Breakfast cereals and snacks," *Sustainable Production and Consumption,* vol. 2, pp. 17-28, 2015.

[5] S. Casani, M. Rouhany and S. Knochel, "A discussion paper on challenges and limitations to water reuse and hygiene in the food industry," *Water Research,* vol. 39, pp. 1134-1146, 2005.

[6] A. Cassano, N. K. Rastogi and A. Basile, "Membrane technologies for water treatment and reuse in the food and beverage industries," in *Advances in Membrane Technologies for Water Treatment*, Cambridge, Woodhead Publishing, 2015, pp. 551-580.

[7] J. Klemes, R. Smith and K. J. K, Handbook of Water and Energy Management in Food Processing, Burlington: Elsevier Science, 2008.

[8] A. Sefghi, "How Much Water is Needed to Produce Food and How Much Do We Waste?," *The Guardian,* p. A10, 10 January 2013.

[9] Institute of Mechanical Engineers, "Global Food : Waste not, Want not," Westminster, 2013.

[10] A. Y. Hoekstra, A. K. Chapagain, M. M. Aldaya and M. M. Mekonnen, "The Water Footprint Assessment Manual," Earthscan, London, 2011.

[11] M. M. Mekonnen and A. Y. Hoekstra, "The green, blue and grey water footprint of crops and deriveed crop products," *Hydrology and Earth Sciences,* vol. 15, no. 5, pp. 1577-1600, 2011.

[12] USGS, "Evapotranspiration - The Water Cycle," 2016. [Online]. Available: https://water.usgs.gov/edu/watercycleevapotranspiration.html. [Accessed 16 February 2017].

[13] R. G. Allen, L. S. Pererira, D. Raes and M. Smith, "Crop Evapotranspiration - Guidelines for computing crop water requirements," Food and Agriculture Organization of the United Nations, 1998.

[14] J. Doorenbos and A. Kassam, "Yield response to water," Food and Agriculture Organization of the United Nations, 1979.

[15] SABMiller, WWF, "Water Footprinting: Identifying & Addressing Water Risks in the Value Chain," 2009.

[16] T. Nurin, "It's Final: AB InBev Closes On Deal To Buy SABMiller," 10 October 2016. [Online]. Available: https://www.forbes.com/sites/taranurin/2016/10/10/its-final-ab-inbev-closes-on-deal-to-buy-sabmiller/#6d96ac16432c. [Accessed 15 March 2017].

[17] A. E. Ercin, M. M. Aldaya and A. Y. Hoekstra, "Corporate Water Foorprint Accounting and Impact Assessment: The Case of the Water Footprint of a Sugar-Containing Carbonated Beverage," *Water Resources Management,* vol. 25, no. 2, pp. 721-741, 2011.

[18] United Nations World Water Assessment Programme, "Water for a Sustainable World," UNESCO, Paris, 2015.

[19] UNICEF, World Health Organization, "Progress on Sanitation and Drinking Water - 2015 update and MDG assessment," 2015.

[20] NJ Department of Environmental Protection, "Water Conservation," 19 January 2017. [Online]. Available: http://www.nj.gov/dep/watersupply/conserve.htm. [Accessed 9 May 2017].

[21] United States Geological Survey, "Water Use in New Jersey," 7 April 2016. [Online]. Available: https://nj.usgs.gov/infodata/wateruse.html. [Accessed 9 May 2017].

[22] A. K. Chapagain and A. Y. Hoekstra, "The water footprint of coffee and tea consumption in the Netherlands," *Ecological Economics*, vol. 64, no. 1, pp. 109-118, 2007.

[23] A. Farah, "Coffee Constituents," in *Coffee Emerging Health Effects and Disease Prevention*, Ames, Wiley-Blackwell, 2012, pp. 21-58.

[24] A. Hicks, "Post-harvest Processing and Quality Assurance for Specialty/Oganic Coffee Products," in *The first Asian regional round-table on sustainable, organic, and specialty coffee production, processing and marketing*, Chiang Mai, 2001.

[25] United States Department of Agriculture, "Foreign Agricultural Service - Global Agricultural Trade System Online," 2017. [Online]. Available: https://apps.fas.usda.gov/gats/default.aspx. [Accessed 11 May 2017].

[26] A. K. Chapagain and A. Y. Hoekstra, "The Water Needed to have the Dutch Drink Coffee," UNESCO-IHE, Delft, 2003.

[27] R. J. Clarke and R. Macrae, Coffee Vol. 2, London: Elsevier Applied Sciences, 1987.

[28] S. I. Mussatto, E. M. S. Machado, S. Martins and J. Teixeira, "Production, Composition, and Application of Coffee and Its Industrial Residues," *Food and Bioprocess Technology*, vol. 4, pp. 661-672, 2011.

[29] J. G. Brennan and A. S. Grandison, Food Processing Handbook, Weinheim: Wiley-VCH, 2011.

[30] M. Huang and M. Zhang, "Tea and coffee powders," in *Handbook of Food Powders - Processes and Properties*, Cambridge, Woodhead Publishing, 2013, pp. 513-531.

[31] S. Humbert, Y. Loerincik, V. Rossi, M. Margni and O. Jolliet, "Life cycle assessment of spray dried soluble cofee and comparison with alternatives (drip filter and capsule espresso)," *Journal of Cleaner Production*, vol. 17, no. 15, pp. 1351-1358, 2009.

[32] B. Pepe, Freehold: A Hometown History, Arcadia Publishing, 2003.

[33] Ocean County Utilities Authority, *Rate History 2009-2018*, 2018.

[34] United States Environmental Protection Agency, "2012 Guidelines for Water Reuse," 2012.

[35] Water Environment Federation, Design of Municipal Wastewater Treatment Plants, Fifth Edition, New York: McGraw-Hill Education, 2010.

[36] K. B. Manoj and H. G. Shwetha, "Performance Evaluation of Coffee Process Wastewater Treatment Plant and Treatability Studies of Coffee Process Wastewater," in *First International Conference on Recent Advances in Science and Engineering*, Bangalore, 2014.

[37] R. Devi, V. Singh and A. Kumar, "COD and BOD reduction from coffee processing wastewater using avacado peel carbon," *Bioresources Technology,* vol. 99, no. 6, pp. 1853-1860, 2008.

[38] A. Cardenas, U. Morales, L. Salgado and T. Zayas, "Electrochemical oxidation of wastewaters from the instant coffee industry using a dimensionally stable RuIrCoOx anode," *ECS Transactions,* vol. 20, no. 1, pp. 291-299, 2009.

[39] C. J. Geankoplis, Transport Processes and Separation Process Principles (Includes Unit Operations), Upper Saddle River: Prentice Hall, 2003.

[40] S. Venikatesan, "Adsorption," in *Separation and Purification Technologies in Biorefineries*, Chichester, Wiley, 2013, pp. 103-148.

[41] S. Rattan, A. K. Parande, V. D. Nagaraju and G. K. Ghiwari, "A comprehensive review on utilization of wastewater from coffee processing," *Environmental Science and Pollution Research International,* vol. 22, no. 9, pp. 6461-6472, 2015.

[42] M. Tokumora, T. Znad and Y. Kawase, "Decolorization of dark brown colored coffee effluent by solar photo-Fenton reaction: Effect of solar dose on decolorization techniques," *Water Research,* vol. 42, no. 18, pp. 4665-4673, 2008.

[43] K. P. Singh, D. Mohan, S. Sinha, T. G. S and D. Gosh, "Color Removal from Wastewater Using Low-Cost Activated Carbon Derived from Agricultural Waste Material," *Industrial Engineering and Chemistry Research,* vol. 42, no. 9, pp. 1965-1976, 2003.

[44] S. R. Syeda, S. A. Ferdousi and K. M. T. Ahmmed, "De-colorization of textile wastewater by adsorption in a fluidized bed of locally availableactivated carbon," *Journal of Environmental Science and Health Part A,* vol. 47, no. 2, pp. 210-220, 2012.

[45] H. Patel and R. T. Vashi, Characterization and Treatment of Textile Wastewater, Waltham: Elsevier, 2015.

[46] A. Karu and U. Gupta, "A review on applications of nanoparticles for the preconcentration of environmental pollutants," *Journal of Materials Chemistry*, vol. 19, no. 44, pp. 8278--8289, 2009.

[47] N. N. Nassar, L. A. Arar, N. N. Marei, M. M. Abu Ghanim, M. S. Dwekat and S. H. Sawalha, "Treatment of olive mill based wastewater by means of magnetic nanoparticle: Decolourization, dephenolization and COD removal," *Environmental Nanotechnology, Monitoring & Management,* Vols. 1-2, pp. 14-23, 2014.

[48] N. N. Nassar and R. Anna, "Rapid Adsorption of Methylene Blue from Aqueous Solutions by Geothite Nanoadsorbents," *Environmental Engineering Science,* vol. 29, no. 8, pp. 790-797, 2012.

[49] N. N. Nassar, N. N. Marei, G. Vitale and L. A. Arar, "Adsorptive removal of dyes from synthetic and real textile wastewater using magnetic iron oxide nanoparticle: Thermodynamic and mechanistic insights," *The Canadian Journal of Chemical Engineering,* vol. 93, no. 11, pp. 1965-1974, 2015.

[50] M. R. Collins, M. P. Youngstrom and M. V. Broder, "Slow Sand and Diatomaceous Earth Filtration," in *Water Treatment Plant Design*, New York City, McGraw-Hill, 2012, pp. 10.1-10.47.

[51] United States Environmental Protection Agency, "Slow Sand Filtration," 2011. [Online]. Available: https://iaspub.epa.gov/tdb/pages/treatment/treatmentOverview.do?treatmentProcessId=-1306063973. [Accessed 2 April 2018].

[52] L. Huisman and W. Wood, "Slow Sand Filtration," World Health Organization, Geneva, 1974.

[53] V. K. Bosak, A. C. VanderZaag, A. Crolla, C. Kinsley, D. Chabot, M. S. S and R. J. Gordon, "Treatment of potato farm wastewater with sand filtration," *Environmental Technology,* vol. 37, no. 13, pp. 1597-1604, 2016.

[54] Y. W. Kang, K. M. Mancl and O. H. Tuovinen, "Treatment of turkey processing wastewater with slow sand filtration," *Bioresource Technology,* vol. 98, no. 7, pp. 1460-1466, 2007.

[55] M. Vanotti, J. Rice, A. Ellison, P. Hunt, F. Humenik and C. Barid, "Solid-Liquid Separation of Swine Manure with Polymer Treatment and Sand Filtration," *Transactions of the ASAE,* vol. 48, no. 4, pp. 1-8, 2005.

[56] I. Sabbah, T. Marsook and S. Basheer, "The effect of pretreatment on anaerobic activity of olive oil mill wastewater," *Process Biochemistry,* vol. 23, no. 12, pp. 1947-1951, 2004.

[57] G. Guven, A. Perendeci and A. Tanyolc, "Electrochemical treatment of simulated beet sugar factory wastewater," *Chemical Engineering Journal,* vol. 151, no. 1-3, pp. 149-159, 2009.

[58] M. Gotsi, N. Kalogerakis, E. Psillakis, P. Samaras and D. Mantazavinos, "Electrochemical oxidation of olive oil mill wastewater," *Water Research,* vol. 39, no. 17, pp. 4177-4187, 2005.

[59] C. Gottschalk, J. A. Libra and A. Saupe, Ozonation of Water and Waste Water: A Practical Guide to Understanding Ozone and Its Applications, Weinheim: Wiley-VCH, 2010.

[60] S. Sharma and R. Sanghi, Wastewater Reuse and Management, New York: Springer, 2013.

[61] P. Canizares, J. Lobato, R. Paz, M. A. Rodrigo and Saez, "Advanced oxidation processes for the treatment of olive-oil mills wastewater," *Chemosphere,* vol. 67, no. 4, pp. 832-838, 2007.

[62] C. Tsioptsias, D. C. Banti and P. Samaras, "Experimental study of degradation of molasses wastewater by biological treatment combined with ozonation," *Journal of Chemical Technology and Biotechnology,* vol. 91, no. 4, pp. 857--864, 2015.

[63] M. Latif, M. A. Qazi, H. Khan, N. Ahmad, N. I. Khan and K. Mahmood, "Physiochemical treatment of textile industry effluents," *Journal of the Chemical Society of Pakistan,* vol. 37, no. 5, pp. 1033-1039, 2015.

[64] D. Yang and J. Yuan, "COD and Color Removal from Real Dyeing Wastewater by Ozonation," *Water Environment Research,* vol. 88, pp. 403-407, 2016.

[65] F. Lipnizki, "Cross-Flow Membrane Applications in the Food Industry," in *Membrane Technology: Membranes for Food Applications*, Weinheim, Wiley-VCH Verlag GmbH & Co, 2010, pp. 1-24.

[66] L. N. Gerschenson, Q. Den and A. Cassano, "Conventional Macroscopic Pretreatment," in *Food Waste Recovery - Processing Technologies and Industrial Techniques,* United Kingdom, Academic Press, 2015, pp. 85-103.

[67] K. Dewettick and T. Trung Le, "Membrane Separations in Food Processing," in *Alternatives to Conventional Food Processing*, Cambridge, The Royal Society of Chemistry, 2011, pp. 184-253.

[68] Suez Water Technologies and Solutions, "Document Library - Filtration and Separation Spectrum," 2017. [Online]. Available: https://www.suezwatertechnologies.com/kcpguest/document-library.do. [Accessed April 2018].

[69] C. Muro, F. Reiera and M. del Carmen Diaz, "Membrane Separation Process in Wastewater Treatment of Food Industry," in *Food Industrial Practices - Methods and Equipment*, Online, InTech, 2012, pp. 253-280.

[70] H. K. Shon, S. Phuntsho, D. S. Chaudhary, S. Vigneswaran and J. Cho, "Nanofiltration for water and wastewater treatment - a mini review," *Drinnking Water Engineering and Science*, vol. 6, pp. 253-280, 2013.

[71] A. B. de Haan and H. Bosch, Industrial Separation Processes - Fundamentals, Berlin: Walter de Gruyter GmbH, 2013.

[72] P. A. Marcelo and S. S. H. Rizvi, "Applications of Membrane Technology in the Dairy Industry," in *Handbook of Membrane Separation: Chemical, Pharmaceutical, Food, and Biotechnical Applications*, Boca Raton, CRC Press, 2009, pp. 505 - 537.

[73] A. Chollangi and M. M. Hossain, "Separation of proteins and lactose from dairy wastewater," *Chemical Engineering and Processing: Process Intensification*, vol. 46, no. 5, pp. 398-404, 2007.

[74] A. W. Mohammad, Y. H. Teow, W. L. Ang, Y. T. Chung, D. L. Oatley-Radcliffe and N. Hilal, "Nanofiltration membranes review: Recent advances and future prospects," *Desalination*, vol. 356, pp. 226-254, 2015.

[75] L. F. Sotoft, K. V. Christensen, R. Andresen and B. Norddahl, "Full scale plant with membrane based concentration of blackcurrant juice on the basis of laboratory and pilot scale tests," *Chemical Engineering and Processing: Process Intensification*, vol. 54, pp. 12-21, 2012.

[76] M. S. Noghabi, S. M. A. Razavi, S. M. Mousavi, M. Elahi and R. Niazmand, "Effect of operating parameters on performance of nanofiltration of sugar beet press water," *Procedia Food Science*, vol. 1, pp. 160-164, 2011.

[77] I. G. Wenten and Khoiruddin, "Reverse osmosis applications: Prospsect and challenges," *Desalination*, vol. 391, pp. 112-125, 2016.

[78] M. Vourch, B. Balannec, B. Chaufer and G. Dorange, "Treatment of dairy wastewater by reverse osmosis for water reuse," *Desalination,* vol. 219, no. 1-3, pp. 190-202, 2008.

[79] T. Coskun, E. Debik and N. M. Demir, "Treatment of olive mill wastewaters by nanofiltration and reverse osmosis membranes," *Desalination,* vol. 259, no. 1-3, pp. 65-70, 2010.

[80] L. Ianniciello, M. Dubourg, A. Leblanc and F. G. Viladomat, "evapeos (R): The Green Future of Instant Coffee," ederna, Toulouse, France, 2014.

[81] S. M. K. Sadr and D. P. Saroj, "Membrane technologies for municipal wastewater treatment," in *Advances in Membrane Technologies for Water Treatment*, Cambridge, Woodhead Publishing, 2015, pp. 443-463.

[82] T. Sparks and G. Chase, Filters and filtration handbook, Oxford: Butterworth-Heinemann, 2016.

[83] New Logic Research, Inc., "VSEP Technology," 2016. [Online]. Available: http://www.vsep.com/technology/index.html. [Accessed 24 January 2017].

[84] O. A. Akoum, M. Y. Jaffrin, L. Ding, P. Paullier and C. Vanhoutte, "An hydrodynamic investigation of microfiltration and ultrafiltration in a vibrating membrane module," *Journal of Membrane Science,* vol. 197, no. 1-2, pp. 37-52, 2002.

[85] S. Rosenblat, "Flow between torsionally oscillating disks," *Journal of Fluid Mechanics,* vol. 8, no. 3, pp. 388-399, 1960.

[86] M. Frappart, M. Y. Jaffrin, L. H. Ding and V. Espina, "Effect of vibration frequency and membrane shear rate on nanofiltration of diluted milk, using a vibratory dynamic filtration system," *Separation and Purification Technology,* vol. 62, no. 1, pp. 212-221, 2008.

[87] O. Akoum, M. Y. Jaffrin and L.-H. Ding, "Concentration of total milk proteins bt high shear ultrafiltration in a vibrating membrane module," *Journal of Membrane Science,* vol. 247, no. 1-2, pp. 211-220, 2005.

[88] New Logic Research, Inc., "Application Note: Membrane Filtration of Fermentation Tank Bottoms," 2017. [Online]. Available: http://www.vsep.com/pdf/Beer-Bottoms-Membrane-Filtration-Case-Study.pdf. [Accessed 24 January 2017].

[89] New Logic Research, Inc., "Bottling plant goes ZLD," 6 February 2017. [Online]. Available: http://www.vsep.com/company/articles/34.html. [Accessed 27 September 2017].

[90] S. Kertesz, Z. Laszlo, E. Forgacs, G. Szabo and C. Hodur, "Dairy wastewater purification by vibratory shear enhanced processing," *Desalination and Water Treatment*, vol. 35, no. 1-3, pp. 195-2011, 2011.

[91] J. Luo, W. Cao, L. Ding, Z. Zhu, Y. Wan and M. Y. Jaffrin, "Treatment of dairy effluent by shear-enhanced membrane filtration: The role of foulants," *Separation and Purification Technology*, vol. 96, pp. 194-203, 2012.

[92] W. Shi and M. M. Benjamin, "Effect of shear rate on fouling in a Vibratory Shear Enhanced Processing (VSEP) RO system," *Journal of Membrane Science*, vol. 366, no. 1-2, pp. 148-157, 2011.

[93] J. A. Dudhbhate and B. S. Zarapkar, "A.T.E.'s solution for waste water management: VSEP, a membrane based system for textile effluent treatment," *Colourage*, vol. 566, pp. 37-39, 2009.

[94] C. S. Slater, M. J. Savelski, P. Kostetskyy and M. Johnson, "Shear-enhanced microfiltration of microalgae in a vibratin membrane module," *Clean Technologies and Environmental Policy*, vol. 17, no. 7, pp. 1743-1755, 2015.

[95] B. S. Shete and N. P. Shinkar, "Dairy Industry Wastewater Sources, Characteristics & its Effects on Environment," *International Journal of Current Engineering and Technology*, vol. 3, no. 5, pp. 1611-1615, 2013.

[96] Food and Agriculture Organization of the United Nations, "The Water-Food-Energy Nexus: A new approach in support of food security and sustainable agriculture," FAO, Rome, 2014.

[97] Energy Information Administration, "First Use of Energy for All Purposes (Fuel and Nonfuel)," 1 March 2010. [Online]. Available: https://www.eia.gov/consumption/manufacturing/data/2010/pdf/Table1_1.pdf. [Accessed 11 May 2017].

[98] S. Toepfl, A. Mathys, V. Heinz and D. Knorr, "Review: Potential of High Hydrostatic Pressure and Pulsed Electric Fields for Energy Efficient and Environmentally Friendly Food Processing," *Food Reviews International*, vol. 22, pp. 405-423, 2006.

[99] B. M. Pastore, "Sustainable P2 Design for Batch-Based Specialty Chemical Manufacture," Rowan University, Glassboro, 2016.

[100] United States Environmental Protection Agency, "Federal Water Pollution Control Act," 2002.

[101] C. Jimenez-Gonzalez and D. J. Constable, Green Chemistry and Engineering: A Practical Design Approach, Hoboken: John Wiley & Sons, Inc, 2011.

[102] M. Goedkoop, M. Oleo, J. Leijting, T. Ponsioen and E. Meijer, "Introduction to LCA with SimaPro," Pre, 2016.

[103] European Life Cycle Database, "Process Data set: Drinking water, water purification treatment; prodction mix, at plant, from groundwater," 2005. [Online]. Available: http://eplca.jrc.ec.europa.eu/ELCD3/datasetdetail/process.xhtml?uuid=db009013-338f-11dd-bd11-0800200c9a66&version=03.00.000. [Accessed February 2017].

[104] European Life Cycle Database, "Process Data set: Waste water treatment; domestic waste water," 2003. [Online]. Available: : http://eplca.jrc.ec.europa.eu/ELCD3/datasetdetail/process.xhtml?uuid=19728650-4cf4-11dd-ae16-0800200c9a66&version=03.00.000. [Accessed February 2017].

[105] European Life Cycle Database, "Process Data set: Waste water treatment; industrial wastewater, organic contaminated," 2003. [Online]. Available: http://eplca.jrc.ec.europa.eu/ELCD3/resource/processes/db009020-338f-11dd-bd11-0800200c9a66?format=html&version=03.00.000. [Accessed February 2017].

[106] U.S. Energy Information Administration, "New Jersey Electrical Profile 2015," January 2017. [Online]. Available: http://www.eia.gov/electricity/state/NewJersey/. [Accessed February 2017].

[107] G. Towler and R. Sinnott, Chemical Engineering Design, Waltham, MA: Butterworth-Heinemann, 2013.

[108] U.S. Energy Information Administration, "New Jersey Natural Gas Industrial Price," 31 January 2018. [Online]. Available: https://www.eia.gov/dnav/ng/hist/n3035nj3m.htm. [Accessed February 2018].

[109] R. M. Felder and R. W. Rousseau, Elementary Principles of Chemical Processes, Hoboken: John Wiley & Sons, 2005.

[110] E. W. Rice, R. B. Barid, A. D. Eaton and L. S. Cleceri, Standard methods for the examination of water and wastewater, Washington, D.C.: American Public Health Association, American Water Works Association, Water Environment Federation, 2012.

[111] Sigma-Aldrich. Inc., "Activated Charcoal Product Information," Sigma-Aldrich, Inc., St. Louis, 2017.

[112] C. L. Yaws and P. K. Narasimhan, "Adsorption Capacity of Activated Carbon for Water Purification," in *Water Encyclopedia, Volumes 1-5*, Hoboken, John Wiley and Sons, 2005, pp. 381-384.

[113] Applied Membranes, Inc., "Water Treatment Guide - Ozone Generation," 2007. [Online]. Available: http://www.watertreatmentguide.com/ozone_generation.htm. [Accessed 2 May 2018].

[114] R. Reidy, "Nanostone Water acquires Ultura," *Filtration Industry Analyst*, vol. 2015, no. 2, p. 1, 2015.